RAQUEL ESTEVES ARROJA

STUDYING THE ROLE OF HYPOXIA IN GLIOBLASTOMA

Department of Biomedical Sciences and Medicine

2020

RAQUEL ESTEVES ARROJA

STUDYING THE ROLE OF HYPOXIA IN GLIOBLASTOMA

Master's in Oncobiology – Molecular Mechanisms of Cancer

Work under the supervision of:

Dr. Patrícia Madureira

Dr. Bibiana Ferreira

Department of Biomedical Sciences and Medicine

2020

STUDYING THE ROLE OF HYPOXIA IN GLIOBLASTOMA

Authorship Statement

I hereby declare to be the author of this work, which is original and unpublished. Authors and papers consulted are duly cited in the text and are listed in the included references.

Raquel Esteves Arroja

(Raquel Esteves Arroja)

Acknowledgments

First of all, I would like to thank my supervisor Dr.Patrícia Madureira. I am deeply grateful for having the amazing opportunity of working with you. Thank you for all the knowledge, support, patience, and friendship. Thank you for making me feel welcome in a different country. It was a pleasure to have learnt from you and there has not been a day when I doubted my choice in a supervisor.

I would also like to thank my co-supervisor, Dr.Bibiana Ferreira, for the support, help and assistance over a great distance.

A special thanks to Dr.Roger Draheim and all of his lab members, especially Fadhael, for the help and for letting me use the lab as my own whenever I needed.

To Brain Tumour Research Centre of Excellence from the University of Portsmouth for the opportunity that has been given to me to learn and grow as a scientist. To all the members of the laboratory for their help when needed, especially to Amy Dexter and Elizabeth Gimmy. Thank you for the coffee cakes, muffins, the support and for making me feel welcome.

Finally, and most importantly, I am forever grateful to my parents, José Manuel Arroja and Florbela Arroja, and my family, for supporting me always and making this experience come true.

Abstract

Glioblastoma (GBM), a grade IV astrocytoma, is the most common type of brain tumour. It is considered one of the most lethal of all cancers and the deadliest among primary brain tumours. It is highly aggressive and invasive, and usually diagnosed among the elderly.

GBM is characterised by the presence of hypoxic regions (low oxygen levels with around 1-3% O_2 depending on the tissue, $pO_2 < 10$ mmHg) and by the existence of a necrotic foci with pseudopalisades and microvascular hyperplasia in its surroundings. As the tumour grows its centre has less access to oxygen and nutrients provenient from the vasculature surrounding the outer layer. To address their needs, cancer cells activate several mechanisms in order to survive. Hypoxia is known to regulate several genes that are associated with angiogenesis, invasion, metabolic changes, and tumour progression. Previous results from our laboratory identified two proteins, ADM and TFRC, that are over- and under-expressed, respectively, in hypoxic GBM cells.

To better understand their role in hypoxic GBM, this study consisted in performing the knockout of *ADM* and *TFRC* in GBM biopsy-derived cell lines – UP-029 and SEBTA-023. The knockout was performed using the CRISPR-Cas9 system and the cells were analysed under normoxic and hypoxic (1% O_2) conditions.

Due to the global COVID-19 pandemic, the research facilities were closed, and the experiments could not be concluded. Thus, the role of ADM and TFRC in hypoxic GBM could not be understood. It is necessary in the future, to continue this study in order to have a better insight of their function in GBM progression. The discovery of new molecular markers and therapeutic targets is crucial in order to fight this deadly type of tumour.

Keywords: Glioblastoma (GBM), Hypoxia, Adrenomedullin (ADM), Transferrin Receptor 1 (TFRC), CRISPR-Cas9.

Resumo

Glioblastoma (GBM) é classificado pela Organização Mundial de Saúde como um astrocitoma de grau IV e é o tipo de tumor do sistema nervoso central mais comum. É considerado um dos tumores mais mortíferos e o mais mortífero de entre os tumores do sistema nervoso central. GBM é altamente invasivo e agressivo e está associado com resistência à quimioterapia. GBM pode ser sub-dividido em dois tipos: primário e secundário. GBM primário é mais agressivo e a sua incidência é comum em pessoas idosas, enquanto que o GBM secundário oferece melhor prognóstico e é diagnosticado geralmente em pessoas de idade inferior a 45 anos.

Pacientes com GBM têm uma sobrevivência média de menos de 15 meses após o seu diagnóstico apesar de todas as abordagens multidisciplinares utilizadas. O tratamento padrão baseia-se na realização de cirurgia (quando esta é possível) seguida de quimioterapia com temozolamida (TMZ) e radioterapia concomitante. Apesar dos vários ensaios clínicos realizados e em curso, apenas três quimioterapêuticos estão aprovados: Temozolamida, Carmustina e Bevacizumab. São necessários novos tratamentos que apresentem menos efeitos secundários e que sejam mais eficazes. Diferentes alternativas para o tratamento de GBM têm sido estudadas nos últimos anos. Entre elas pode-se enumerar: imunoterapia, como o uso de células dendríticas, vacinas peptídicas, células CAR-T, inibidores de checkpoints imunes e vírus oncolíticos; *Tumour Treating Fields* (*TTFields*) e *Laser Interstitial Thermal Therapy* (*LITT*). Existem vários ensaios clínicos em diferentes fases que podem vir a demonstrar-se promissores no futuro.

GBM tem como características patológicas a existência de centro necrótico com pseudopaliçadas e hiperplasia microvascular na sua região circundante. É também caracterizado pela existência de regiões hipóxicas. Uma região é considerada hipóxica quando os níveis de oxigénio são baixos (com cerca de 1-3% O_2 dependendo do tecido) com pO_2 inferior a 10mmHg. À medida que o tumor cresce, a região central tem menos acesso a oxigénio e nutrientes, fornecidos pelos vasos sanguíneos, em comparação com as regiões mais superficiais. De forma a obter oxigénio e nutrientes necessários, as células cancerígenas ativam vários mecanismos de forma a sobreviverem. A hipóxia regula vários genes e proteínas que estão associados com

angiogénese, invasão e reprogramação metabólica, favorecendo a progressão tumoral. Esta é uma característica do GBM e está associada à sua progressão.

Adrenomedulina (ADM) é uma hormona que desempenha um efeito vasodilatador e que está sobre-expressa em vários tipos de cancro (por exemplo: cancro da mama, pulmão, próstata). ADM desempenha um papel importante no processo de angiogénese e crescimento tumoral. TFRC é um recetor de transferrina que medeia a entrada de ferro dentro da célula através de endocitose e que está expresso na superfície da maior parte das células. Tal como ADM, TFRC está expresso de forma anormal em vários tipos de cancro como por exemplo cancro da mama, cólon e ovário. Sabe-se que a hipóxia induz a transcrição de ambos os genes. Resultados obtidos anteriormente no nosso laboratório identificaram estas duas proteínas, ADM e TFRC, sobre- e sub-expressas, respetivamente, em linhas celulares de GBM.

O principal objetivo deste estudo é a compreensão do papel destas duas proteínas em GBM hipóxico. Para tal, realizou-se o *knockout* (KO) dos genes *ADM* e *TFRC* em linhas celulares de GBM prevenientes de biópsias de pacientes – UP-029 e SEBTA-023. O *knockout* foi realizado utilizando o sistema de edição do genoma CRISPR-Cas9 e as células foram analisadas em condições de normóxia e hipóxia (1% O_2).

Para avaliar as condições de hipóxia, as células *wild-type* foram expostas a diferentes condições de hipóxia. As células pertencentes à linha celular UP-029 foram expostas durante 24h e 48h, as SEBTA-023 durante 6h e 24h e a presença de várias proteínas alvo de hipóxia e de HIF-1 foram analisadas (HIF-1α, HIF-2α, CA IX, NDRG1 e PDK1) através de *Western Blotting*. A presença das proteínas alvo em comparação com células sem tratamento confirmam as condições de hipóxia.

O sistema CRISPR/Cas9 é um sistema de edição do genoma que utiliza a nuclease Caspase 9 (Cas9) para criar uma quebra da cadeia dupla num locus genómico de interesse. Esta técnica consiste na introdução de um plasmídeo CRISPR/Cas9 que contém sequências de *guide RNAs* (gRNAs), sequências estas que são complementares à sequência de DNA alvo, que guiam a Cas9 ao local de corte. Após o corte, a célula tenta reparar este erro e acaba por criar uma mutação Indel, realizando assim o *knockout*.

De modo a fazer o knockout dos dois genes, foram desenhados 4 gRNAs que posteriormente foram clonados num plasmídeo CRISPR, pSpCas9(BB)-2A-Puro

(PX459) vetor V2.0. A clonagem foi confirmada e os plasmídeos foram transfetados nas duas linhas celulares – UP-029 e SEBTA-023.

As células transfectadas foram analisadas através de *Western Blotting*. A presença de ADM não foi possível de detetar através de *Western Blotting*, possivelmente devido ao seu tamanho (6 kDa) ou devido a esta proteína ser secretada. Outras técnicas foram utilizadas (dotblot, ELISA, PCR) de modo a tentar ultrapassar este problema, no entanto a sua otimização não foi possível e teve de ser adiada. As células com KO de *TFRC* foram analisadas, no entanto não se conseguiu isolar clones com KO. A análise de células com KO de *TFRC* e a otimização de técnicas que comprovem a presença de ADM têm de ser continuadas, no entanto o fecho dos laboratórios devido à pandemia COVID-19, não o permitiu. Para além de continuar o isolamento de clones com KO de *TRFC* e *ADM*, é necessário avaliar o papel destas duas proteínas em condições de normóxia e hipóxia realizando ensaios funcionais. No futuro é sugerida a realização de ensaios de tubulogénese em relação às células WT e com KO de *ADM*. É sugerido também a realização de ensaios de viabilidade (MTS) e de sensibilidade a *stress* oxidativo (tratamento com H_2O_2) em relação a ambas as células WT e com KO de *ADM* e *TFRC*. A continuação deste estudo é necessária para uma melhor compreensão do papel destas duas proteínas, ADM e TFRC, na progressão de GBM. A descoberta de novos marcadores associados com a progressão de GBM é necessária para combater este tipo de tumor e fornecer um melhor prognóstico aos pacientes.

Palavras chave: Glioblastoma (GBM), Hipóxia, Adrenomedulina (ADM), Recetor da Transferrina (TFRC), CRISPR-Cas9.

List of Contents

List of Figures

List of Tables

List of Abbreviations

A:

ADM – Adrenomedullin

AKT – Protein Kinase B

ALT – Alternative Lengthening of Telomeres

Amp – Ampicillin

Ang – 1 – Angiopoietin-1

Ang-2 – Angiopoietin-2

APC - Antigen Presenting Cells

APS – Ammonium Persulphate Solution

Arg – Arginine

ASCL1 - Achaete-Scute Family BHLH Transcription Factor 1

ATP – Adenosine Triphosphate

ATRX – Alpha-Thalassemia Mental Retardation x-linked

B:

BBB – Blood-Brain-Barrier

BCA - Bicinchoninic Acid

BCL-2 - B-cell Lymphoma 2

BiCNU - Carmustine

BRCA – Breast Cancer gene

BSA – Bovine Serum Albumin

BV – Bevacizumab

C:

CA IX – Carbonic Anhydrase 9

CA XII – Carbonic Anhydrase 12

$CaCl_2$ – Calcium chloride

CAF – Cancer-associated Fibroblasts

cAMP - cyclic Adenosine Monophosphate

CAR – Chimeric Antigen Receptor

Cas9 – Caspase 9

CBF1 – Immunoglobulin kappa J

CBP/p300 - CREB-binding protein/E1A binding protein p300

CCR5 – C-C Chemokine Receptor type 5

CDKN2A – Cyclin Dependent Kinase Inhibitor 2A

CFU - Colony Forming Units

CGRP - Calcitonin Gene-Related Peptide

CHI3L1 – Chitinase 3 Like 1

CI – Confidence Interval

Cl^- - Chloride

CMV - Cytomegalovirus

CNS – Central Nervous System

CO_2 – Carbon Dioxide

CpG - Cytosine-phosphate-guanine

CRISPR – Clustered Regularly Interspaced Palindromic Repeats

CRLR - Calcitonin Receptor-Like Receptor

CSC – Cancer Stem Cell

CT – Computer Tomography

C-TAD - C-terminal Activation Domain

Cu^+ - Cuprous ion

Cu^{2+} - Cupric ion

CXCL1 - C-X-C Chemokine Ligand 1

CXCL12 - C-X-C Chemokine Ligand 12

CXCL2 - C-X-C Chemokine Ligand 2

CXCR4 - C-X-C Chemokine Receptor type 4

D:

DAMPs - Damage-Associated Molecular Patterns

DBS – Double Strand Break

DC – Dendritic Cells

DCX - Doublecortin

DLL3 - Delta-like 3

DMEM - Dulbecco's Modified Eagle's Medium

DNA - Deoxyribonucleic acid

E:

E2F – E2 Factor

EDTA – Ethylenediamine Tetraacetic Acid

EGFR – Epidermal Growth Factor Receptor

ELISA - Enzyme-Linked Immunosorbent Assay

EMT – Epithelial-to-Mesenchymal Transition

eNOS – Endothelial Nitric Oxide Synthase

EphA2 - Ephrin type-A receptor 2

F:

FAK - Focal Adhesion Kinase

FBS - Fetal Bovine Serum

FDA – Food and Drug Administration

Fe^{2+} - Ferrous ion

Fe^{3+} - Ferric ion

Fe_3O_4 - Iron oxide magnetite

FGF-2 – Fibroblast Growth Factor 2

FIH - Factor inhibiting HIF1

fMRI – Functional Magnetic Resonance Imaging

FVII – Factor VII

G:

GABRA1 - Gamma-aminobutyric acid type A receptor subunit alpha1

GBM – Glioblastoma

G-CIMP – Glioma Cytosine-phosphate-guanine island methylator phenotype

GFAP - Glial Fibrillary Acidic Protein

GLUT1 - Glucose Transporter 1

GLUT3 - Glucose Transporter 3

gRNA – Guide RNA

GSC – Glioblastoma Stem Cell

Gy – Gray

H:

HBSS - Hanks' Balanced Salt Solution

HCl – Hydrochloric Acid

HDR – Homology-directed Repair

HIF – Hypoxia Inducible Factor

HK2 – Hexokinase 2

HRE – HIF-responsive Element

I:

ICD – Immunogenic Cell Death

IDH – Isocitrate Dehydrogenase

IGF 2 - Insulin growth factor 2

IgG – Immunoglobulin G

IL-13Rα – Interleukin-13 Receptor α

iMRI – Intraoperative Magnetic Resonance Imaging

ITT – Intention To Treat

K:

KCl – Potassium Chloride

KO – Knockout

KPS – Karnofsky Performance Status

L:

LB - Lysogeny broth

LDHA - Lactate dehydrogenase A

LITT – Laser Interstitial Thermal Therapy

LOH – Loss of Heterozygosity

LOX - Lysyl Oxydase

M:

MAP – Mitogen-activated-protein

MCT1 - Monocarboxylate Transporter 1

MCT4 – Monocarboxylate Transporter 4

MDM2 – Mouse Double Minute 2 Homolog

MERTK – Tyrosine-protein Kinase MER

MET - Hepatocyte growth factor receptor

MET – Mesenchymal-to-Epithelial Transition

$MgCl_2$ – Magnesium Chloride

MGMT - O^6-methylguanine-DNA-methyltransferase

$MgSO_4$ – Magnesium Sulfate

MHC - Major Histocompatibility Complex

MLH1 – mutL Homolog 1

MMP – Matrix Metalloproteinase

MMR – Mismatch Repair

mOS – median Overall Survival

MRI – Magnetic Resonance Imaging

MSH2 – mutS Homolog 2

MTIC - [(methyl-triazene-1-yl)-imidazole-4-carboxamide]

mTOR – Mammalian Target of Rapamycin

N:

NAb – Neutralising Antibodies

NaCl – Sodium Chloride

NADPH – Nicotinamide Adenine Dinucleotide Phosphate

NDRG1 - N-myc Downstream Regulated 1

NEFL - Neurofilament Light

NES – Nestin

NF1 - Neurofibromin 1

NFAT - Calcineurin-nuclear Factor of the Activated T-cell

NHEJ – Non-Homologous End Joining

NO – Nitric Oxide

NOS – Nitric Oxide Synthase

NP-40 - Nonyl Phenoxypolyethoxylethanol

NPs – Nanoparticules

N-TAD - N-terminal activation domain

O:

O_2 - Oxygen

OCT-4 - Octamer-binding transcription factor

OD – Optical Density

OS – Overall Survival

OXPHOS – Oxidative Phosphorylation

P:

p21 – Protein 21

PAM – Protospacer Adjacent Motif

PAR-2 – Protease-Activator Receptor 2

PBS – Phosphate-Buffered Saline

PCR - Polymerase Chain Reaction

PD-1 - Programmed cell Death protein 1

PDGF – Platelet-derived Growth Factor

PDGFR – Platelet-derived Growth Factor Receptor

PDK1 - Pyruvate dehydrogenase kinase 1

PD-L1 - Programmed Death-Ligand 1

PFK1 – Phosphofructokinase 1

PFS – Progression-Free Survival

Pgn - Plasminogen

PHD - Prolyl hydroxylase domain

pI – Isoelectric Point

PI3K - Phosphoinositide 3-kinase

PIP2 - Phosphatidylinositol 4, 5 bisphosphate

PIP3 - phosphatidylinositol 3, 4, 5 triphosphate

PlGF – Placental Growth Factor

Plm – Plasmin

PLOD2 – Procollagen-Lysine, 2-Oxoglutarate 5-Dioxygenase 2

pO_2 – oxygen partial pressure

PTEN – Phosphatase and Tensin Homolog

Puro – Puromycin

R:

RAMP - Receptor Activity Modifying Protein

RB – Retinoblastoma

RISC – Recurrence-Initiating Stem-like Cancer

RNA – Ribonucleic Acid

ROBO1 – Roundabout Guidance Receptor 1

ROS – Reactive Oxygen Species

S:

SDS – Sodium Dodecyl Sulfate

SDS-PAGE - Sodium Dodecyl Sulfate – Polyacrylamide Gel Electrophoresis

sgRNA – Single-guided RNA

SLC12A5 - Solute Carrier Family 12 Member 5

SOX - Sry-type HMG box

SRC - Proto-Oncogene Tyrosine-Protein Kinase Src

STAT - Signal Transducer and Activator of Transcription

SWI/SNF2 – SWItch/Sucrose Non Fermentable

SYT1 - Synaptotagmin 1

T:

TAA – Tumour Associated Antigens

TAM – Tumour-associated Macrophages

TBS-T - Tris-Buffered Saline-Tween

TCA – Tricarboxylic Acid Cycle

TCF4 - Transcription factor 4

TEMED - Tetramethylethylenediamine

TF – Tissue Factor

TF - Transferrin

TFRC – Transferrin Receptor 1

TGF-β - Transforming Growth Factor – β

TMZ – Temozolomide

TP53 – Tumour Protein 53

tPA - Tissue-type Plasminogen Activator

TRPC6 - Transient Receptor Potential 6

TSG – Tumour Suppressor Gene

TTFields – Tumour Treating Fields

TWIST1 - Twist family bHLH transcription factor 1

Ty – Tyrosine

U:

uPA - Urokinase-type Plasminogen Activator

uPAR – Urokinase-type Plasminogen Activator Receptor

UV – Ultraviolet

V:

Val - Valine

VEGF – Vascular Endothelial Growth Factor

VEGFR – Vascular Endothelial Growth Factor Receptor

VPF – Vascular Permeability Factor

W:

WHO – World Health Organization

WT – Wild-Type

Z:

ZEB1/2 - Zing finger E-box binding homeobox ½

Others:

2-HG – 2-hydroxyglutarate

5-ALA - 5-Aminolevulinic Acid

1. Introduction:

1.1. Cancer

A cell becomes cancerous due to genetic and environmental factors. Every person has a different genetic susceptibility to develop cancer, which together with their lifestyle and environmental exposures over time may contribute to cancer development. The exposure to carcinogens is present on a daily basis. Carcinogens are physical and chemical substances that cause cancer. Physical carcinogens such as ultraviolet (UV) (e.g. sun and solarium) and ionizing radiation (X-rays) are of great importance. Chemical carcinogens such as alcohol, tobacco, hydrocarbons (e.g. benzene and diethylstilbestrol) and asbestos are also noteworthy (Weiderpass, 2010; Weinberg, 2014). Environmental pollution, as well as lifestyle (diet, obesity and lack of exercise), play an important role in cancer development. (Anand et al., 2008; Lewandowska et al., 2019; Weiderpass, 2010). Different types of cancer are linked to different carcinogens exposure and lifestyle factors. A few examples are listed in the table below (Table 1.1).

Table 1.1 – Examples of types of cancer linked to carcinogens exposure and lifestyle factors.
(Anand et al., 2008; Lewandowska et al., 2019; Weiderpass, 2010; Weinberg, 2014).

Carcinogen / Lifestyle factor		Type of cancer
UV radiation		Melanoma
Asbestos		Mesothelioma
Alcohol		Mouth, liver, breast, oesophagus and larynx cancer
Tobacco		Lung, mouth, bladder, larynx and kidney cancer
Benzene		Acute leukaemia
Diet	**High in nitrates, low in vegetables**	Stomach and oesophagus cancer
	High in fat, low in fibre	Bowel, pancreas, prostate and breast cancer
	High red meat consumption	Gastrointestinal and colorectal cancer

Urban air pollution	Lung cancer
Obesity	Colon, breast, oesophagus and endometrium cancer

Mutations in the DNA caused by environmental factors and other carcinogens are considered somatic mutations. These are passed to daughter cells after cell division but are not inherited by the offspring (Alexandrov et al., 2013; Pecorino, 2012). Mutations are not only induced by the exposure to environmental factors and other carcinogens but they can also be spontaneous due to DNA lesions (e.g. during DNA replication, free radicals) that are not repaired by the DNA repair system (Alexandrov et al., 2013; Loeb & Loeb, 2017).

In addition to somatic mutations, germline mutations can occur in cancer susceptibility genes and may be inherited by the offspring leading to an increased risk of developing cancer. These mutations are the cause of hereditary cancer syndromes that account for 10% of all cancers. The most frequent syndromes are the following: Li-Fraumeni syndrome (mutation in Tumour Protein 53 (*TP53*)), Hereditary Breast and Ovarian Cancer syndrome (mutation in Breast Cancer gene 1 and 2 (*BRCA1/2*)), Cowden syndrome (mutation in Phosphatase and Tensin Homolog (*PTEN*)) and Lynch syndrome (mutation in DNA Mismatch Repair (MMR) genes such as mutL Homolog 1 (*MLH1*) and mutS Homolog 2 (*MSH2*)) (Chavarri-Guerra et al., 2020; Valdez et al., 2017).

Cancer cells usually acquire capabilities that normal and healthy cells do not have. They have their own way of escaping the normal controls of proliferation sent by neighbouring cells and “become the masters of their own destinies” (Hanahan & Weinberg, 2011). They can become immortal, resist cell death and evade growth suppressors. Their metabolism is reprogrammed contributing to their abnormal proliferation capabilities. Their genome is unstable and usually has several mutations. Mutations occur in the DNA of healthy cells constantly but most of them are repaired by DNA repair systems. There are two classes of genes that play important roles in initiating cancer and are commonly mutated in cancer: Tumour Suppressor Genes (TSG) and oncogenes. TSGs inhibit cell division and cancer development while oncogenes enhance it. Mutations that inactivate the expression of TSGs are typically observed in cancer cells contributing to their loss of suppressive properties and

subsequent cancer development. Contrarily to TSGs, mutations in proto-oncogenes that activate these genes confer a selective advantage to cancer development and cell growth. The combination of mutations in oncogenes and TSGs leads to a deregulation of the cell cycle control and to an abnormal interaction between the cancer cells and the microenvironment. This gives them the ability to divide when they should not and form aberrant masses of cells in the body (Hanahan & Weinberg, 2011; Miller, 2018; Strachan & Read, 2011; Stratton et al., 2009; Weinberg, 1996).

This genomic instability that is frequent in cancer cells contributes to the accumulation of subsequent somatic mutations. Cancer cells usually present numerous passenger mutations but only a small number of driver mutations. While driver mutations confer growth advantage and contribute to the development of the tumour, passenger mutations do not (Helleday et al., 2014; Stratton et al., 2009). The role of passenger mutations has been debated recently since they have been described as mini-drivers and latent drivers (Aparisi et al., 2019; Castro-Giner et al., 2015; Nussinov & Tsai, 2015). Castro-Giner *et al*. (2015) highlighted the existence of "mini-driver" mutations as mutations that provide a small selective advantage. Latent drivers, as described by Nussinov *et al.* (2015) act as passenger driver but drive cancer development when combined with other mutations (Nussinov & Tsai, 2015). Several genes need to be mutated for cancer to be formed. It is believed that common epithelial cancers need 5-7 driver mutations while hematopoietic cancers need a smaller number of driver mutations for cancer development (Helleday et al., 2014; Strachan & Read, 2011; Stratton et al., 2009).

The development of cancer is a multistep process. As cells start to divide uncontrollably (hyperplasia) due to deregulation of the cell cycle control and faulty communication with the microenvironment, the tissue and their surroundings become disorganized and abnormal (dysplasia). This mass of cells constitutes at this point a carcinoma *in situ* that is not invasive. The tumour may remain limited to this site or it may acquire more mutations that allow it to become malignant, acquire motile and invasive characteristics, spread through the blood vessels (disseminate) and metastasize if the microenvironment in the host organ is favourable. As the tumour grows, its access to nutrients and oxygen becomes limited. In order to survive, it induces the development of new vessels, angiogenesis. This process also contributes

to cancer cell metastasis through the blood vessels (Figure 1.1) (Weinberg, 1996, 2014).

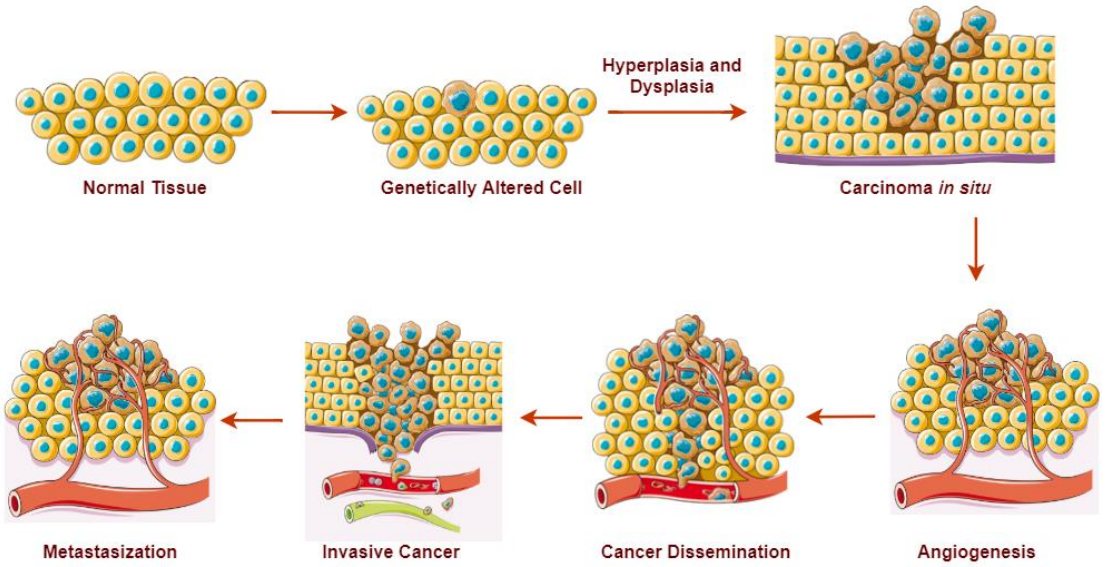

Figure 1.1 – Cancer development is a multistep process.
A genetically altered cell divides uncontrollably (hyperplasia) leading to the disorganization of the tissue and their surroundings (dysplasia). A carcinoma *in situ* can be formed and disseminate throughout the body if the cells acquire motility and invasive capabilities. Figure adapted from Weinberg, 1996, 2014.

The tumour microenvironment also has an important role in cancer development and progression. Tumour cells recruit and reprogram normal cells, such as fibroblasts, immune and vascular cells, so they can act as contributors to cancer progression. The tumour microenvironment is constituted by Cancer-Associated Fibroblasts (CAFs), endothelial cells, pericytes, Tumour Associated Macrophages (TAMs), and other immune cells. Growth promoting signals, such as chemokines, cytokines and growth factors are also present in the microenvironment being secreted by both tumour and stromal cells within the tumour microenvironment. The secretion of these proteins, together with the recruitment of key cells, promotes cancer cell proliferation, angiogenesis and invasion making the interactions between tumour cells and the microenvironment essential for cancer progression (Denton et al., 2018; Yuan et al., 2016). Immune cells, in the microenvironment, play an important role however, cancer cells can avoid the immune system, preventing their destruction (Hanahan & Weinberg, 2011).

There are different types of cancer and they are divided according to their cells of origin as described below (Weinberg, 2014).

The most common type of cancer has origin in epithelial tissues and it is denominated carcinoma. It is responsible for 80% of cancer-related deaths in the Western World and it can be divided into two major subtypes: adenocarcinoma and squamous cell carcinoma. The first subtype has origin in epithelial cells with secretory function while the second is originated by epithelial cells with structural function (Weinberg, 2014).

Sarcomas have origin in mesenchymal cells and represent only 1% of all existing cancers. Among the most common sarcomas we can include osteosarcoma (origin in osteoblasts), liposarcoma (origin in adipocytes) and fibrosarcoma (origin in fibroblasts) (Weinberg, 2014).

Melanoma has origin in the melanocytes. Most of the melanomas take place in the pigmented cells of the skin (skin melanoma) but it can also occur in the retina (ocular melanoma) (Weinberg, 2014). It has a high tendency to metastasize to distant tissues such as brain, lungs and small intestine (Zbytek et al., 2008).

Cancers with origin in blood-forming tissues are denominated hematopoietic and can be divided into two major groups: leukaemia and lymphomas. Leukaemia has origin in the hematopoietic cell lineages and do not form solid tumours, moving freely in the blood flow. Leukaemia can be sub-divided into lymphocytic or myeloid according to the cells that are affected, and it can be acute or chronic. Lymphocytic leukaemias have origin in both T and B cells (lymphocytic lineage) and Myeloid leukaemias have origin in cells from the myeloid lineage. Lymphomas have origin in the lymphocytic lineage. These usually form solid tumour masses in the lymph nodes (Weinberg, 2014).

Cancers that have origin in cells from the peripheral and central nervous systems (CNS) are denominated neuroectodermal. They can be subdivided into primary and secondary. Primary CNS tumours are located in the CNS, in the CNS envelopes and in the nerves localised in the skull and spine. These include gliomas, neuroblastomas, medulloblastomas and schwannomas. Secondary CNS tumours are CNS metastases (Preusser & Weller, 2017; Weinberg, 2014). Glioma is a common term used to characterise primary brain tumours which include tumours of astrocytic

origin, such as glioblastomas and astrocytomas, ependymomas, oligodendrogliomas and mixed gliomas (Hanif et al., 2017). Glioblastoma is considered to be one of the most lethal and untreatable human tumours and the deadliest among primary brain tumours (Monteiro et al., 2017; Paolillo et al., 2018).

1.2. Glioblastoma

Glioblastoma (GBM) is the most common type of primary malignant brain tumour. It is classified by the World Health Organization (WHO) as a grade IV astrocytoma (Monteiro et al., 2017). The WHO classifies gliomas into grade I to IV according to their increasing level of malignancy. Grade IV gliomas are usually highly invasive and malignant. GBM is the most aggressive and invasive type of tumour among all the gliomas (Hanif et al., 2017).

1.2.1. Glioblastoma classification and subtypes

According to clinical characteristics, GBM can be sub-divided into primary and secondary GBM (Figure 1.2.). Primary GBM arise *de novo* and without indications of previous lesions. It is aggressive, highly invasive, and more common among the elderly. Secondary GBM arises from a prior lower grade astrocytoma and it is less common than primary GBM. It is associated with a better prognosis and usually appears in people under 45 years old (de Vleeschouwer, 2017; Hanif et al., 2017).

1.2.1.1. Primary Glioblastoma

Primary GBM can be divided into 4 subtypes: Classical, Mesenchymal, Neural and Proneural (Figure 1.2.) (Verhaak et al., 2010).

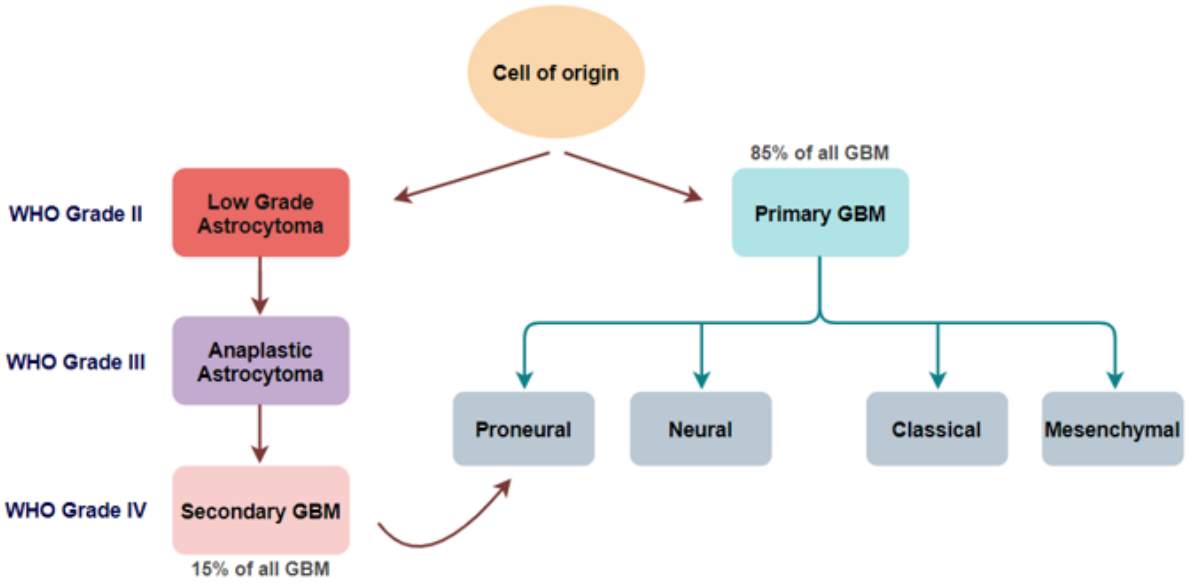

Figure 1.2 – Classification and subtypes of glioblastoma.
GBM can be divided in two types: primary (85%) and secondary (15%). Primary GBM can be divided in Neural, Classical and Mesenchymal. Proneural is a subtype of both primary and secondary GBM. Figure adapted from Hanif et al., 2017.

Primary GBM usually has mutations or amplification of the Epidermal Growth Factor Receptor (*EGFR*). Most of the GBMs that have EGFR overexpressed also have the *EGFR* gene mutated. Mutant EGFRvIII is observed in primary GBM. It is originated by the loss of the exons 2 to 7 of *EGFR* that leads to a deletion of 267 amino acids in the extracellular domain resulting in the constant activation of the receptor (de Vleeschouwer, 2017).

Activation of EGFR signalling pathway leads to the activation of two other oncogenic pathways, RAS and Phosphoinositide 3-kinase (PI3K) pathways, known to be related to cell growth, proliferation, survival and angiogenesis. RAS activates RAL-GEF, MAPK/ERK and PI3K pathways. RAS recruits, binds and activates RAF (Mitogen-activated-protein (MAP) kinase kinase kinase), RAF phosphorylates and activates MEK (MAP kinase kinase) and MEK in its turn phosphorylates and activates ERK (MAP kinase) (Figure 1.3) (de Vleeschouwer, 2017; Moghadam et al., 2017; Neel et al., 2011). In this way, the amplification or mutation of *EGFR* leads to its constitutive activity resulting in higher proliferation and GBM pathogenesis.

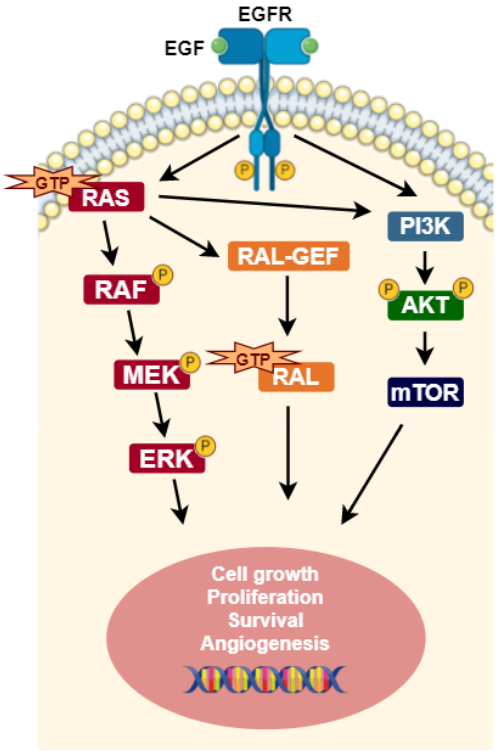

Figure 1.3 – EGFR signalling pathway.
EGFR when activated induces the activation of RAS and PI3K signalling pathways and their downstream intermediates. In its turn, RAS activates RAL-GEF and PI3K pathways. The activation of these pathways leads to the transcription of target genes related to cell growth, proliferation, survival and angiogenesis contributing to tumour progression. Figure adapted from Shackelford & Shaw, 2009; Weinberg, 2014.

Another alteration that is common in primary GBMs is the deletion or mutation of the tumour suppressor *PTEN*. *PTEN* mutations are usually seen in advanced stages of primary GBM. Loss of Heterozygosity (LOH) is a genetic event in which a heterozygous locus in a cell becomes homozygous due to the loss of one allele. It is usually associated with the loss of the wild-type allele in hereditary cancer syndromes (Ryland et al., 2015; Schwarzenbach, 2013). LOH of chromosome 10q is common in GBM (both primary and secondary GBM) and is related to *PTEN* deletion. When a growth factor binds a growth factor receptor, PI3K phosphorylates Phosphatidylinositol 4, 5 bisphosphate (PIP2) into Phosphatidylinositol 3, 4, 5 triphosphate PIP3. PIP3 activates and recruits protein kinase B (AKT) which in its turn activates mTORC1. PTEN is a negative regulator of this pathway and dephosphorylates PIP3 into PIP2, hence inhibiting AKT (Figure 1.4). With the loss of *PTEN*, the PI3K/AKT signalling pathway is constitutively active and this leads to cell growth, proliferation and inhibition of apoptosis (de Vleeschouwer, 2017; Ohgaki et al., 2004).

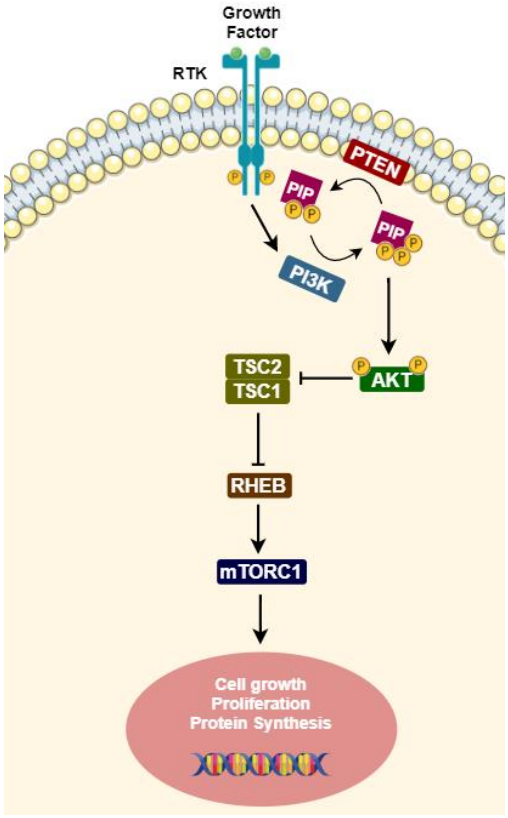

Figure 1.4 – PI3K signalling pathway.
PI3K pathway is activated when a growth factor binds a receptor tyrosine kinase (RTK). RTK suffers autophosphorylation and phosphorylates PI3K activating it. PI3K phosphorylates PIP2 into PIP3 activating the downstream intermediates AKT and mTORC1. PTEN dephosphorylates PIP3 into PIP2 acting as a negative suppressor inhibiting AKT activation. When activated, PI3K pathway leads to the transcription of genes related to cell growth, proliferation and protein synthesis contributing to tumour progression. Figure adapted from Ding et al., 2011.

Cyclin Dependent Kinase Inhibitor 2A, CDKN2A-p16^{INK4a} deletion is also a common alteration in primary GBMs. CDKN2A belongs to the INK family. CDKN2A acts in the Retinoblastoma (RB) pathway. CDKN2A- p16^{INK4a} deletions can be found on both primary and secondary GBM but they are more common in primary GBM (de Vleeschouwer, 2017).

RB plays an important role in the cell cycle. In non-proliferating cells, RB is hypo-phosphorylated and binds to E2 factor (E2F). This prevents the transcription of genes that are necessary for mitosis, stopping the cell cycle at the G1/S checkpoint. In proliferating cells, growth factors induce the expression of cyclin D1 and activation of Cyclin-dependent Kinase-cyclin complexes (CDK-cyclin) that phosphorylate RB. As

RB is phosphorylated, E2F is released and it induces the transcription of genes that promote DNA synthesis and cell proliferation (Figure 1.5) (de Vleeschouwer, 2017).

The RB pathway is regulated negatively by CDKNs. CDKNs compete with cyclins for CDK binding and prevent RB phosphorylation. When CDKNs are deleted (for example CDKN2A-p16^{INK4a} deletion), this competition does not occur which allows CDK-cyclin binding and RB phosphorylation. E2F is free to be released and induces the transcription of genes that lead to cell proliferation (Figure 1.5) (de Vleeschouwer, 2017).

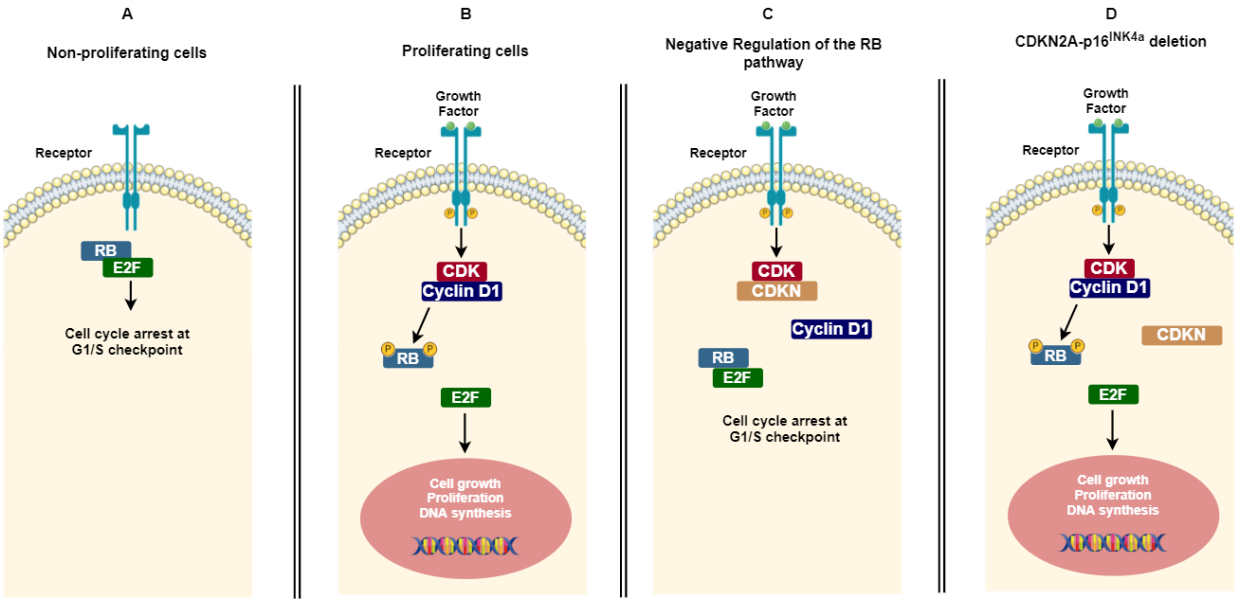

Figure 1.5 – RB signalling pathway and CDKN2A- p16^{INK4a} deletion.
(**A**) In non-proliferating cells, RB is hypo-phosphorylated and binds E2F and the cell cycle is arrested at G1/S checkpoint. (**B**) In proliferating cells, CDK-cyclin D1 phosphorylates RB causing E2F to be released and promote the transcription of target genes. (**C**) This pathway can be regulated negatively by CDKN (e.g. CDKN2A- p16^{INK4a}) proteins that compete with cyclins for CDK binding preventing RB phosphorylation. (**D**) With CDKN2A- p16^{INK4a} deletion, there is no competition for the CDK binding and RB can be phosphorylated and E2F is free to promote transcription of target genes. Figure adapted from de Vleeschouwer, 2017.

1.2.1.2. Secondary Glioblastoma

Secondary GBM is less aggressive than primary GBM and it is usually Proneural (Hanif et al., 2017).

Secondary GBM frequent alterations include overexpression of Platelet Derived Growth Factor A and Platelet Derived Growth Factor Receptor Alpha

(PDGFA/PDGFRa), Loss of Heterozygosity (LOH) of 1p/19q and mutations of *TP53*, Isocitrate Dehydrogenase 1/2 (*IDH1/2*) and Alpha-thalassemia mental retardation X-linked (*ATRX*) (de Vleeschouwer, 2017; Hanif et al., 2017).

PDGFRa is a growth factor receptor related to the promotion of angiogenesis and PDGFA is its ligand. They are both targets of cancer cells and their overexpression leads to an increased angiogenic activity which contributes to tumour growth (de Vleeschouwer, 2017).

TP53 pathway is related to cell death and differentiation, cell cycle control and DNA damage response. *TP53* pathway is activated when DNA damage occurs. p53 increases Protein 21 (p21) transcription to stop the cell cycle on G1 phase. p21 is a CDNK that binds to a cyclin and inhibits its function. This stops the cell cycle and gives time for DNA repair to take place. In cases where DNA repair is not possible/effective, p53 activates mechanisms of cell death to prevent the division of cells with damaged DNA (Figure 1.6) (de Vleeschouwer, 2017).

p53 pathway has a negative feedback mechanism. p53 induces the transcription of Mouse Double Minute 2 Homolog (*MDM2*) which in its turn induces p53 degradation by the proteasome (Figure 1.7). If *TP53* is mutated, the DNA damage is not repaired. Usually, in human gliomas, *TP53* has missense mutations that target essential exons for DNA binding. Another alteration usually seen in GBMs is MDM2 amplification. These alterations lead to a non-functional or non-existent p53 and to the proliferation of cells with damaged DNA (Chao, 2014; de Vleeschouwer, 2017).

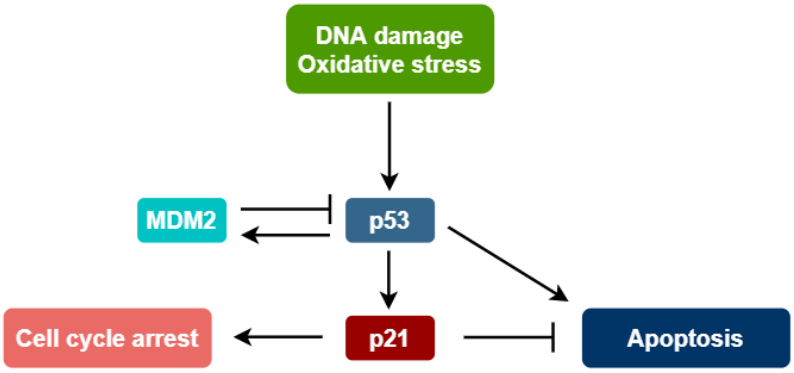

Figure 1.6 – p53 pathway.
p53, activated by DNA damage and oxidative stress, increases p21 transcription to arrest the cell cycle on G1 phase. With the cell cycle stopped, the DNA has time to be repaired. p53 induces apoptosis if there is more DNA damage that repair. Figure adapted from Strachan & Read, 2011.

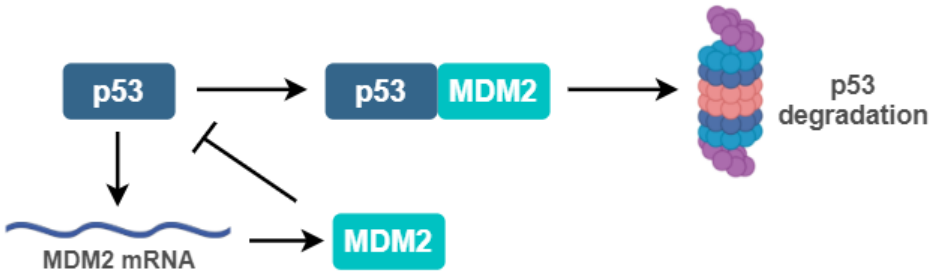

Figure 1.7 – Negative feedback mechanism of TP53.
p53 induces the transcription of MDM2 and in its turn, MDM2 induces the degradation of p53 by the proteasome. Figure adapted from Nag et al., 2013.

IDH 1/2 mutations are present in 70% of low-grade gliomas and secondary GBMs. *IDH1* mutations are believed to be the most reliable marker to differentiate primary from secondary GBMs and they are associated with a good patient outcome. In 2016, the WHO updated the classification of the CNS tumours according to their histopathological and molecular features. According to this classification, GBM is subdivided in GBM IDH-wildtype (WT) (90% of all cases) and GBM IDH-mutant (de Vleeschouwer, 2017; Louis et al., 2016; Monteiro et al., 2017; Nørøxe et al., 2016).

IDH enzymes are responsible for the oxidative carboxylation of isocitrate to α-ketoglutarate producing Nicotinamide Adenine Dinucleotide Phosphate (NADPH) (Figure 1.8 a.). There are five metabolic *IDH* genes that code for three IDH enzymes. IDH1 can be found in the cytosol and peroxisome and it delivers energy to produce

peroxisomal enzymes that affect several metabolic pathways. IDH2 and IDH3 can be found in the mitochondria, participating in the Tricarboxylic Acid Cycle (TCA) and contributing to the cell growth (Juan Huang et al., 2019; Monteiro et al., 2017; Nørøxe et al., 2016).

Figure 1.8 – Catalytic reaction performed by IDH wild-type and IDH mutant.
a. The enzyme IDH catalyses the oxidative decarboxylation of isocitrate in α-ketoglutarate producing NADPH. **b.** With IDH mutated, the reaction shown in a. still occurs but at a low rate and α-ketoglutarate is converted into the oncometabolite 2-HG, consuming NADPH and leaving the cell vulnerable to oxidative stress. Adapted from Juan Huang et al., 2019.

When *IDH* is mutated, the activity of the IDH protein is reduced by approximately 50%, so the production of α-ketoglutarate and NADPH decreases and the production of the oncometabolite, 2-hydroxyglutarate (2-HG), and $NADP^+$ increases (Figure 1.8 b.). This oncometabolite leaves the cell susceptible to oxidative stress and may cause epigenetic changes such as hypermethylation in human gliomas (Abdullah et al., 2016; Juan Huang et al., 2019; Nørøxe et al., 2016). 2-HG also upregulates VEGF and promotes the production of HIF-1α and consequent glioma invasion (Juan Huang et al., 2019).

As *IDH* is mutated, the normal function of the mitochondria becomes compromised as well as the production of bioenergy and intermediates. Taking that into account, IDH-mutant GBM cells have their growth lowered when compared with IDH-WT GBM, which translates into a better patient outcome (Monteiro et al., 2017; Nørøxe et al., 2016).

ATRX is a gene that was first discovered in patients with the α-thalassemia, x-linked mental retardation syndrome (ATRX syndrome). The ATRX protein is a member of the SWItch/Sucrose Non Fermentable (SWI/SNF2) family with a key role in chromatin remodelling and exists as two isoforms (180 and 280 kDa). *ATRX* is usually inactive in

gliomas due to deletions, mutations or gene fusions (Haase et al., 2018; Nandakumar et al., 2017).

Alternative Lengthening of Telomeres (ALT) is a non-telomerase-dependent telomere lengthening mechanism. A correlation between *ATRX* mutations and ALT was discovered and *ATRX* loss in gliomas has been shown to promote ALT. ALT promotion leads to telomere elongation which consequently leads to unlimited proliferation and pathogenesis. *ATRX* loss has also been associated with DNA damage and replicative stress (Chung et al., 2012; Haase et al., 2018; Nandakumar et al., 2017).

1.2.1.3. GBM subtypes

GBM can be divided into 4 subtypes according to their molecular pathogenesis and gene expression patterns: Classical, Mesenchymal, Neural and Proneural. (Figure 1.2.)

The classical subtype is classified by the amplification or mutation of *EGFR*, loss of *PTEN* and *CDKN2A* (CDKN2A-p16^{INK4a} deletion) and high expression of Nestin (*NES*) and the Notch and Sonic Hedgehog signalling pathways proteins. Paired loss of chromosome 10 and amplification of chromosome 7 is also a common event observed in classical subtype GBMs (de Vleeschouwer, 2017; Hanif et al., 2017; Monteiro et al., 2017; Verhaak et al., 2010a).

The mesenchymal subtype can be classified by the expression of mesenchymal markers such as Hepatocyte growth factor receptor (MET) and Chitinase 3 Like 1 (CHI3L1) and astrocytic markers such as CD44 and MER Tyrosine-protein Kinase (MERTK). It is also usually classified by mutations or deletion of the Neurofibromin 1 (*NF1*) gene, *CDKN2A* and *TP53*. NF1 functions as a negative regulator of the RAS pathway and its loss leads to the constitutive activation of RAS hence promoting oncogenesis. Like the classical subtype, the mesenchymal type usually shows gain of chromosome 7 and loss of chromosome 10 (de Vleeschouwer, 2017; Hanif et al., 2017; Monteiro et al., 2017; Verhaak et al., 2010b).

The neural subtype expresses a strong composition of neuron markers that are involved in the nervous system function and development. These markers are Gamma-

Aminobutyric acid type A Receptor subunit alpha1 (GABRA1), Synaptotagmin 1 (SYT1), Neurofilament Light (NEFL) and Solute Carrier Family 12 Member 5 (SLC12A5) (de Vleeschouwer, 2017; Monteiro et al., 2017; Verhaak et al., 2010).

The proneural subtype is classified by the amplification of PDGFRA and alterations in *TP53*, *PI3K* and *IDH1*. It also contains a high expression of proneural developmental genes such as Sry-type HMG box (*SOX*), Delta-like 3 (*DLL3*), Doublecortin (*DCX*), Transcription factor 4 (*TCF4*) and Achaete-Scute Family BHLH Transcription Factor 1 (*ASCL1*) (de Vleeschouwer, 2017; Monteiro et al., 2017; Verhaak et al., 2010).

A new subset of tumours was recently identified, Glioma Cytosine-phosphate-guanine (CpG) island methylator phenotype, G-CIMP. These tumours can be characterized by distinct copy number alterations, DNA methylation patterns and transcriptomic profiles when compared to the other four GBM subtypes. They are closely related to *IDH* mutations and almost all the IDH-mutant gliomas are G-CIMP positive (G-CIMP+). IDH-mutant/G-CIMP+ tumours have a better patient prognosis than IDH-mutant/G-CIMP- (G-CIPM negative) tumours. Most of the times they also have gain of chromosome 8 and 10 and alterations in the MYC pathway (de Vleeschouwer, 2017; Malta et al., 2017).

MGMT (O^6-methylguanine-DNA-methyltransferase) gene promoter methylation is one of the most important prognostic markers since it is associated with better patient prognosis. It is associated with G-CIMP status and *IDH* mutations. G-CIMP+, *IDH* mutations and MGMT gene promoter methylation, per se, are considered favourable prognostic biomarkers. However, patients with the three combined mutations are believed to have better overall survival (OS) than patients with the *MGMT* methylation biomarker alone (de Vleeschouwer, 2017; Malta et al., 2017).

1.3. Hypoxia and glioblastoma

Hypoxia is a biological condition that is characterized by the deficiency of oxygen in a cell or organism with oxygen partial pressure (pO_2) lower than 10 mmHg. As a tumour grows, the oxygen distribution throughout the tumour becomes defective and the centre of the tumour has less access to oxygen than the outer layer. This leads to deficiency of O_2 and the existence of hypoxic and/or necrotic zones usually in central

regions of the tumour (Figure 1.9). A main characteristic of GBM is the presence of multiple hypoxic regions that are associated with GBM aggressiveness and chemo-resistance. Within the main GBM pathological features is the existence of necrotic foci with pseudopalisades and microvascular hyperplasia in its surroundings (Figure 1.10) (Daniel J. Brat et al., 2004; Monteiro et al., 2017; Walsh et al., 2014).

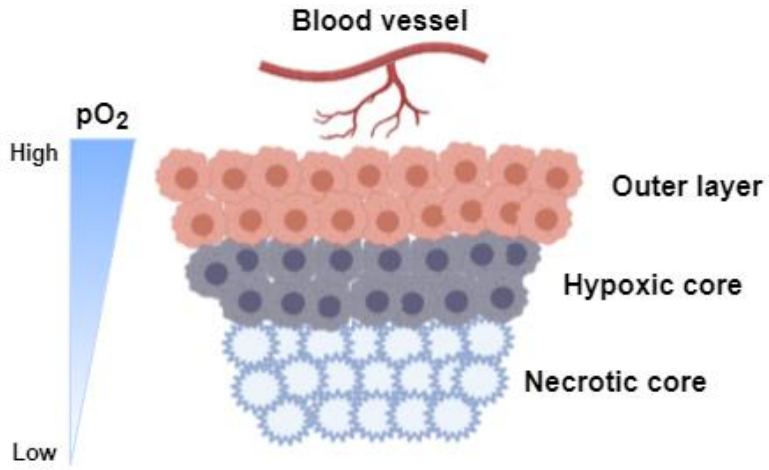

Figure 1.9 – Heterogeneity of oxygen distribution throughout the tumour.
The outer layer, surrounded by the blood vessels, has better access to oxygen having a better diffusion of O_2. As it approaches the centre of the tumour, the diffusion of O_2 becomes less efficient leading to hypoxic and necrotic tissues. Figure adapted from Luo & Wang, 2019.

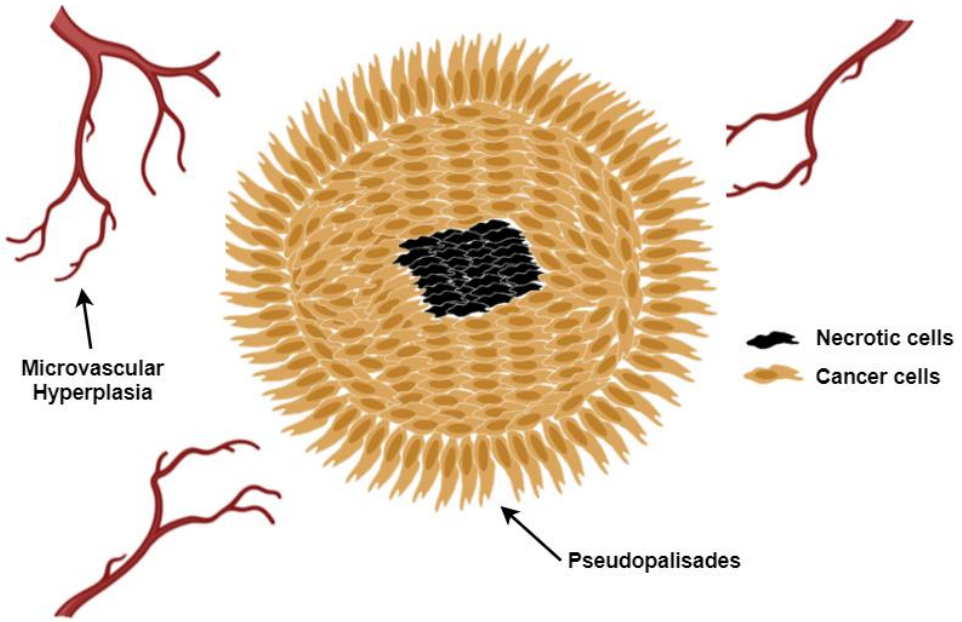

Figure 1.10 – GBM pathological features.
GBM is characterised by the existence of necrotic foci with pseudopalisades and microvascular hyperplasia in its surroundings. Pseudopalisades have origin in the migration of tumour cells from a hypoxic region and they establish a perpendicular orientation to the necrotic centre. Microvascular hyperplasia is an impaired form of angiogenesis and proliferation of cells that form microaggregates at the edge of the sprouting vessels. Adapted from Monteiro et al., 2017.

The pseudopalisades are believed to have origin in the migration of cells from a hypoxic region and usually have their long axis perpendicular to the necrotic centre. Microvascular hyperplasia refers to an exacerbated proliferation of endothelial cells, pericytes and smooth muscle cells that form microaggregates at the edge of the sprouting vessels. The formation of "glomeruloid bodies" can occur which is a characteristic of GBMs and these are the most exaggerated form of microvascular hyperplasia. The formation of this new vasculature due to hypoxic conditions promotes tumour expansion and invasion which is a major problem in patients with GBM (D. J. Brat & van Meir, 2001; Daniel J. Brat et al., 2002; Kaur et al., 2004; Monteiro et al., 2017; Rong et al., 2006).

1.3.1. Hypoxia-Inducible Factors (HIFs)

Hypoxia is regulated predominantly by Hypoxia-Inducible Factors (HIFs). HIFs are heterodimeric transcription factors and they are constituted by 2 subunits: HIF-α and HIF-β. HIF- α has 3 isoforms: HIF-1α, HIF-2α and HIF-3α that are regulated by O_2;

whereas HIF-β is constitutively expressed and is O_2 independent (Majmundar et al., 2010; Monteiro et al., 2017; Walsh et al., 2014).

HIF-1α has a ubiquitous expression which means that it is expressed in all cells, while HIF-2α and HIF-3α are only expressed in certain tissues (e.g. endothelial cells, renal interstitial cells, type II pneumocytes, liver parenchymal cells and myeloid lineage cells). HIF-α has two transactivation domains, N-terminal activation domain (N-TAD) and C-terminal activation domain (C-TAD). The N-TAD regulates HIF-α stability and the C-TAD regulates HIF-α transcriptional activation under hypoxic conditions (Majmundar et al., 2010; Monteiro et al., 2017; Walsh et al., 2014).

HIF-α is regulated by two hydroxylases: Prolyl Hydroxylase domain (PHD) and Factor Inhibiting HIF (FIH) that are O_2 and Fe^{2+} dependent. HIF-α stability is altered depending on the O_2 conditions (normoxia or hypoxia). Under normoxic conditions, PDH and FIH are active and switch off HIF-α activity. PHD hydroxylates proline residues on HIF-α (P402 and P564) and allows the von Hippel-Lindau (VHL) tumour suppressor protein to bind HIF-α. This binding leads to HIF-α ubiquitination and degradation by the 26s proteasome. FIH hydroxylates an asparagine residue on HIF-α (N803) and inhibits its transactivation function (C-TAD becomes inactive) and the recruitment of HIF-α co-activators such as CREB-binding protein/E1A binding protein p300 (CBP/p300) (Figure 1.11). It is known that FIH also binds to VHL and acts as a corepressor (Fan et al., 2014; Mahon et al., 2001; Monteiro et al., 2017; Schofield & Ratcliffe, 2004; Walsh et al., 2014).

Under hypoxic conditions, PDH and FIH are inactive. VHL is not capable to bind HIF-α and HIF-α is stable. C-TAD is active and CBP/p300 co-activator and HIF-β are recruited and interact with HIF-α forming a heterodimer. This heterodimer binds to a core DNA sequence in the HIF-responsive element (HRE) and HIF target genes are transcribed (Figure 1.11). HIF initiates hypoxia-derived processes that lead to tumour growth, proliferation, and metastasis (Monteiro et al., 2017; Schofield & Ratcliffe, 2004; Walsh et al., 2014).

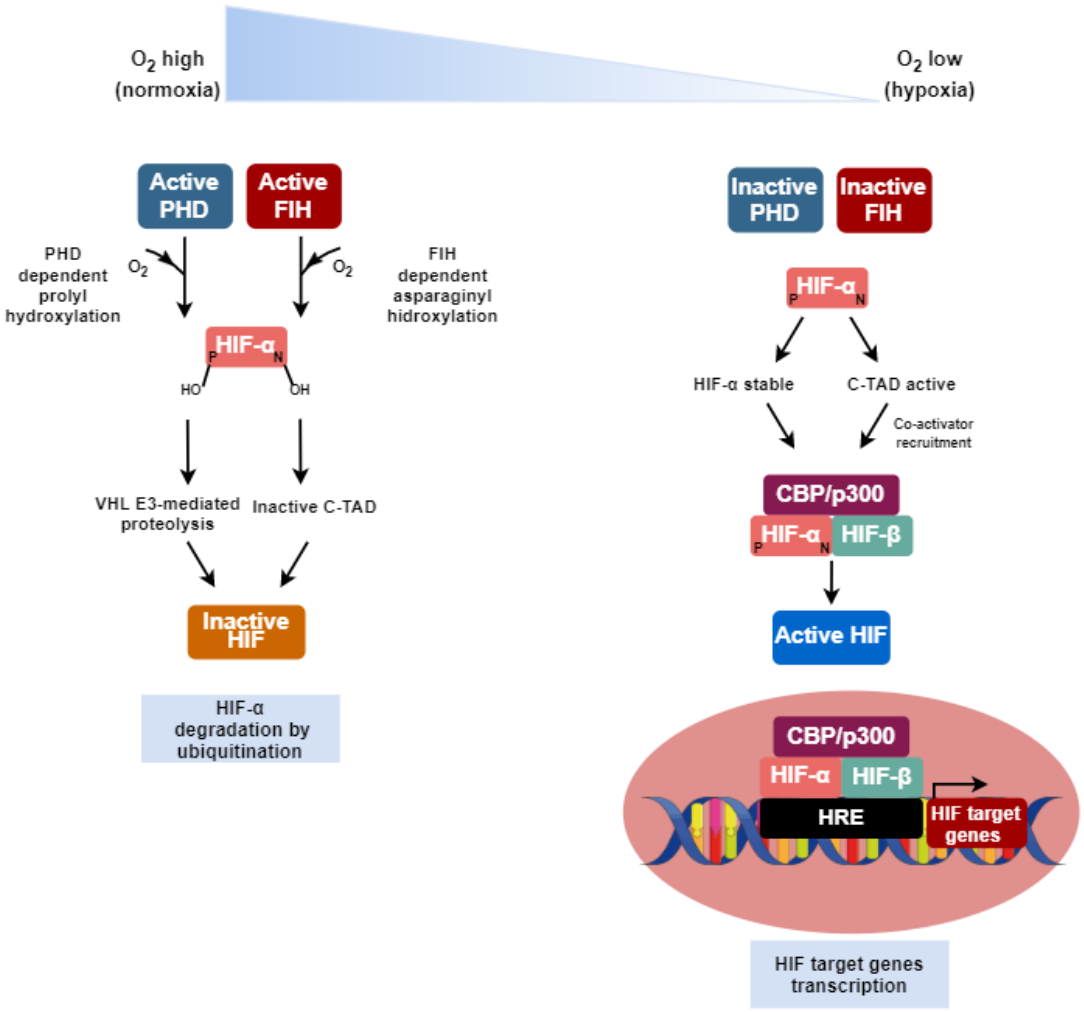

Figure 1.11 – HIF regulation under normoxic and hypoxic conditions.
Under normoxic conditions (high levels of O_2), PHD and FIH are active and switch off HIF-1α activity. FIH inhibits HIF-1α by inactivating C-TAD and HIF-1α co-activators. PHD allows VHL to bind HIF-1α and leading it to ubiquitination and consequent degradation by the proteasome. Under hypoxic conditions (low levels of O_2), PHD and FIH are inactive, allowing HIF-α, CBP/p300 and HIF-β to bind the HRE on the DNA leading to HIF target genes transcription. Figure adapted from Masson & Ratcliffe, 2003.

Several genetic alterations in signalling pathways lead to HIF activation. These alterations are associated with tumour progression, for example, mutations in PI3K/AKT/mTOR and RAS pathways. Genetic alterations common in GBM, such as the activation of EGFR and loss of *TP53* and *PTEN*, can lead to an increase of HIF-1α expression. The loss of *PTEN* and the activation of EGFR activates the PI3K/AKT/mTOR pathway and HIF-1α expression (Figure 1.12). Ravi *et al*. (2000) suggested that p53 inhibits HIF-1α by promoting MDM2-mediated ubiquitination and its degradation. So, the loss of *TP53* leads to the stabilization of HIF-1α and to an

increase of its expression (Figure 1.13) (Bertout et al., 2008; Monteiro et al., 2017; Ravi et al., 2000).

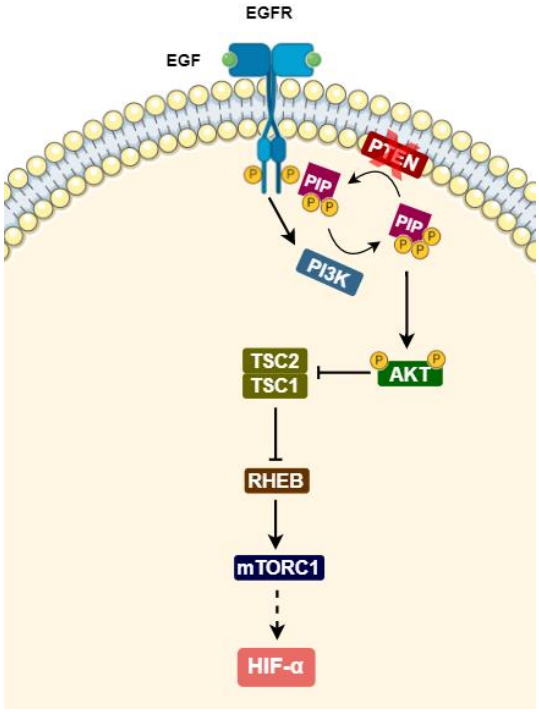

Figure 1.12 – PI3K pathway when PTEN is inactive leads to an increase of HIF-1α expression.
When PTEN is inactivated, PIP3 is active, phosphorylates and activates AKT activating downstream intermediates and promoting HIF-1α expression. Figure adapted from Ding et al., 2011; Monteiro et al., 2017.

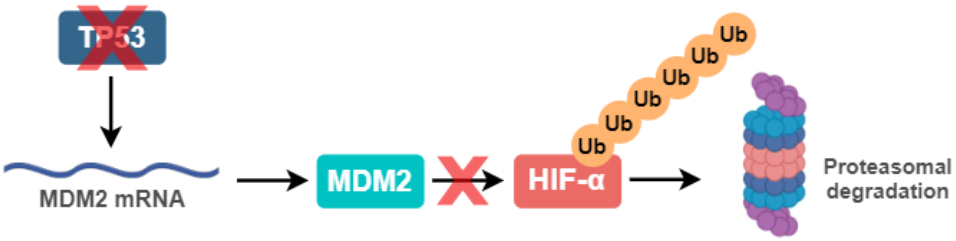

Figure 1.13 – Loss of TP53 leads to an increase of HIF-1α expression.
P53 inhibits HIF-1α through MDM2-mediated ubiquitination and subsequent proteasomal degradation. With its loss, HIF-1α expression is stabilized and its expression increases. Figure adapted from Monteiro et al., 2017.

HIF regulates several biological processes and hundreds of genes that are involved in tumour progression. Some examples are highlighted in the figure below (Figure 1.14)

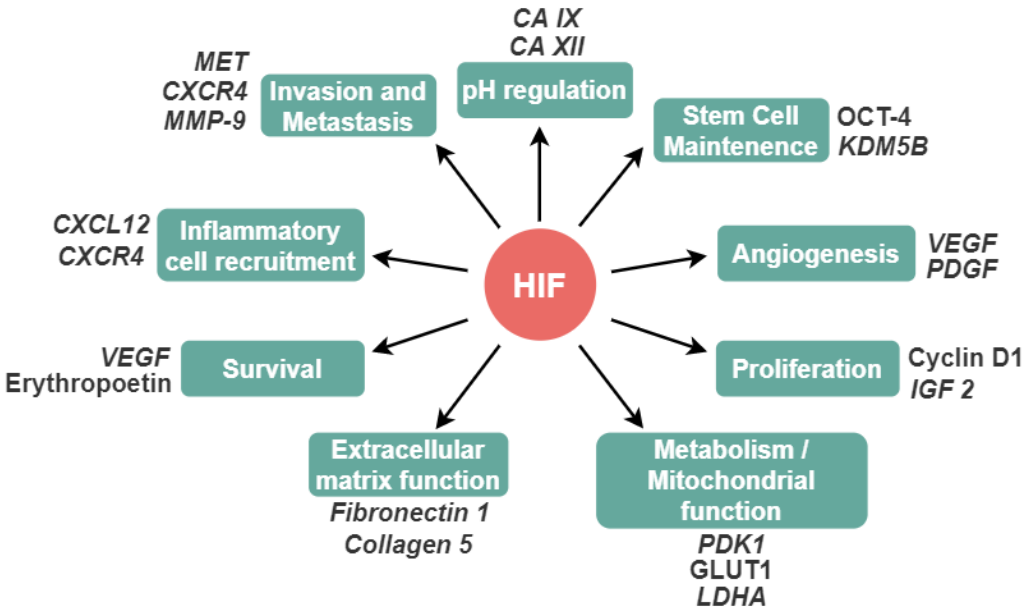

Figure 1.14 – Examples of genes and proteins regulated by HIFs and their respective biological process involved.
Examples include: proliferation (cyclin D1 and *IGF2*); metabolism/mitochondrial function (*PDK1*, GLUT1 and *LDHA*); extracellular matrix function (*collagen 5* and *fibronectin 1*); survival (*VEGF* and erythropoietin); inflammatory cell recruitment (*CXCL12* and *CXCR4*); invasion and metastasis (*MET* and *CXCR4*); pH regulation (*CA IX* and *CA XII*); stem cell maintenance (OCT-4 and *KDM5B*) and angiogenesis (*VEGF* and *PDGF*) (Bertout et al., 2008; Favaro et al., 2011; Walsh et al., 2014). Figure adapted from Bertout et al., 2008.

1.3.2. Angiogenesis

Just like normal tissues, but at a higher rate due to their high metabolism and proliferation, cancer tissues require nutrients and oxygen, that are provided to them by the vasculature. Growing tumours are usually deprived of O_2, glucose and other nutrients. This occurs as a consequence of increased metabolic activity and high proliferation rate. As they grow, the oxygen distribution throughout the tumour is not homogeneous and it leads to a deficiency of O_2, usually in central regions. A tumour can grow to a size of 1-2 mm^3 before their supply of nutrients and O_2 become limited. To overcome this problem and address their needs, new blood vessels are generated

from previous vessels through a biological process known as angiogenesis (Hanahan & Weinberg, 2011; Hillen & Griffioen, 2007; Ravi et al., 2000).

Angiogenesis plays an important role in embryonic development, placenta formation, wound healing, neovascular ocular diseases and tumour growth. This process is regulated through proteins with pro- and anti-angiogenic functions and usually there is a balance between these angiogenic factors. However, in pathological angiogenesis, which is the case of tumour angiogenesis, there is a shift in this balance and the expression of pro-angiogenic factors is upregulated (Srinivasan et al., 2015).

GBM is one of the most vascularized tumours with a high level of pro-angiogenic factors and, as previously mentioned, it is characterized by high levels of microvascular hyperplasia near hypoxic regions (Kaur et al., 2004; Monteiro et al., 2017).

As mentioned before, the deficient oxygen distribution throughout the tumour due to an accelerated metabolism and tumour proliferation leads to the generation of new blood vessels. Hypoxia is considered the main promotor of tumour angiogenesis. Under hypoxic conditions, HIF promotes the transcription of several angiogenic factors including VEGF, PDGF and Angiopoietin-2 (Ang-2) (Schito, 2019).

VEGF is a pro-angiogenic factor that is secreted by cancer cells under hypoxic conditions and that acts in endothelial cells, by binding to VEGFR-1 and -2, stimulating them to proliferate. In order to provide support for the new vessels, endothelial cells secrete another pro-angiogenic factor, PDGF that acts in the pericytes and stimulates their proliferation through PDGFR binding (Figure 1.15) (Alberts et al., 2015; Arvelo et al., 2016).

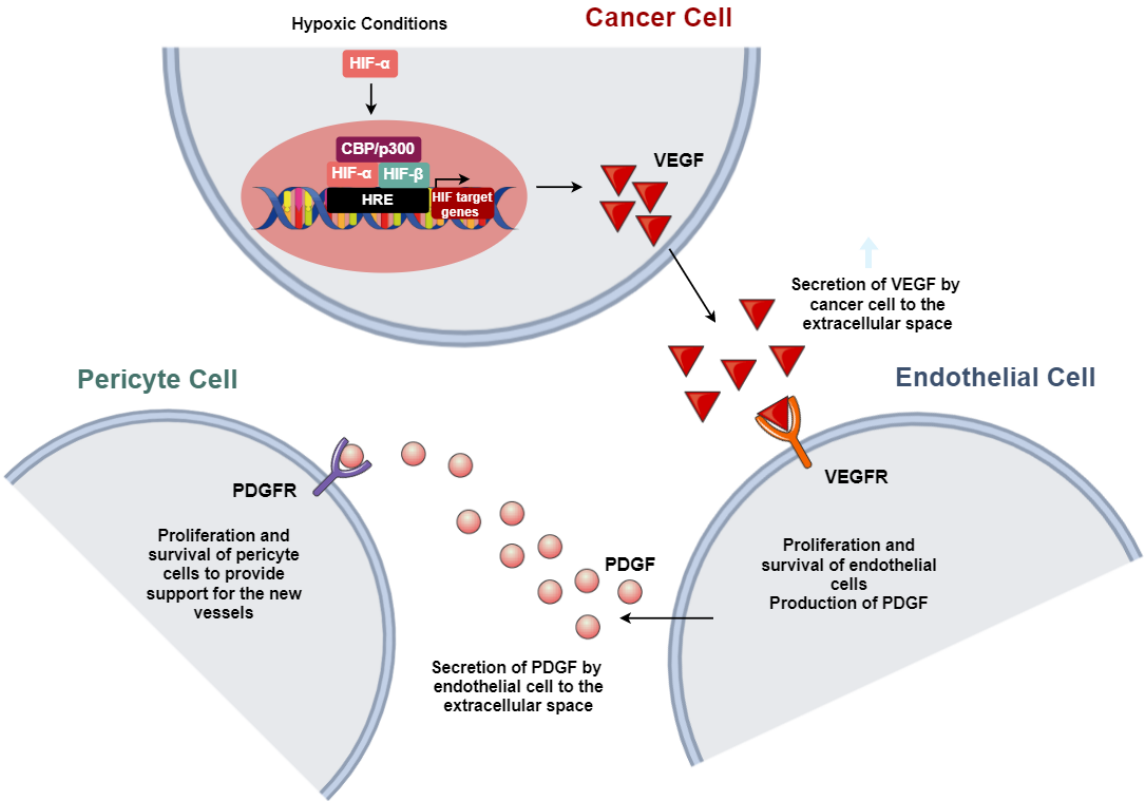

Figure 1.15 – Hypoxia promotes angiogenesis by activating endothelial and pericyte cells proliferation.
When in hypoxic conditions, cancer cells release pro-angiogenic factors to the extracellular space, such as VEGF, that binds to VEGFR in endothelial cells stimulating them to proliferate and produce PDGF. PDGF is released to the extracellular space and bind PDGFR in pericyte cells stimulating their proliferation to provide support for the new vessels. Both endothelial and pericyte cells are needed to form new vessels. Figure adapted from Buddhini, 2013.

In GBM, VEGFR-1 and -2 are upregulated in endothelial cells when compared with endothelial cells of normal brain. Also, in hypoxic regions of GBM, the concentration of VEGF is 200-300-fold higher than in serum (Kaur et al., 2004; Takano et al., 1996). VEGF is a Vascular Permeability Factor (VPF) and its overexpression leads to dilated vessels, and leaky and permeable vasculature (Dvorak, 2002; Mahase et al., 2017; Walsh et al., 2014). VEGF also stimulates Endothelial NOS (Nitric Oxide Synthase) (eNOS) increasing the production of Nitric Oxide (NO) which leads to vasodilation (Shibuya, 2013). This defective and leaky vasculature leads to abnormal blood flow and consequent heterogenous oxygen distribution. Their abnormal pericyte and EC coverage also facilitates the intravasation of tumour cells into the bloodstream (Jain et al., 2007; Mahase et al., 2017; Walsh et al., 2014).

Amplification of EGFR upregulates VEGF by increasing the levels of HIF-1α through a PI3K-dependent pathway. This might also support the high level of angiogenesis and vascularization in GBM (Clarke et al., 2001; Kaur et al., 2004).

Aside from hypoxia, VEGF expression and glioma angiogenesis can also be affected by genetic alterations. As previously mentioned, GBM frequently has loss of *PTEN*. The loss of *PTEN* function activates the PI3K pathway and lead to the upregulation of VEGF contributing to angiogenesis (Kaur et al., 2004).

Angiopoietins -1 and -2 (Ang-1 and -2) also play important roles in the process of angiogenesis. Ang-1 binds to Tie2 receptor activating it ensuring vasculature stabilization and integrity (non-leaky vasculature). Ang-2 acts as a Tie2 agonist by binding to it, inhibiting its phosphorylation by Ang-1. In VEGF absence, Ang-2 works as an anti-angiogenic factor, and promotes EC death and blood vessel regression leading to hypoxic conditions. In hypoxic conditions, VEGF and Ang-2 expressions are increased and together promote new blood vessels sprouting and tumour angiogenesis. In VEGF presence, Ang-2 plays a role of pro-angiogenic factor. The vasculature formed is disorganized and abnormal due to Ang-1 inhibition by Ang-2 (Eklund & Saharinen, 2013; Z. Huang & Bao, 2004; Kaur et al., 2004).

Placenta Growth Factor (PlGF) is a member of the VEGF family. PlGF homodimers bind to VEGFR-1 however, it can form a heterodimer with VEGF and bind to heterodimeric VEGFR-1/VEGFR-2 (Kaur et al., 2004). It is a pro-angiogenic factor and is also shown to be upregulated in GBM cells under hypoxic conditions and in hypervacularized brain tumours (Kaur et al., 2004; Nomura et al., 1998).

The tumour microenvironment also contributes to the process of angiogenesis. The Extracellular Matrix is present in all tissues and organs and provides biochemical and structural support for its cellular components. It is responsible for cell-cell communication, adhesion, cell movement and proliferation. It is composed mainly of collagen, proteoglycans, fibronectin and laminin. The ECM activates signalling pathways and has an important role in tumour progression. It not only influences tumour growth but also its response to therapy (Frantz et al., 2010; Walker et al., 2018). CAFs are found in connective tissue that elaborates ECM components and basal membrane. They produce growth factors, cytokines and chemokines and release CXC-chemokine ligand 12 (CXCL12) and Fibroblast Growth Factor Receptor-2

(FGFR-2) that stimulates angiogenesis through the recruitment of endothelial cells. They also secrete CXC-chemokine ligand 1 (CXCL1) and CXC-chemokine ligand 2 (CXCL2) that recruits tumour-associated macrophages. They are associated with angiogenesis by releasing pro-angiogenic factors such as VEGF (Arvelo et al., 2016; Riabov et al., 2014).

1.3.3. Invasion

As mentioned before, cancer cells can gain mobility and invade other tissues. For invasion to occur, cancer cells and their microenvironment release factors that help them through this process. At the time that angiogenesis occurs, factors that degrade and modify the extracellular matrix are released. The microenvironment regulates tumour invasion by secreting cytokines and chemokines and by secretion and activation of proteases, such as Matrix Metalloproteinases (MMPs) and plasmin. MMPs belong to the family of endopeptidases and can be divided into five subtypes according to their substrate: collagenases, stromelysins, membrane-type, gelatinases and other metalloproteinases. They play an important role in tumour invasion by degrading the ECM. MMPs are secreted in their inactive form and they are activated by serine proteases, like plasmin (Plm). Plasminogen (Pgn), the zymogen (i.e. proteolytically inactive precursor of a protease) of plasmin, is a single chain glycoprotein of 791 aminoacids that is produced in the liver and released in the bloodstream. It is cleaved by two serine proteases, urokinase-type Plasminogen Activator (uPA) and Tissue-type Plasminogen Activator (tPA), becoming plasmin. uPA and tPA cleave the Arg^{561}-Val^{562} ($Arginine^{561}$-$Valine^{562}$) peptide bond in a molecule of plasminogen resulting in the double-chain enzyme plasmin. Plasmin also promotes its own activation by converting pro-uPA into uPA. Plasmin cleaves the N-terminal pro-domain of the inactive forms of some MMPs (pro-MMPs) leading to their activation and consequently to the degradation of the ECM (Figure 1.16) (Aisina & Mukhametova, 2014; Klein et al., 2004; Schaller & Gerber, 2011; van Zijl et al., 2011).

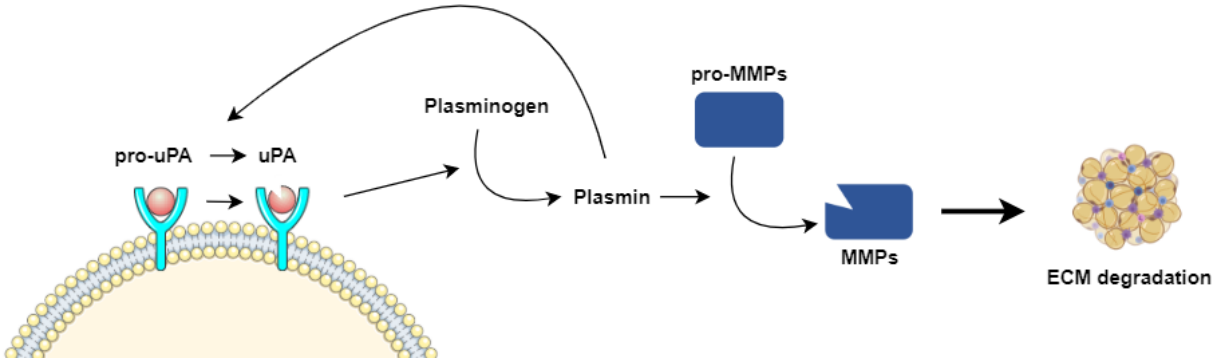

Figure 1.16 – Plasminogen-plasmin system promotes ECM degradation.
Plasminogen is cleaved by uPA becoming the enzyme Plasmin. Plasmin promotes its own expression by activating pro-uPA into uPA and activates MMPs that are essential in degrading the ECM. Figure adapted from Blasi & Carmeliet, 2002.

MMP-2 and -9 degrade type IV collagen, gelatine and fibronectin in the ECM and were shown to be upregulated by HIF-1α in GBM (Emara & Allalunis-Turner, 2014; Kaur et al., 2005). uPA/uPAR system, that is overexpressed by hypoxia, is also of great importance since it is overexpressed in GBM (Daniel J. Brat et al., 2004b; Gupta et al., 2011; Raghu et al., 2011). Both overexpression of uPA/uPAR and MMP-2 and -9 contribute to GBM invasiveness.

Cancer cells can go through a process known as Epithelial-to-Mesenchymal Transition (EMT). EMT can be classified into three different subtypes: EMT during embryogenesis and organ development; EMT associated with tissue regeneration and organ fibrosis, and EMT associated with tumour progression and metastasis. Through this process, epithelial cells can change their epithelial phenotype to mesenchymal and acquire invasive and motile properties. This usually occurs through signals they receive from the microenvironment. Cells that once had cell-cell adhesion become individualized, their polarity changes from apical-basal to front-rear, their cytoskeletal organization is rearranged, and they express mesenchymal markers. (Derynck & Weinberg, 2019; Kalluri & Weinberg, 2009).

Hypoxia is known to promote EMT through the activation of several pathways and proteins. Protein for immunoglobulin kappa J (CBF1) is highly expressed in GBM pseudopalisades and hypoxic areas. CBF1 is a transcriptional regulator of the Notch pathway that is known to induce EMT in various tumours. Zing finger E-box binding homeobox 1 (ZEB1) is also expressed in the pseudopalisades and hypoxic areas of GBM. ZEB1 regulates Roundabout Guidance Receptor 1 (ROBO1) leading to the N-

cadherin anchorage to the cytoskeleton and promotion of GBM cells migration and invasion. Twist family bHLH transcription factor 1 (TWIST1) is also induced by hypoxia and has an important role in EMT induction through activation of several pathways and proteins related to tumour progression and invasion. TWIST1 induces cell-cell and cell-substrate interactions and cytoskeleton reorganization leading to GBM cell migration and invasion. High expression of Procollagen-Lysine, 2-Oxoglutarate 5-Dioxygenase 2 (PLOD2) is related to poor overall survival and poor progression free survival in patients with GBM. PLOD2 induces Focal Adhesion Kinase (FAK) phosphorylation at residue Tyr^{397} ($Tyrosine^{397}$) which leads to an increase in focal adhesions and contributes to GBM cell migration and invasion (Monteiro et al., 2017). A study conducted by Srivastava *et al.* (2018), showed that FAT1 expression in hypoxic GBM leads to the promotion of EMT by inducing EMT markers such as Snail, Lysyl Oxidase (LOX), N-cadherin and Vimentin (C. Srivastava et al., 2018).

Other proteins have been shown to promote GBM cell migration and invasion in response to hypoxia. These are described in the table below:

Table 1.2 – List of proteins induced by hypoxia that were shown to promote GBM cell invasion.
(Monteiro et al., 2017; Proescholdt et al., 2005)

List of proteins	Biological process involved / Function	Mechanism
Carbonic Anhydrase 9 – CA IX	ECM degradation	CA IX is involved in the regulation of intercellular pH. Overexpression of CA IX leads to the acidification of the extracellular space and consequent tissue degradation and GBM cell migration and invasion (Monteiro et al., 2017; Proescholdt et al., 2005).
EGFR	ECM degradation	Hypoxia stimulates EGFRvIII (common EGFR mutation in GBM) and Integrin β3 interaction. This interaction leads to the activation of Integrin β3/SRC/FAK/EGFRvIII signalling axis and consequently to the activation of pathways intermediates (ERK, AKT and STAT3), upregulation of MMP-2 and -9 and subsequently to GBM invasion (Monteiro et al., 2017).

Integrins	ECM degradation	Integrins αvβ3 and αvβ5 are recruited to the GBM cell membrane in a hypoxic environment. They activate FAK which leads to GBM invasion promotion (Monteiro et al., 2017).
CXCR4	Chemokine receptor	CXCR4, an CXCL12 receptor, is highly expressed in GBM hypoxic areas. CXCL12 expression in hypoxic endothelial cells is induced by HIF-1α and CXCR4 overexpression leading to migration through the blood vessels (Monteiro et al., 2017).
C-C chemokine receptor type 5 – CCR5	Chemokine receptor	CCR5 is upregulated by hypoxia in GBM cells. CCR5 high expression is associated with poor overall survival and disease-free survival (Monteiro et al., 2017). Wang *et al.* (2016) demonstrated that the knockdown of *CCR5* in GBM cell lines (U87) leads to decreased invasive capability which suggests an important role in GBM invasion (Wang et al., 2016).
Cyclin G2	Cytoskeleton dynamics	Cyclin G2 is overexpressed in GBM pseudopalisades and hypoxic regions. Cyclin G2 induces cortactin to the leading edge of migrating cells promoting its phosphorylation and leading to cell ruffle formation, migration and invasion (Monteiro et al., 2017).
Tissue Factor - TF	Haemostasis	TF is usually upregulated in hypoxic GBM. TF regulates haemostasis when binding to Factor VII (FVII) and plays an important role in the regulation of blood coagulation. The migration and invasion effects of TF/FVII in GBM are mediated through the activation of Protease Activated Receptor 2 (PAR-2) and ERK signalling pathways (Monteiro et al., 2017).
Ephrin type-A receptor 2 - EphA2	Cell mobility	EphA2 activates AKT and initiates AKT-dependent EphA2 phosphorylation at residue Ser^{897} ($Serine^{897}$). This phosphorylation (P-Ser^{897}-EphA2) is necessary

		for lamellipodia formation and GBM cells invasion (Monteiro et al., 2017).
Transient Receptor Potential 6 – TRPC6	Cation channel	TRPC6 is upregulated in hypoxic GBM. TRPC6 induction leads to the activation of Calcineurin-nuclear Factor of the Activated T-cell (NFAT) pathway and consequent GBM cells invasion (Monteiro et al., 2017).

GBM invades the surrounding tissue and rarely metastasizes outside of the brain. GBM cells migrate through two types of extracellular spaces in the brain: perivascular space around the blood vessels and space between the brain parenchyma and white matter fibre tracts (Paw et al., 2015; Vollmann-Zwerenz et al., 2020).

GBM is a heterogeneous tumour that has Cancer Stem Cells (CSCs). These cells have as characteristics the capacity of self-renewal and generation of differentiated progeny and are distinguished for their constant proliferation and tumour initiation when transplanted into a host (Cheng et al., 2013; Z. Yu et al., 2012). Glioblastoma Stem Cells (GSCs) are considered one of the major causes of GBM invasiveness and relapse (Xie et al., 2014). These cells express high levels of VEGF under both normoxic and hypoxic conditions. They also express CXCL12, contributing to vasculature formation by inducing endothelial cell migration, promoting angiogenesis and further invasion. They contribute to pericyte expression since most pericytes in GBM are derived from GSCs transdifferentiation (Bao et al., 2006; Cheng et al., 2013; Folkins et al., 2009; Lathia et al., 2015).

1.3.4. Metabolic reprogramming

In 1924, Otto Warburg observed a phenomenon that was later denominated “The Warburg Effect” (Figure 1.17). Warburg observed that cancer cells, even under normoxic conditions, prefer to produce Adenosine Triphosphate (ATP) via glycolysis than via Oxidative Phosphorylation (OXPHOS). As glycolysis is a less efficient way to produce ATP (~4mol ATP/mol glucose) when compared to OXPHOS (~36 mol ATP/mol glucose), cancer cells need to uptake more glucose in order to maintain their energy needs (Heiden et al., 2009; D. Huang et al., 2014; Warburg, 1925). However,

glycolysis not only serves to produce ATP, but it also produces glycolytic intermediates that are needed in several biosynthetic pathways (e.g. lipids and nucleotides synthesis) which benefits proliferating cells. Most glucose is used for their production rather than for ATP generation. Glycolysis is faster than OXPHOS which together with its increase contributes to the fast supply of these essential precursors. This switch also avoids the unnecessary catabolic oxidation of carbon bonds into CO_2 (Hanahan & Weinberg, 2011; Heiden et al., 2009; Weinberg, 2014).

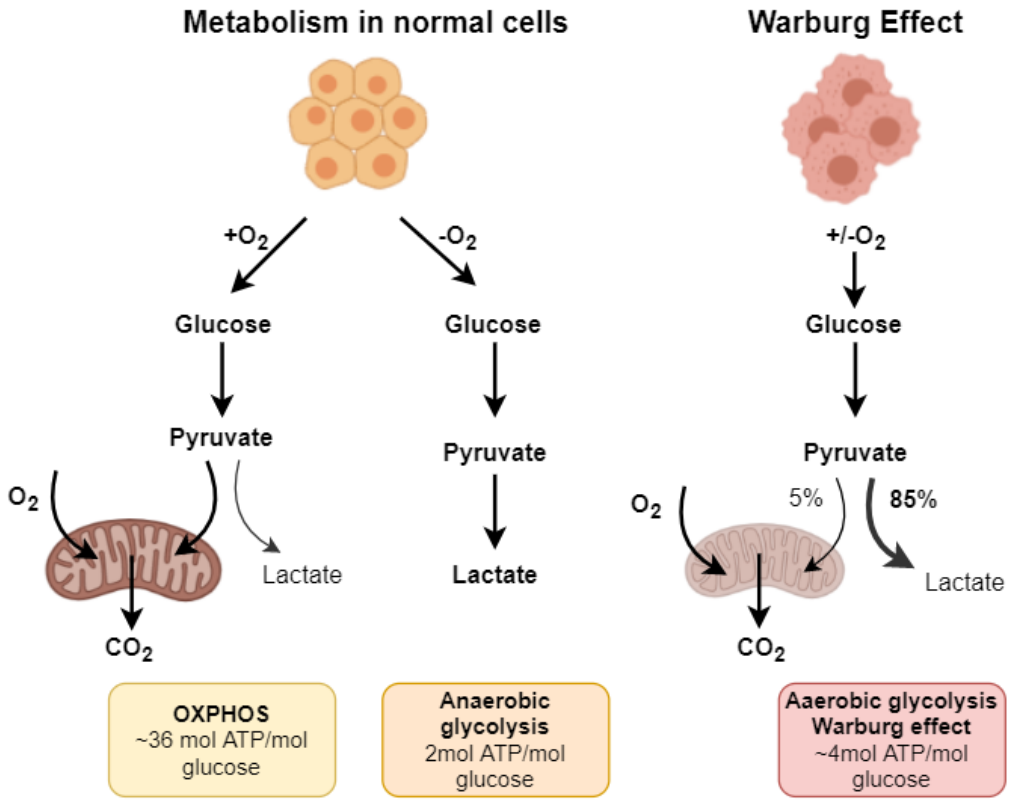

Figure 1.17 – Metabolism in normal cells vs Metabolism in cancer cells (Warburg Effect).
In normal cells, cells produce ATP mainly through oxidative phosphorylation, while in tumour cells, energy is obtained mainly through aerobic glycolysis – Warburg effect. Figure adapted from Heiden et al., 2009.

HIF-1α facilitates the Warburg Effect in GBM cells by regulating metabolic genes such as glycolytic enzymes (LDHA, Hexokinase 2 (HK2), PDK1, Aldolase, Phosphofructokinase 1 (PFK1)), Glucose Transporters 1 and 3 (GLUT1 and GLUT3),

pH regulators (CA IX and CA XII) and lactate transporters (Monocarboxylate Transporter 4 (MCT4)) (Agnihotri & Zadeh, 2016; Mahase et al., 2017).

GLUT 1 and GLUT3 are proteins that transport glucose through the plasma membrane (Werner et al., 2016). The overexpression of GLUT1 and GLUT3 guarantee sufficient glucose uptake by the cells. HK2, PFK1 and Aldolase are enzymes that are involved in different glycolysis steps (Figure 1.18). Their upregulation enhances the glucose flux (Agnihotri & Zadeh, 2016; D. Huang et al., 2014; Mahase et al., 2017; Werner et al., 2016).

MCT4, a lactate transporter, and LDHA, an enzyme that converts pyruvate in lactate (Figure 1.18), are overexpressed in GBM promoting lactate production due to hypoxia (Agnihotri & Zadeh, 2016; D. Huang et al., 2014). The increase in lactate production leads to tumour microenvironment acidification promoting local inflammation recruiting immune cells such as macrophages that in its turn secrete cytokines and growth factors driving tumour growth and invasion. Also, via MCT1, lactate can induce endothelial cell migration and tumour angiogenesis (Agnihotri & Zadeh, 2016).

CA IX and CA XII are transmembrane isoenzymes that contribute to pH regulation by CO_2 hydration ($CO_2 + H_2O \Leftrightarrow HCO_3^- + H^+$). Their overexpression makes the cytosol alkaline due to HCO_3^- production. At the same time, H^+ ions are transferred out of the cell and make the microenvironment acidic facilitating tissue degradation, GBM cell death and invasion (Amiri et al., 2016; Proescholdt et al., 2005, 2012). CA IX also contributes to lactate export by cooperating with MCTs (Pastorekova & Gillies, 2019).

HIF-1α also upregulates *PDK1*, deactivating pyruvate dehydrogenase. It prevents pyruvate oxidation and conversion into acetyl-coenzyme A and its entry into the TCA cycle and increases the amount of lactate in the cytosol (Agnihotri & Zadeh, 2016; Mahase et al., 2017). As PDK1 reduces the production of Reactive Oxygen Species (ROS) in cells, PDK1 overexpression under hypoxic stress protects the cells from ROS damage (D. Huang et al., 2014).

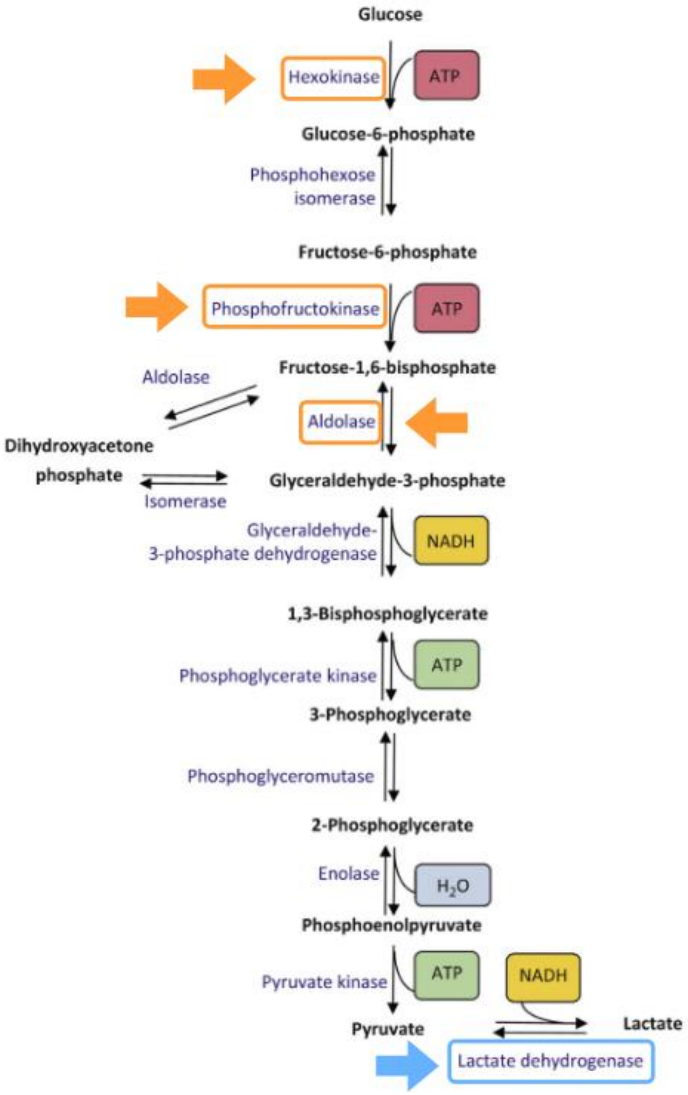

Figure 1.18 – Glycolysis steps.
Hexokinase, phosphofructokinase, aldolase and lactate dehydrogenase, highlighted in the figure, participate in different steps of glycolysis and are overexpressed in GBM due to hypoxia. Figure adapted from Werner et al., 2016.

1.4. Glioblastoma treatment

GBM is usually diagnosed in patients with a median age of 64 years old however it can occur at any age (Davis, 2016). Regardless of the multidisciplinary approaches known, GBM has a high rate of mortality and a median survival of less than 15 months after diagnosis (Davis, 2016; de Vleeschouwer, 2017). After the diagnosis, usually performed by Computer Tomography (CT) or Magnetic Resonance Imaging (MRI) scan, the current standard therapy is surgical resection of the tumour (when possible) followed by concomitant radiotherapy and chemotherapy with temozolomide (Stupp

regimen) (Davis, 2016; Stupp et al., 2005). Despite the high number of clinical trials already performed, there is no standard therapy for recurrent or progressive GBM besides palliative care, reoperation, re-irradiation and systemic and combined therapies (Davis, 2016; de Vleeschouwer, 2017).

1.4.1. Surgery

Surgery is the first approach used to treat GBM. After diagnosis, it is needed to determine if a patient is a good candidate for surgery using the Karnofsky Performance Status (KPS) scale (Table 1.3). KPS ≥70 is the minimum required for surgery to be performed although some exceptions can be made for patients with KPS <70. Even though the surgical procedure for GBM intends a maximal resection of the tumour, most times due to GBM invasiveness to other areas of the brain, especially to the eloquent cortex (i.e. speech and motor control cortex), the complete removal is not possible (Davis, 2016; Rajaratnam et al., 2020; Young et al., 2015).

Table 1.3 – Karnofsky performance status scale adapted from Young et al., 2015.

Patient status	Criteria (%)
Able to carry on normal activity and to work; no special care needed	**100%** Normal no complaints; no evidence of disease
	90% Able to carry on normal activity; minor signs or symptoms of disease
	80% Normal activity with effort; some signs or symptoms of disease
Unable to work; able to live at home and care for most personal needs; varying amount of assistance needed	**70%** Cares for self; unable to carry on normal activity or to do active work
	60% Requires occasional assistance but is able to care for most personal needs
	50%

	Requires considerable assistance and frequent medical care
Unable to care for self; requires equivalent of institutional or hospital care; disease may be progressing rapidly	**40%** Disabled; requires special care and assistance
	30% Severely disabled; hospital admission is indicated although death not imminent
	20% Very sick; hospital admission necessary; active supportive treatment necessary
	10% Moribund; fatal processes progressing rapidly
	0% Dead

Distinguish between non-neoplastic brain and tumour tissue during surgery is challenging. The use of fluorescent dyes (e.g. 5-Aminolevulinic Acid (5-ALA)), functional MRI (fMRI) and intraoperative MRI (iMRI) are techniques used to overcome this issue (Davis, 2016; Rajaratnam et al., 2020; Young et al., 2015).

When the tumour is located in an inoperable area of the brain or when the patient suffers of multiple comorbidities that do not allow them to tolerate surgery, a biopsy of the tissue is performed. The biopsy allows the removal of a small tissue specimen for pathological diagnosis with minimal invasiveness (Young et al., 2015).

Surgical approach must be evaluated for each patient individually in order to maximize the quality of life and survival, minimize morbidity and maintain pre-operative KPS (Young et al., 2015).

1.4.2. Radiotherapy and Chemotherapy

After surgery, GBM patients are subjected to radiotherapy and chemotherapy. Radiotherapy plays an important role in GBM treatment due to its possibility of relapse. The current standard radiotherapy dosage according to the Stupp regimen (Stupp et al., 2005) is a total of 60 Gy (Grays) in fractions of 2 Gy administered 5 days a week for 6 weeks. Concurrently, temozolomide (TMZ) is administrated at a dose of 75mg/m^2

daily for six weeks. After a rest period of one month, TMZ chemotherapy is restarted at a dose of 150 mg/m^2 daily for 5 days for the first month. If this dose is tolerated, it can be increased up to 200 mg/m^2 for 5 days per month. TMZ is administrated for 6 months after radiotherapy but many physicians continue TMZ administration for 12-18 months even though it is not proved to improve survival (Davis, 2016; Rajaratnam et al., 2020; Stupp et al., 2005).

Temozolomide is a DNA alkylating agent that forms methyl-triazene-1-yl)-imidazole-4-carboxamide (MTIC), that methylates the 6-OH on guanine residues. This results in DNA double-strand breaks and apoptosis due to guanine mispair with thymine (Anjum et al., 2017; de Vleeschouwer, 2017; Rajaratnam et al., 2020). *MGMT* gene encodes for a DNA-repair protein that removes alkyl groups from O^6 position of guanine. Its epigenetic silencing leads to diminished DNA-repair activity which is favourable for the treatment with temozolomide. The use of temozolomide combined with radiotherapy for newly diagnosed GBM with methylation of *MGMT* promoter showed survival advantage among patients when compared with radiotherapy alone (Hegi et al., 2005). Besides Temozolomide, there are two other chemotherapeutic agents approved for GBM treatment by the Food and Drug Administration (FDA) – Bevacizumab (BV) and Carmustine (BiCNU). Bevacizumab is an anti-VEGF monoclonal antibody that was approved in 2009 for recurrent GBM (Cohen et al., 2009). It is the first antiangiogenic therapy that has been approved for cancer and it binds to VEGF preventing its binding to the VEGFR and the activation of downstream pathways and subsequent angiogenesis (Rajaratnam et al., 2020). Even though it does not seem to improve patients' overall survival it has been observed to improve patients' progression-free survival (PFS) in patients with newly-diagnosed GBM (10.7 months vs 7.3 months when compared with placebo group) (Gilbert et al., 2014). Carmustine is a nitrosourea compound that was used before TMZ to treat GBM. It has cytotoxic action and has been avoided in the present due to severe side-effects (bone marrow suppression and liver and kidney toxicity) (Anjum et al., 2017; de Vleeschouwer, 2017; Rajaratnam et al., 2020). However, local therapy with Carmustine wafers (Gliadel®) in the resection cavity after surgery has been shown to improve patients' median survival in recurrent and newly diagnosed GBM (Chowdhary et al., 2015). The dosage regimens used are described in the table below (Table 1.4).

Table 1.4 – Dosage regimen of approved chemotherapeutic agents for the treatment of GBM by the FDA (Food and Drug Administration).
Adapted from Rajaratnam et al., 2020.

Chemotherapeutic Agent	Disease Type	Dosage Regimen
Temozolomide	Newly diagnosed	**Concurrent:** 75mg/m^2 daily for six weeks
		Adjuvant: rest period of 4 weeks. 1st cycle:150 mg/m^2 daily for 5 days in a 28-day cycle 2nd – 6th cycles: 150-200 mg/m^2 daily for 5 days in a 28-day cycle
Bevacizumab	Recurrent	10 mg/kg as intravenous infusion every 2 weeks (until disease progression or unacceptable toxicity)
Carmustine implant	Newly diagnosed/Recurrent	Eight 7.7 mg wafers with a total of 61.6 mg implanted intracranially

As previously mentioned, GBM progression is driven by altered signalling pathways. Targeting these pathways or/and their intermediates is an approach used in several types of cancer that needs to be adapted to GBM therapy. Several ongoing clinical trials are investigating these drugs and their effect in GBM. Some examples of published clinical trials and their targets are listed in the table below (Table 1.5) (le Rhun et al., 2019; Rajaratnam et al., 2020).

Table 1.5 – Targets and drugs used in clinical trials for GBM.
Rajaratnam et al., 2020

Target	Treatment	Clinical Trial Phase	Disease Type	Conclusion	Reference / ClinicalTrials.gov Identifier:
EGFR	Lapatinib (+TMZ+RT)	II	Primary	Requires further studies due to small number of patients	(A. Yu et al., 2017) NCT01591577
	Dacomitinib	II	Recurrent	Limited activity as a single agent	(Sepúlveda-Sánchez et al., 2017) NCT01520870
PI3K	Buparlisib	II	Recurrent	Lack of efficacy	(Wen et al., 2019) NCT01339052
mTORC1/2	Vistusertib (+TMZ)	I	Recurrent	Requires further studies with additional targeted agent	(Lapointe et al., 2019) NCT02619864
	Everolimus (+RT +TMZ vs RT + TMZ)	II	Primary	Increase of toxicity and no improvement of PFS	(Chinnaiyan et al., 2018) NCT01062399
	Temsirolimus (+sorafenib (RAF kinases inhibitor))	I / II	Recurrent	Toxicity of grade 3	(Schiff et al., 2018) NCT00329719
PDGF	Tandutinib	I / II	Recurrent	Lack of efficacy	(Batchelor et al., 2017) NCT00379080
MET	Onartuzumab (+bevacizumab vs placebo + bevacizumab)	II	Recurrent	No evidence of clinical benefit	(T. Cloughesy et al., 2017) NCT01632228
CDK4/6	Palbociclib	II	Recurrent	Not effective as a single agent	(Taylor et al., 2018) NCT01227434

Most of the clinical trials published so far did not reveal promising outcomes for GBM treatment however there are 450* new ongoing clinical trials at different stages of development that may prove to be encouraging in the future (Rajaratnam et al., 2020). *data acquired from clinicaltrials.gov on 04/09/2020.

1.4.3. New Therapies

The therapies used in GBM treatment trigger side effects like nausea, hair loss and weakening of the immune system. New therapies with fewer side effects and higher efficacy are needed in order to fight this deadly tumour. Some new strategies for the treatment of GBM have been emerging. Among them is Tumour Treating Fields (TTFields). TTFields is a technology approved by the FDA, in 2011, for the treatment of recurrent GBM, as monotherapy, and in 2015 for newly diagnosed GBM together with chemotherapy. This therapy has been approved in the form of a device named Optune that is placed on the patients' shaved scalp and creates alternating electric fields of low intensity and intermediate frequency that are delivered continuously. These fields disrupt cell division, cell cycle is arrested by interference with the mitotic spindle and apoptosis is induced without affecting non-dividing cells. This device is portable and is intended for continuous home use (Hottinger et al., 2016; Rajaratnam et al., 2020; Stupp et al., 2012, 2015). Along with TMZ, TTFields increase overall survival and progression-free survival in newly-diagnosed GBM without serious side effects other than skin irritation. Overall ITT population: median Progression-Free Survival (PFS): 7.1 months (95% CI 5.9-8.2) (TMZ + TTFields) vs 4.0 months (95% CI 3.3-5.2) (TMZ). Median Overall Survival (OS): 19.6 months (95% CI 16.6-24.4) (TMZ + TTFields) vs 16.6 months (95% CI 13.6-19.2) (TMZ) (Hottinger et al., 2016; Stupp et al., 2017; Taphoorn et al., 2018).

Another new therapy that recently emerged for GBM treatment is Laser Interstitial Thermal Therapy (LITT). LITT offers treatment when surgical resection of the tumour is not possible by destroying the cancer cells with localized high temperature. This approach has the advantage of being minimally invasive and its efficacy has been observed in recurrent GBM as an alternative to surgery (Thomas et al., 2016). Even though it has been suggested to enhance PFS of difficult access high-grade gliomas, more studies are needed to understand if LITT is a good substitute to standard surgery

(Mohammadi et al., 2014; Rajaratnam et al., 2020). In 2018, Kamath, A. *et al*. performed a study in patients with difficult access newly-diagnosed GBM and recurrent GBM. They stated that LITT is safe and showed an increase in overall survival in patients with recurrent GBM but more studies are needed for this patient's group (Kamath et al., 2018).

The interest in immunotherapy as a cancer treatment is evident since the late 1800's however, it was in the past 15 years that several advances were made. It provides promise and hope of transforming cancer therapy. Research in cancer immunotherapy has presented breakthroughs for several types of cancers (Lee Ventola, 2017). Immunotherapy approaches have also been developed for GBM treatment. These include immune checkpoint inhibitors, dendritic cell and peptide vaccines, Chimeric Antigen Receptor (CAR) T-Cell and viral therapies. The most extensively studied immunotherapy is the immune checkpoint inhibitors. The immune system relies on immune checkpoints to prevent the attack of healthy cells. Cancer cells take advantage of these checkpoints to avoid detection by the immune system. Immune checkpoint inhibitors are antibodies that target immune checkpoint proteins, so cancer cells do not take advantage of them, increasing the pre-existing anti-cancer response by the immune system. Programmed cell Death 1 (PD-1) and its ligand, Programmed Death-Ligand 1 (PD-L1), are two of the most studied immune checkpoint proteins (Tivnan et al., 2017). Berghoff, A. *et al.* (2015) showed that PD-L1 was present in most GBM samples examined considering it and its receptor (PD-1) important targets for future investigation (Berghoff et al., 2015; Vlahovic et al., 2015). Currently, there are several clinical trials ongoing using immune checkpoint inhibitors such as nivolumab (anti-PD-1), pembrolizumab (anti-PD-1), atezolizumab (anti-PD-L1), durvalumab (anti-PD-L1) and pidilizumab (anti-PD-1) for treatment of GBM (Jing Huang et al., 2017; Lim et al., 2018; Tivnan et al., 2017).

In T-Cell therapy, T cells are modified to express CARs, being later expanded and inserted in the patient. CARs can recognise Tumour Associated Antigens (TAAs), bound to the tumour cells and specifically kill them. This therapy is not approved for GBM treatment but there are some clinical trials ongoing especially targeting EGFRvIII (Bagley et al., 2018).

Viral therapy in its turn is based on the use of immunogenic oncolytic virus that are only able to replicate inside the cancer cells leading them to immunogenic cell death (ICD). During ICD, TAAs and cellular proteins known as Damage-Associated Molecular Patterns (DAMPs) are released increasing the immune response and leading to anti-tumour immunity (Aurelian, 2016; Martikainen & Essand, 2019). Some studies demonstrated good patient outcomes using oncolytic viruses, such as PVSRIPO, DNX-2401 and Toca511, in patients with recurrent GBM (T. F. Cloughesy et al., 2018; Desjardins et al., 2018; Lang et al., 2018). There is not any FDA-approved viral treatment for GBM but there are many ongoing clinical trials at different clinical stages. In most clinical trials, the virus is introduced intratumorally avoiding the action of Neutralising Antibodies (NAb) (Martikainen & Essand, 2019). Even though the BBB is disrupted in most cases of GBM, there can be regions with intact BBB that restricts the entry of the viruses when systemically administered (Sarkaria et al., 2018). At the same time, systemic delivery can be advantageous in order to reach sites that cannot be reached by intratumoural administration (Martikainen & Essand, 2019).

Therapy with Dendritic Cells (DC) has gained attention due to its ability to boost anti-tumour immunity. DCs are Antigen Presenting Cells (APCs) that take up tumour antigens presenting them to CD8+ and CD4+ T-cells via Major Histocompatibility Complex (MHC) Class I. They are extracted from the patient and presented to tumour antigens. When reintroduced into the patient, these DCs activate CD8+ and CD4+ T-cells response leading to a tumour-specific immune response and subsequent cell death (Desjardins et al., 2016; Tivnan et al., 2017). There are several ongoing phase I-III clinical trials. In 2018, Liau, L. *et al.* (2018) presented the results for the first phase III clinical trial using DCs therapy in newly-diagnosed GBM in which they state that the vaccine is safe and suggest survival benefit (mOS: 15 months (95% CI 13.2-16.8) (Stupp regimen) vs 23.1 months (95% CI 21.2-25.4) (DC-Vax-L overall ITT population) after surgery) (Liau et al., 2018; S. Srivastava et al., 2019; Stupp et al., 2005).

Lastly, peptide vaccines function in a similar way to DCs vaccines. Peptide vaccines are constituted of peptide sequences (antigens) that will trigger immune responses through APCs. APCs present the antigen via MHC and activate T-cells that proceed to target tumour cells and kill them. This type of vaccines has the advantage of being highly specific but at the same time is limited by poor immunogenicity of the peptides (Zhang et al., 2019). There are several ongoing clinical trials using peptide vaccines

especially targeting EGFRvIII (Lim et al., 2018; McGranahan et al., 2019; Sayegh et al., 2014).

The use of nanocarriers to delivery drugs has also been discussed for GBM. They emerged as a promising approach to overcome the challenge of crossing the Blood-Brain-Barrier (BBB) and to optimize drug delivery. These nanocarriers can be liposomes, dendrimers, micelles and nanoparticles (NPs). They have four main characteristics: a shell; a core that can be anionic, cationic or hydrophobic, depending of what needs to be carried; surface targeting molecules (e.g. antibodies, proteins, peptides); and the cargo (e.g. chemotherapeutics, proteins). Nanocarriers can also carry bio-cargoes, such as plasmids that code for proteins involved in apoptosis or agents to perform genetic knockout using CRISPR/cas9 or knockdown using siRNAs. (Glaser et al., 2017; Shergalis et al., 2018). One of the strategies that use nanocarriers is hyperthermic treatment. This treatment uses thermoseeds and magnetic NPs that apply heat in the area where the tumour is located. NanoTherm® (MagForce Nanotechnologies, Germany) was approved in Europe to treat GBM in combination with radiotherapy. It consists of iron oxide magnetite (Fe_3O_4) nanoparticles of 12 nm with aminosilane coating that are introduced directly into the tumour. They have an intrinsic magnetic moment that is stimulated by a magnetic field creating heat. It was demonstrated to be safe by Maier-Hauff *et al.* (2011), where the use of NanoTherm® in recurrent GBM patients together with radiotherapy showed an increase in the overall survival when compared with conventional therapies (12.6 months vs 6.2 months) (Glaser et al., 2017; Maier-Hauff et al., 2011; Shergalis et al., 2018).

1.4.4. Resistance to therapy

After initial treatment, some tumour cells can remain around the surgical cavity leading to GBM recurrence. Tumour heterogeneity is one of the main reasons why these cells survived the initial therapies and why GBM patients have such poor prognosis. The complexity of GBM became clear with the advances in genomic studies. GBM heterogeneity is caused by differences in the cell of origin and genetic and epigenetic alterations that these cells undergo. These alterations generate different types of cells, Tumour Initiating Cells (TICs) that can clonally expand and

establish heterogeneous clonal cell populations (Figure 1.19) (Osuka & van Meir, 2017).

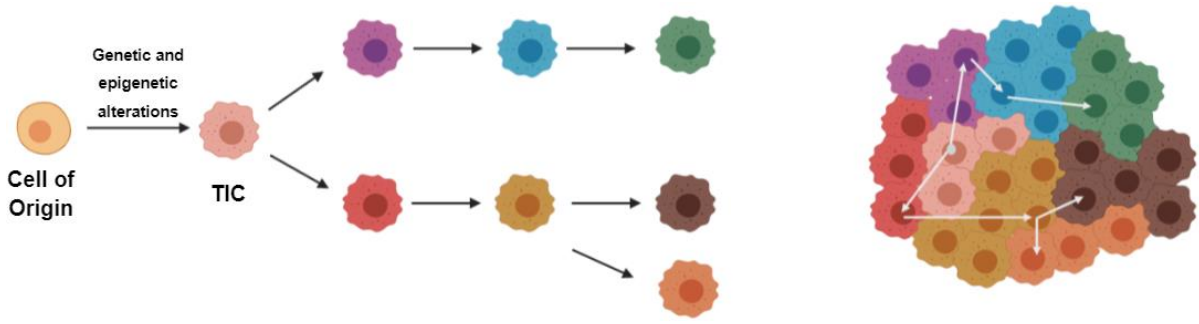

Figure 1.19 – Tumour clonal expansion.
An original cell (neural stem cell, CNS progenitor cell, mature astrocyte or neuron) is subjected to genetic and epigenetic modifications which makes it a tumour initiating cell (TIC) that can clonally expand and form a heterogeneous clonal cell population. Figure adapted from Osuka & van Meir, 2017.

GBM stem cells, as mentioned before, are considered one of the major causes of GBM relapse. They show high-level of chemo- and radio-resistance allowing them to survive to the initial GBM treatment and initiate tumour recurrence. They are an important target in the search for more efficient therapies for GBM treatment (Lathia et al., 2015; Osuka & van Meir, 2017).

Some findings have demonstrated that there is a subgroup of cells that may have derived from GSCs and that can initiate tumour recurrence. They are named Recurrence-Initiating Stem-like Cancer (RISC) cells and are more aggressive than GSCs. RISC cells have stem-like characteristic and survive the initial therapies developing innate and adaptive resistance to the treatment due to genetic and epigenetic modifications (Osuka & van Meir, 2017).

Hypoxia also influences GBM resistance and recurrence (Luo & Wang, 2019; Muz et al., 2015). Hypoxia contributes to treatment resistance by controlling several processes such as the cell cycle arrest, inhibiting apoptosis and senescence, regulating autophagy and mitochondrial activity, promoting invasion and affecting drug delivery. When in normoxic conditions, cells are vulnerable to radiation due to oxygen fixation leading to irreversible DNA damage. However, under hypoxic conditions, cells are resistant to ionizing radiation as a result of the diminished production of DNA

radicals due to low presence of oxygen (Gray et al., 1953; Hill et al., 2015; Muz et al., 2015). Also, both chemo- and radiotherapy are more efficient in rapidly proliferating cells (G2/M phase) and less efficient in cells at the end of the S phase. Consequently, slow-proliferating, quiescent and stem-cell-like cells that are localized in the most hypoxic regions of the tumour are the most resistant to treatment (Muz et al., 2015; Pawlik & Keyomarsi, 2004). The faulty vasculature created through tumour angiogenesis caused by hypoxia also confer treatment resistance, since chemotherapeutic drugs might not be able to reach the tumour site under these conditions (Muz et al., 2015).

ZEB1, as mentioned in section 1.3.3., is induced by hypoxia promoting GBM invasion. ZEB1 has been shown to promote chemoresistance to GBM treatment. Siebzehnrubl *et al.* (2013), demonstrated that ZEB1 knockdown increases sensitivity to TMZ *in vitro* and *in vivo*. It upregulates c-MYB that in its turn increases the expression of MGMT, that is related to TMZ resistance (Siebzehnrubl et al., 2013).

To conclude, the necessity for new and more effective treatment options against GBM is paramount in order to fight this deadly type of tumour and prevent its recurrence.

Previous work from my supervisor lab identified two proteins that were differentially expressed in hypoxic GBM cells compared to normoxic conditions, namely Adrenomedullin (ADM) and Transferrin Receptor 1 (TFRC). These proteins can potentially play an important role in GBM progression and therefore constitute promising molecular targets for GBM treatment in the future (Chédeville et al., 2020).

1.5. Adrenomedullin (ADM)

Adrenomedullin is a 52 amino-acids peptide hormone with an internal disulphide bond that forms a ring structure. It is synthesized as part of a longer precursor molecule of 185 residues designated preproadrenomedullin (Figure 1.20). It belongs to the Calcitonin Gene-Related Peptide (CGRP) superfamily and acts through a Calcitonin Receptor-Like Receptor (CRLR) associated with three modifying proteins (Receptor Activity Modifying Protein (RAMP) 1, RAMP2 and RAMP3). Co-expression of RAMP2 and RAMP3 with CRLR produces an ADM receptor. The interaction of ADM with its

receptor regulates vasodilatation in a direct and indirect way. The direct way activates adenyl cyclase increasing cyclic AMP (cAMP) intracellularly. The indirect way increases intracellular calcium which activates eNOS and increases the production of NO. It also increases NO production through the activation of PI3K/AKT pathway (Patel et al., 2017).

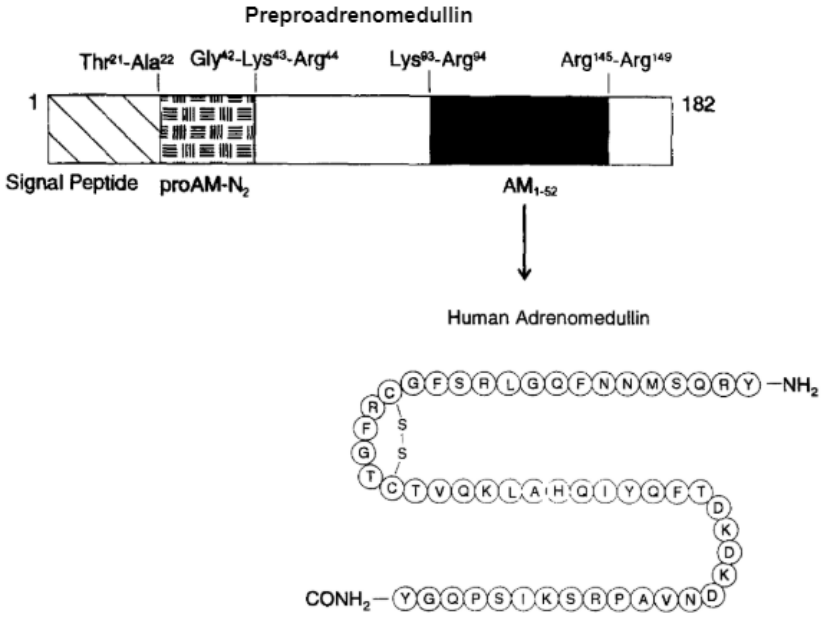

Figure 1.20 – Preproadrenomedullin and human adrenomedullin structures.
AM - ADM. Figure adapted from Schell et al., 1996.

ADM can act as a hormone or a cytokine. Under physiological conditions, it has a strong vasodilatory effect and plays an important role in angiogenesis. (Patel et al., 2017). ADM can induce angiogenic activity through the PI3K/AKT, MAPK and FAK pathways in vascular endothelial cells (W. Kim et al., 2003; Patel et al., 2017; Ribatti et al., 2005). ADM also upregulates VEGF and Basic Fibroblast Growth Factor (bFGF) through the ADM receptor and the PI3K pathway (Maki et al., 2011).

ADM is highly expressed in a large variety of tumours (e.g. breast and lung carcinomas, GBM, prostate adenocarcinoma) and plays an important role in cancer growth and tumour angiogenesis (Deville et al., 2010; Nikitenko et al., 2006).

As mentioned before hypoxia stimulates angiogenesis. Besides VEGF, hypoxia is proven to increase ADM expression (through HRE binding in the ADM gene promoter

region) and its expression is stabilized by HIF-1α. It promotes tumour angiogenesis and acts as an anti-apoptotic factor inhibiting hypoxic cell death (Deville et al., 2010; Metellus et al., 2011; Ribatti et al., 2005). It has been proposed that ADM, under hypoxic conditions, upregulates the expression of B-cell Lymphoma 2 (BCL-2), an anti-apoptotic protein, inhibiting hypoxic induced apoptosis (Oehler et al., 2001). Also, ADM-overexpressing tumour cells have been shown to express lower levels of pro-apoptotic factors (e.g. Bax, Caspase 8 and Bid) supporting ADM as a survival factor for tumour cells (Martinez et al., 2002).

ADM has been shown to be overexpressed in GBM, a highly vascularized tumour. Metellus *et al.* (2011) showed upregulation of *ADM* in GBM patient's biopsy-derived cells. *In situ* analysis showed that ADM was induced especially near the necrotic foci, in the hypoxic regions of the tumour, suggesting hypoxic regulation of ADM. U87 and U373, two commercial GBM cell lines, were exposed to hypoxic conditions and showed ADM induction. Additionally, when re-exposed to normal levels of O_2, ADM expression resumed to basal levels, confirming ADM induction by hypoxia (Metellus et al., 2011).

Moreover, recent results from our lab showed that ADM was upregulated in GBM cells under hypoxic conditions and that it is associated with substantial lower overall survival (Chédeville et al., 2020). ADM might constitute a potential target for GBM therapy and the comprehension of its role in hypoxic GBM is crucial.

1.6. Transferrin Receptor 1 (TFRC)

Transferrin Receptor 1 is a transmembrane protein that interacts with iron-loaded transferrin (TF) to mediate iron import into the cell through endocytosis (Daniels-Wells & Penichet, 2016; Johnsen et al., 2019). It consists of two identical subunits of 90 kDa linked by disulphide bonds. Each subunit can bind one TF molecule and can intake four ferric irons (Fe^{3+}) into the cell during each TFRC-mediated endocytosis cycle (Figure 1.21) (Johnsen et al., 2019). TFRC is ubiquitously expressed on the surface of most cells (Shen et al., 2018). It is expressed at a low level, however in rapidly proliferating cells it is expressed at a higher level. TFRC is abnormally overexpressed in several tumours (e.g. breast, colon, ovarian, brain cancer) contributing to cancer proliferation and progression. Its expression is also associated with poor cancer prognosis (Daniels-Wells & Penichet, 2016; Shen et al., 2018).

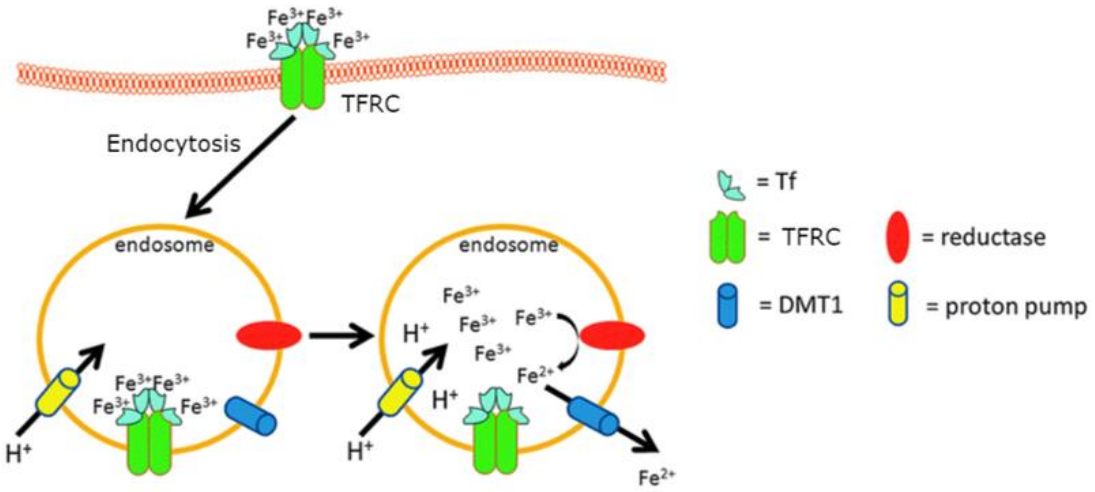

Figure 1.21 – Representation of iron uptake by TFRC.
Fe^{3+} attached to transferrin binds TFRC entering the cell by endocytosis. In the endosome, H^+ enters, there is a decrease in pH, expression of Divalent Metal Transporter 1 (DMT1) and Fe^{3+} detachment from transferrin. Fe^{3+} is reduced into Fe^{2+} and is released in the cytosol. Figure adapted from Lawen & Lane, 2013.

Iron is an essential nutrient and it is required for many biological processes such as electron transport, DNA synthesis, mitochondrial respiration and cell proliferation. However, high concentrations of intracellular iron lead to ROS formation and cell death (Jones et al., 2006; Peyssonnaux et al., 2008; Shen et al., 2018). Iron is also needed to hydroxylate HIF-α through PHD and FIH activation (Janke et al., 2013; Jones et al., 2006; Peyssonnaux et al., 2008).

Hypoxia is known to induce the transcription of the *TFRC* gene (Peyssonnaux et al., 2008; Shen et al., 2018). It has been demonstrated to be overexpressed in GBM (Daniels et al., 2006; Prior et al., 1989; Shen et al., 2018), however recent results from our lab demonstrated that TFRC was downregulated in GBM cells under hypoxic conditions (Chédeville et al., 2020). PHD and FIH need Fe^{2+} in order to be active. The downregulation of TFRC in hypoxic GBM is an interesting result. We hypothesized that the downregulation of TFRC under hypoxic conditions could be a cancer mechanism to inactive PHD and FIH, allowing HIF target genes' transcription and GBM progression.

1.7. Study objective

GBM is one of the deadliest types of cancer due to its aggressiveness, high invasiveness and resistance to treatment. It is associated with poor patient prognosis and its study and comprehension is crucial.

Hypoxia is a hallmark of GBM. It is known to contribute to GBM progression, invasiveness and chemo-resistance.

The main objective of this study is to characterize the role of ADM and TFRC proteins in hypoxic GBMs. To this end the main objective of this research work is to perform the knockout of these two genes using the CRISPR/Cas9 system in two GBM patient's biopsy-derived cell lines, UP-029 and SEBTA-023, and analyse their role under normoxic and hypoxic conditions.

2. Methodology

2.1. gRNA cloning using pSpCas9(BB)-2A-Puro (PX459) vector V2.0

In order to knockout the genes of interest, a CRISPR plasmid, pSpCas9(BB)-2A-Puro (PX459) vector V2.0 (Addgene #62988 (Appendix A – Figure A.1)), was used. This plasmid can be expressed in mammalian cells. It contains the gene that codes for Cas9 prevenient from *Streptococcus pyogenes* and genes that confer resistance to ampicillin (for selective bacterial growth) and puromycin (for growth in eukaryotic cells). This plasmid can be digested by BbsI for cloning of the gRNAs. These gRNAs were designed with overhangs that can bind the sites where BbsI cut in the plasmid (Figure 2.1). To perform the knockout of both genes (*TFRC* and *ADM*), 2 gRNAs were designed for each gene to minimize the off-target probability. The gRNAs were designed using the CRISPR Design tool available at http://tools.genome-engineering.org and confirmed using the BLAST tool (NCBI) (available at https://blast.ncbi.nlm.nih.gov/Blast.cgi) to confirm the inexistence of off-target activity.

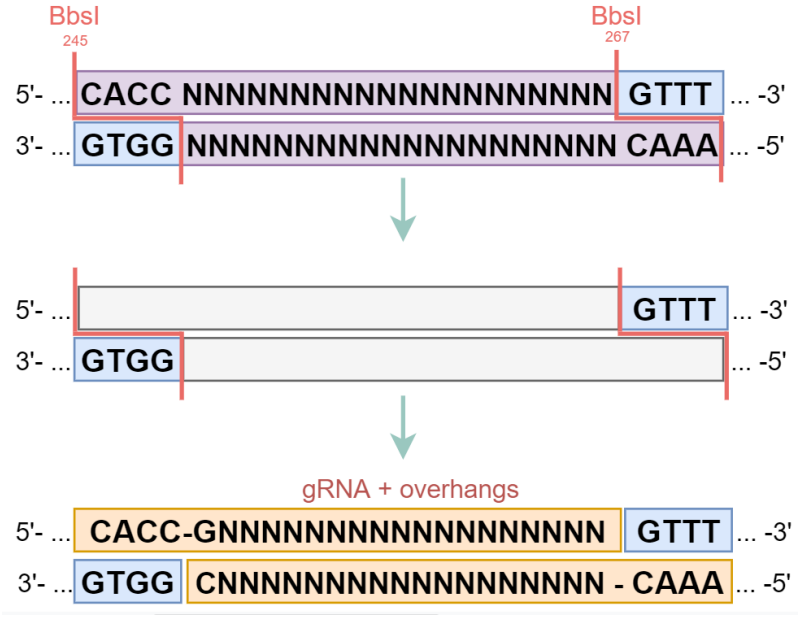

Figure 2.1 – Schematic representation of the gRNAs cloning in the PX459 plasmid. BbsI, a restriction enzyme, cuts after nucleotides 245 and 267 in the PX459 plasmid. The gRNAs are designed with complementary overhangs that bind the site where BbsI cuts in the plasmid.

2.1.1. pSpCas9(BB)-2A -Puro (PX459) vector V2.0 digestion

PX459 vector was digested with the restriction enzyme, BbsI for linearization and insertion of the gRNAs. The digestion solution contained 10 µg of PX459 plasmid (12µl), 5µl of 10X Buffer G (Thermo-Fisher Scientific), 5µl of BbsI enzyme (10U/µl) (Thermo-Fisher Scientific) and 28µl of ddH_2O. The solution was incubated at 37ºC for 8h.

2.1.2. Plasmid purification

For the PX459 linearized plasmid purification, first we performed an electrophoresis in a 0,8% agarose gel for 4h at 50V. To the samples, it was added 6µl of 10X DNA Loading Buffer (Appendix B). The mixture was loaded in the gel and ran for 4 hours at 50V. Gel Doc™ EZ Imaging System and ChemiDoc™ MP Imaging System (BIO-RAD) were used to visualize the gel.

To purify the PX459 plasmid, GenElute™ Gel Extraction Kit from SIGMA-ALDRICH and Zymogen Gel DNA Recovery Kit from Zymo Research were used. The DNA fragment of interest was excised from the gel with a clean scalpel and weighted. To 100 mg of gel, it was added a 300 µl of a Gel Solubilization Solution containing guanidine thiocyanate and incubated at 55-60ºC for 10 minutes or until the gel was dissolved (vortex for 2-3 minutes during incubation to help dissolving). To 100 mg of gel volume, 100 µl of 100% Isopropanol was added to the melted agarose. The solution was transferred to a binding column and centrifuged for 1 minute at 16000g. The flow-through liquid was discarded. 700 µl of Wash Solution was added to the column and centrifuged for 1 minute at 16000 g. The flow-through liquid was discarded and centrifuged once more at the same conditions without adding any additional Wash Solution. The column was transferred to a clean collection tube and 50 µl of Elution Buffer (containing 10mM Tris buffer pH 8.5-9) was added to the centre of the membrane and incubated for 1 minute at room temperature. After the incubation, the column was centrifuged at 16000g for 1 minute. The purified DNA was quantified using a Nanodrop Spectrophotometer and stored at -20ºC.

2.1.3. Oligonucleotides annealing

For each gRNA, we incubated a mixture containing 1µl of Forward oligo (100µM), 1µl of reverse oligo (100µM), 1µl of 10X T4 Ligation Buffer (Promega) and 7µl of ddH_2O at 37ºC for 30 minutes, followed by an incubation at 95ºC for 5 minutes letting them cool down slowly to 25ºC for oligonucleotides annealing.

2.1.4. Ligation reaction

The annealed oligonucleotides from step 2.1.3. were diluted in a ratio of 1:150 in ddH_2O. Each reaction contained 1µl of BbsI digested plasmid from step 2.1.1. (90 ng), 1µl of oligo duplex (0.5 ng), 1µl of 10X T4 Ligation Buffer (Promega), 0.5µl of T4 DNA Ligase (Promega) and 6.5 µl of ddH_2O. One reaction was performed without adding the oligo duplex (negative control). All the reactions were incubated at 16ºC for 16h.

2.1.5. Competent Bacteria

The bacterial cells used were STBL4 *E. coli*. Always working by the flame, 5 µl of STBL4 glycerol stock was inoculated into 5ml of LB (Lysogeny broth) medium and incubated at 37ºC for approximately 16 hours shaking at 200 rpm. After 16 hours, 1ml of the growth bacterial cell culture was inoculated into 100 ml of LB medium and incubated at 37ºC at 200 rpm until optical density (OD 600 nm) was 0.4. The grown culture was then incubated at 4ºC for 10 minutes followed by a centrifugation at 4000g for 10 minutes at 4ºC. The resulting pellet was resuspended with 50 ml of ice cold 100 mM calcium chloride ($CaCl_2$) solution, incubated on ice for 20 minutes and centrifuged at 4000 g for 10 minutes at 4ºC. The resulting pellet was then resuspended with 10 ml of ice cold 100 mM $CaCl_2$ and 10% of glycerol solution. 100 µl aliquots were prepared in 1.5ml tubes and stored at -80ºC.

2.1.6. Transformation of competent bacteria

To transform competent bacteria, plates with LB agar + ampicillin (100 µg/ml) were prepared. To each tube of 100 µl of STLB4 competent bacteria, 2 µl of 1.6 mM β-mercaptoethanol were added and mixed by flicking the tube. Then, 4 µl of each ligation (step 2.1.4.) were added to the tube, mixed by flicking the tube and incubated for 30

minutes on ice. After this incubation, the tubes were quickly transferred and incubated for 1 minute at 42ºC (heat shock) and then for 2 minutes on ice. 200 µl of SOC medium (Appendix B) were added to the tubes and incubated at 37ºC for 1 hour shaking at 200 rpm. Finally, the transformed STBL4 cells were plated in LB agar + ampicillin plates. One plate was plated with the negative control reaction and two other plates were plated with 5 ng and 50 ng of circular/uncut pX459 plasmid to calculate the efficacy of transformation (Figure 2.2). All plates were plated according to Figure 2.1 and incubated at 37ºC for approximately 16 hours. After this incubation, the plates were stored at 4ºC. All the procedure was performed in aseptic conditions using a Bunsen burner flame.

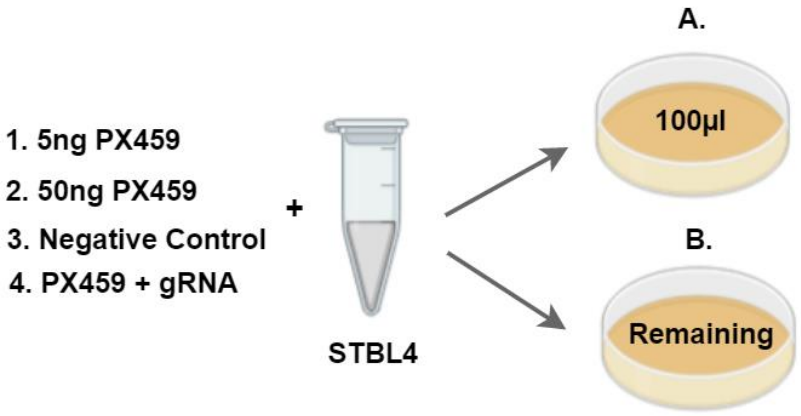

Figure 2.2 – Schematic representation of the transformation of competent bacteria step.
Each reaction was plated in two different plates: 100µl in plate A. and the remaining reaction in plate B.

2.1.7. Selection of positive clones for CRISPR

To select the clones that contain the plasmid (positive clones), a Polymerase Chain Reaction (PCR) was performed. 10 µl of NZYTaq 2x Green Master Mix, 1 µl of U6 Forward primer (10 µM) (Appendix A – Table A.1), 1 µl of gRNA Reverse primer (10 µM) for each gRNA and 8 µl of ddH_2O were added to a 0.2 ml PCR tube. The colonies in the LB agar + ampicillin plates were picked with a yellow pipette tip and dipped in the tubes with the PCR mix. One of the tubes was used as negative control and contained the PCR mix and empty plasmid. The reactions were then submitted to the following PCR conditions:

1) Initial denaturation step - 95ºC for 5 minutes; 2) Denaturation step - 95ºC for 30 seconds; 3) Annealing step - 56ºC for 30 seconds; 4) Amplification step - 72ºC for 30 seconds; 5) Go to step 2) 30 times and 6) Final amplification step- 72ºC for 10 minutes. (Applied biosystems veriti thermal cycler – ThermoFisher).

The PCR products were then subjected to an electrophoresis in a 1.5% agarose gel. 3 µl of the EZ 1kB DNA ladder (BIO-RAD) (Appendix C – Figure C.1) was loaded in the first well and 15 µl of each PCR product in the following wells. The run was performed at 120V for 30 minutes. Gel Doc™ EZ Imaging System and ChemiDoc™ MP Imaging System (BIO-RAD) were used to visualize the gel.

2.1.8. DNA extraction

15 ml tubes were prepared with 3 ml of LB medium containing 100 µg/ml of ampicillin. The yellow pipette tips used to pick the colonies were discarded into the tubes after being dipped in the PCR mixture (step 2.1.7.) and the tubes were incubated at 37ºC for approximately 16 hours, shaking at 200 rpm. After visualisation and analysis of the PCR products, 1.5 ml of the bacterial growth containing positive clones were transferred from the 15ml tubes to 1.5 ml Eppendorf tubes to extract plasmid DNA. This procedure was performed under aseptic conditions using a Bunsen burner flame.

100 µl of 100% glycerol and 400µl of bacterial growth containing positive clones was transferred to 1.5 ml Eppendorf tubes to make glycerol stocks. The tubes were stored at -80ºC.

2.1.8.1. DNA miniprep

Plasmid DNA was extracted from the bacterial growth using E.Z.N.A.® Plasmid DNA Mini Kit II (OMEGA Bio-Tek) and QIAprep Spin Miniprep Kit (QIAGEN). Tubes with bacterial growth containing positive clones were centrifuged at 10000 g for 3 minutes at room temperature. The supernatant was discarded, and the pellet was resuspended in 250 µl of Solution I which contains RNase and transferred to a clean 1.5 ml Eppendorf tube. 250 µl of Solution II (cell lysis solution) was added and mixed thoroughly by inverting the tube 4–6 times until the mixture becomes clear. When clear,

350 µl of Solution III was added to the mixture and the tube was immediately inverted 4-6 times until a flocculent precipitate is formed. The solution was centrifuged at 13000 g for 10 minutes. The supernatant was pipetted into a kit binding column and centrifuged at 13000 g for 1 minute. The flow-through liquid was discarded, 500 µl of Solution HBC containing guanidine hydrochloride was added and centrifuged for 1 minute at 13000 g. The flow-through liquid was discarded and 700 µl of Wash Buffer was added to the column and centrifuged again for 1 minute at 13000 g. The flow-through liquid was discarded, and another centrifugation was performed under the same conditions without adding any additional Wash Buffer. The column was placed in a new 1.5 ml Eppendorf tube. To elute the DNA, 50 µl of ddH_2O-MiliQ was added to the centre of the column and incubated for 1 minute at room temperature. After the incubation, a centrifugation was performed at 12000g for 1 minute. The DNA extracted was quantified using a Nanodrop Spectrophotometer and stored at -20ºC.

2.1.8.2. DNA midiprep

100 ml of LB broth and 100 µl of ampicillin (100 mg/ml) were added to a 500 ml Erlenmeyer flask. With a yellow pipette tip, a scratch of the glycerol stock was pipetted into the Erlenmeyer flasks and incubated at 37ºC for approximately 16 hours shaking at 200 rpm.

The plasmid DNA was extracted using E.Z.N.A.® Plasmid DNA Midi Kit (OMEGA Bio-Tek) and PureYield™ Plasmid Midiprep System (Promega). 50 ml of bacterial growth containing positive clones was centrifuged at 5000 g for 15 minutes at room temperature. The supernatant was discarded and the pellet was resuspended in 3 ml of Solution I containing RNase. 3 ml of Solution II (cell lysis solution) was added to the tube, mixed gently by inverting the tube 3-5 times and incubated for 3 minutes at room temperature. After the incubation, 3 ml of Solution III (salting out) was added and mixed gently by inverting the tube 3-5 times. The mixture was incubated for 3 minutes until a white flocculent precipitate was formed and centrifuged at 4000g for 40 minutes. 3.5 ml of the supernatant was transferred to a kit binding column and centrifuged at 4000 g for 3 minutes. The flow-through liquid was discarded and this step was repeated until all the supernatant has been transferred to the column. 3.5 ml of HBC buffer containing guanidine hydrochloride was added to the column and centrifuged at 4000 g for 3

minutes. The flow-through liquid was discarded, 3.5 ml of Wash Buffer was added and centrifuged at the same conditions. This step was repeated and followed by a centrifugation at 4000 g for 10 minutes without adding any additional Wash Buffer. The columns were transferred to a 15 ml nuclease-free tube and 500 µl of ddH_2O-MiliQ was added to elute the DNA. It was incubated at room temperature for 3 minutes and centrifuged at 4000 g for 5 minutes. After elution, the DNA extracted was quantified using a Nanodrop Spectrophotometer and stored at -20ºC.

2.1.9. Sequencing

The plasmid DNA was prepared for sequencing according to the instructions of the Sequencing Company. Sequencing was performed by NZYTech (Portugal) and TubeSeq Service by Eurofins Genomics (Germany).

Table 2.1 – List of plasmids obtained after cloning.

Gene	Plasmids
TFRC	TFRC gRNA1-PX459
	TFRC gRNA2-PX459
ADM	ADM gRNA1-PX459
	ADM gRNA2-PX459

2.2. Cell Lines and Cell Culture

The cell lines used, UP-029 and SEBTA-023, were obtained from patients with GBM provided to the Brain Tumour Research Centre, University of Portsmouth. The cell lines had the following molecular characteristics:

-UP-029: methylated MGMT promoter, IDH1 wild-type. The patient was 66 years old at the time of diagnosis.

-SEBTA-023: methylated MGMT promoter, IDH1 wild-type, GFAP+; no 1p19q deletion. The patient was 70 years old at the time of diagnosis.

2.2.1. Ethical Statement

Human adult glioblastoma biopsy-derived primary cell cultures: UP-029 and SEBTA-023 were obtained from patients from King's College Hospital, London, under ethics permission (REC reference number: 11/SC/0048, 29 August 2018).

2.2.2. Cell Culture

Both cell lines (UP-029 and SEBTA-023) were maintained and cultured at the University of Portsmouth in a high glucose (4500 mg/l) Dulbecco's modified Eagle's medium (DMEM) (Gibco-ThermoFisher) supplemented with 10% Fetal Bovine Serum (FBS). They were grown in a humidified incubator at 37ºC with a 5% CO_2 atmosphere and tested regularly for mycoplasma presence. All the cells used tested negative for mycoplasma presence in the several tests performed.

Cell stocks of UP-029 and SEBTA-023 cells were taken out of the liquid nitrogen container and left to thaw in a water bath at 37ºC. After thawing, they were plated in 75 cm^2 flasks with 11 ml of DMEM medium. After 24 hours, the cell medium was replaced for fresh medium.

2.2.2.1. Cell passage and plates preparation

To passage cells, the medium was aspirated from the flask, followed by washing the cells with 3 ml of Hanks' Balanced Salt Solution (HBSS) (Gibco-ThermoFisher). To detach the cells, 3 ml of TrypLE Express (Gibco-ThermoFisher) were added to the flask that was further incubated for 2 minutes in a humidified incubator at 37ºC, 5% CO_2. After observing at the microscope that the detachment was complete, the cell suspension was transferred to a 15 ml tube with 5 ml of DMEM medium and centrifuged for 5 minutes at 1000 g at room temperature. The resultant cell pellet was resuspended in 5ml of DMEM medium. 0.5 ml of the cell suspension were transferred to a new 75 cm^2 flask containing 11.5 ml of DMEM medium.

2.2.2.2. Cells transfection

In order to count the number of cells in suspension, a Countess II FL Automated cell counter (ThermoFisher) was used. 10 µl of the cell suspension was mixed with 10 µl of Trypan Blue stain 0.4% (Invitrogen) and 10 µl of this solution was transferred into a cell counter chamber using a p20 pipette. The counter chamber was introduced into the Countess II FL Automated cell counter and the number of live cells was obtained. 100 mm plates were plated with $1x10^6$ - $2x10^6$ cells, the number of cells required to transfect the next day, in 10ml of DMEM medium.

Cell transfection was performed using the jetPRIME® transfection reagent (Polyplus-transfection™). jetPRIME® is suitable for genome editing using CRISPR/Cas9 technology by transient transfection. jetPRIME reagent, a cationic polymer-based reagent, has strong interaction with the nucleic acids forming a complex with the DNA. This complex enters the cells easily by endocytosis by binding the anionic cell-surface proteoglycans. The plasmid DNA is released from the endosome via a proton sponge-mechanism (osmotic rupture) and can be imported to the nucleus. This import takes place when the nuclear envelope disappears during mitosis (https://www.polyplus-transfection.com/resources/product-literature/).

For an optimal transfection, a cell confluence of 60-80% is required. The transfection was performed according to the guidelines described in the table below (Table 2.2) with a 1:2 DNA to jetPRIME® reagent ratio (w/v).

Table 2.2 – Guidelines for transfection with jetPRIME® transfection reagent (Polyplus-transfection™).

Culture Vessel	Volume of jetPRIME® buffer (µl)	Amount of DNA (µg)	Volume of jetPRIME® reagent (µl)
100mm plate	500	5-15	10-45

500 µl of jetPRIME® buffer were added to 1.5 ml Eppendorf tubes, followed by 7 µg of each plasmid DNA (TFRC gRNA1, TFRC gRNA2, ADM gRNA1 and ADM gRNA2). The mixture was vortexed and spin down. 15 µl of jetPRIME® reagent were

added to the mixture, vortexed and spin down. The reactions were incubated at room temperature for 10 minutes and added to the cells (UP-029 and SEBTA-023) by mixing slowly. Negative control was performed using cells form each cell line that were not transfected. All the plates were incubated in a humidified incubator at 37ºC with a 5% CO_2 atmosphere.

24 hours later, the medium was removed and replaced with fresh DMEM medium. 6 µl of puromycin (3 µg/ml) were added to the cells and incubated for 48 hours in a humidified incubator at 37ºC with a 5% CO_2 atmosphere. 48 hours later, the medium was removed and replaced with fresh DMEM medium.

2.2.2.3. Isolation of clonal cell lines

With the aim of making single cell KO clones, the transfected cells were serially diluted. First, the cells were washed, detached and centrifuged as mentioned in 2.2.2.1.. After counting the number of live cells in the cell suspension, the volume needed to have 800 cells was calculated and transferred to Tube 1 together with 12ml of DMEM medium. From Tube 1, 1ml was transferred to Tube 2 with 9 ml of DMEM medium (1:10 dilution giving rise to 80 cells). From Tube 1, 100 µl were pipetted into each well of a 96-wells plate (Plate A) and from Tube 2, 100 µl were pipetted into each well of a 96-wells plate (Plate B) being Plate B a dilution of Plate A (1:10) (Figure 2.3). All the plates were incubated in a humidified incubator at 37ºC with a 5% CO_2 atmosphere. After confluency, the cells were passed to 12-wells, 6-wells and 60 mm plates.

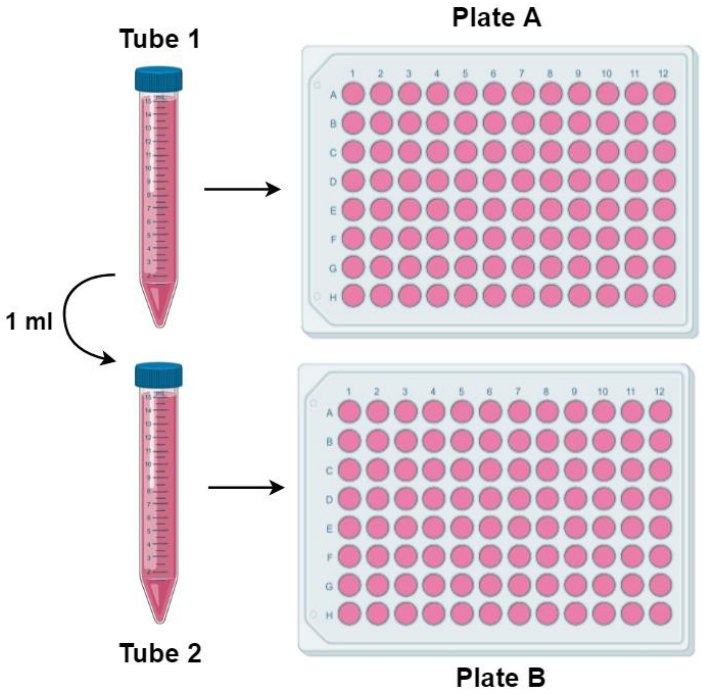

Figure 2.3. - Schematic representation of the isolation of clonal cells step.

2.2.2.4. Hypoxia

For hypoxia experiments, cells were exposed to hypoxic conditions in a humidified incubator with O_2 levels regulated to 1% and 5% CO_2 during different exposure times. In 60 mm plates, UP-029 cells were exposed to hypoxia conditions for 24 and 48 hours. SEBTA-023 cells were exposed for 6 and 24 hours of hypoxia.

2.3. Western-Blotting

2.3.1. Cell lysates and BCA assay

In order to obtain lysates containing all proteins from the cells, the medium from each 60 mm plate was discarded followed by washing the cells with 1 ml of Phosphate-buffered saline (PBS) and removing it thereafter. 60-100µl of Lysis Buffer (Appendix B) were added to each plate followed by scrapping to lyse the cells. The cell lysates were transferred to 1.5 ml tubes, incubated on ice for 10 minutes and centrifuged at 15000 g for 15 minutes at 4ºC. After the centrifugation, the supernatants were transferred to new 1.5 ml tubes and stored at -80ºC.

Before running the gels, the protein concentration in each sample was determined using the Pierce™ Bicinchoninic Acid (BCA) Protein Assay Kit (Thermo-Fisher) according to the manufacturer's instructions. The BCA assay is based on the biuret reaction which consists of the reduction of Cu^{2+} to Cu^{+} by protein in an alkaline medium. This allows the highly sensitive detection of the cuprous cation Cu^{+} by BCA. When BCA reacts with Cu+, a purple coloured complex is formed and a strong linear absorbance at 562 nm is exhibited which is directly proportional to protein concentration (Wilson & Walker, 2010).

The samples were prepared in 96-wells plates. 200µl of BCA Reagent (50:1: Reagent A : Reagent B, Pierce) were added to each well from rows A and B (Figure 2.4). A linear calibration curve was established with a range of BSA amounts between 2-20 µg using Bovine Serum Albumin (BSA) (2 µg/µl) and added in row A. Four µl of each sample, Non-treated (NT) and treated at different time points (TP), were added in row B according to Figure 2.3.

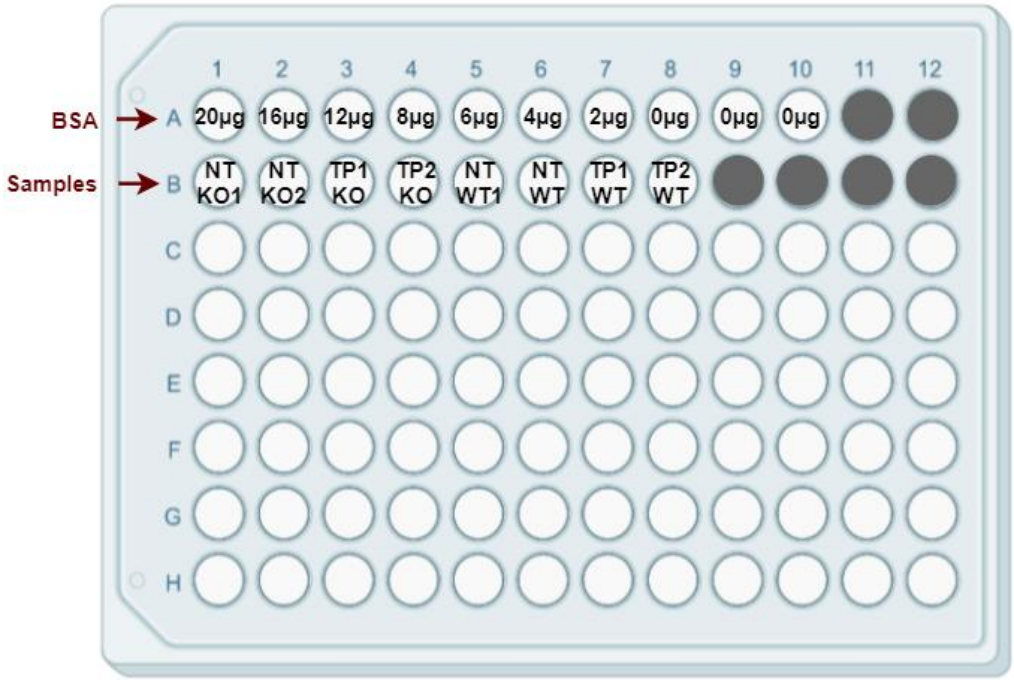

Figure 2.4 – Schematic representation of the 96-wells plate used in the BCA assay and the solutions added.
NT – Non-treated; **TP –** Time Point; **KO –** Knockout; **WT –** Wild-type

The plate was then incubated at 37ºC for 30 minutes and analysed after that using Polar Optima Omega plate reader (BMG Labtech).

2.3.2. Western Blotting

Western-blotting is a technique that is broadly used in molecular biology. It allows the identification of proteins by separating them by their molecular weight in an acrylamide gel through applying an electric current. First, the proteins are submitted to a Sodium Dodecyl Sulfate – Polyacrylamide Gel Electrophoresis (SDS-PAGE). The proteins mixture is boiled in β-mercaptoethanol and Sodium Dodecyl Sulfate (SDS). β-mercaptoethanol breaks proteins' disulphide bridges while SDS, an anionic detergent, binds and denatures them. SDS molecules surround the proteins giving them negative charge which allows them to migrate towards the positive electrode (anode).

The electrophoresis gel is divided in two different gels: stacking and running gel. The stacking gel in comparison with the running gel is prepared with a pH 6.8 buffer (running gel – pH 8.8 buffer) and has a lower concentration of acrylamide:bisacrylamide. The stacking gel is used to concentrate the proteins in a sharp band before reaching the running gel, so they can start migrating at the same time. This happens due to the differences in ionic strength and pH between the running buffer and the stacking gel. The running buffer (pH=8.3) has a higher pH than the stacking gel (pH=6.8), so glycine ions (pI=5.97) (from the running buffer) that are negatively charged (pH>pI) become neutrally charged (pH≈pI) and migrate slower than the SDS-protein complexes. Chloride ions (Cl^-) (from Tris-HCl) migrate faster than both the SDS-protein complexes and glycine ions in this order: Cl^- ions > SDS-protein complexes > Glycine ions. The SDS-proteins complexes stay between the glycine ions and Cl^- ions, forming a concentrated sharp band. As the running gel has a higher pH (pH=8.8) than the stacking gel (pH=6.8), the glycinate ions present in the mixture that were once concentrated with the protein-SDS complex, become negatively charged and migrate faster than the SDS-protein complex together with the Cl^- ions, leaving them to migrate at their own rate according to their molecular weight. As proteins have different sizes, smaller proteins migrate faster and more easily through the pores than larger proteins. After the run, the proteins were transferred to a nitrocellulose

membrane and detected using specific antibodies that bind to the protein of interest (Nelson & Cox, 2013; Wilson & Walker, 2010; Yang & Mahmood, 2012).

After protein quantification using the BCA assay, the proteins were prepared to load into the SDS-PAGE gel. Loading fractions containing 50 µg/40 µl of protein in 1X Protein Loading Buffer (Appendix B) were denatured by heating at 99ºC. The gel was cast in a BIO-RAD Mini-PROTEAN Tetra Cell Casting Module and it was constituted by two gels with different characteristics: stacking and running gel (Table 2.3). The more acrylamide:bisacrylamide the tighter the pores in the gel, so the running gel was made according to the size of the protein of interest – 7% and 10% (Table 2.3). 3 µl of the molecular weight marker Precision Plus Protein All Blue Standards (BIO-RAD) (Appendix C – Figure C.2) and 18 µl of each sample were loaded in the gel wells. The gels were submerged in 1X Running Buffer (Appendix B) and ran at an initial voltage of 110V until the proteins reach the running gel and 130V afterwards for approximately 80 minutes.

Table 2.3. – Composition of running and staking gels used for Western-blotting.

Running Gels			**Stacking Gel**	
	7%	**10%**		**1 Gel**
1M Tris pH 8.8	3ml	3ml	**1M Tris pH 6.8**	312.5µl
30% acrylamide:bisacrylamide	1.9ml	2.7ml	**30% acrylamide:bisacrylamide**	550µl
H_2O	3ml	2.2ml	**H_2O**	2.3ml
10% SDS	80µl	80µl	**10% SDS**	25µl
25% APS	32µl	32µl	**25% APS**	12.5µl
TEMED	12µl	12µl	**TEMED**	7.5µl

After electrophoresis, the proteins were transferred onto a nitrocellulose membrane using an electric field according to the sandwich method. This allows the proteins to move out of the gel and onto the membrane (Yang & Mahmood, 2012). The gel was placed in a gel holder on top of a sponge and a filter, followed by the nitrocellulose membrane and another filter and sponge. The gel holder was then emerged in 1X Transfer Buffer (Appendix B) together with 2 ice packs in a Mini Trans-Blot®

Electrophoretic Transfer Cell (BIO-RAD) and the transfer was performed at 110V for 1 hour.

The membranes were blocked with Odyssey® Blocking Buffer (LI-COR) for at least 30 minutes at room temperature with shaking on a plate mixer to prevent non-specific antibody binding to the membrane. After 30 minutes, the blocking buffer was removed, and the membranes were incubated with a primary antibody overnight (approximately 16 hours) at 4ºC with shaking. The primary antibody (Table 2.4) was removed and the membranes were washed 5 times for 5 minutes each with 1X Tris-Buffered Saline - Tween (TBS-T) (Appendix B). The 1X TBS-T solution was removed, and the membranes were incubated with the secondary antibody (Table 2.4) for 1 hour at room temperature with shaking in a plate mixer. The membranes were washed again with TBS-T under the same conditions and visualised using the Odyssey® CLx Imaging System (LI-COR). The images were further analysed using the Image Studio Lite software (LI-COR).

The antibodies used were diluted in 1X TBS-T. Primary Antibody – 1:500 dilution; Secondary Antibody – 1:5000 dilution.

Table 2.4. – List of antibodies used for Western-blotting.

Antibody	Description	Reference	Company
Primary Antibodies			
HIF-1α	Mouse IgG	sc-13515	Santa Cruz Biotechnology
HIF-2α	Mouse IgG	sc-46691	Santa Cruz Biotechnology
TFRC	Mouse IgG	sc-51829	Santa Cruz Biotechnology
CA IX	Mouse IgG	sc-365900	Santa Cruz Biotechnology
NDRG1	Mouse IgG	sc-398291	Santa Cruz Biotechnology
PDK1	Mouse IgG	sc-293160	Santa Cruz Biotechnology

α-tubulin	Mouse IgG	sc-5286	Santa Cruz Biotechnology
Secondary Antibodies			
Anti-mouse	Goat anti-mouse IgG	926-32210	LI-COR

3. Results

3.1. gRNA cloning using pSpCas9(BB)-2A-Puro (PX459) vector V2.0

Several genome editing technologies have emerged in the last few years including the CRISPR/Cas9 system. Cas9 is a nuclease that promotes genome editing by generating a Double Strand Break (DSB) in a specific genomic locus. DSB are usually repaired through Non-Homologous End Joining (NHEJ) which can lead to mutations in the form of insertions or deletions (Indels) or Homology-directed Repair (HDR). If Indels occur in coding regions they can lead to frameshift mutations or premature stop codons that can mediate gene knockouts (Ran et al., 2013).

Type II CRISPR is the best characterized type of CRISPR/Cas9 that is provenient from the bacteria *Streptococcus pyogenes*. The CRISPR/Cas9 system relies on the use of single-guided RNAs (sgRNAs) or guide-RNAs (gRNAs). gRNAs consist of non-coding sequences of approximately 20bp that pair with the complementary DNA target sequence guiding the Cas9 nuclease to the specific site. It requires that the target DNA precedes a 5'-NGG PAM (Protospacer Adjacent Motif) for the Cas9 to recognise the target site (Figure 3.1). A DBS is usually generated approximately 3bp upstream of the PAM (Ran et al., 2013). The CRISPR/Cas9 system is of enormous importance in basic research and translational medicine. It provides important research tools that can have a significant impact in gene therapy and human diseases, especially in the cancer genetics field. (Jacinto et al., 2020).

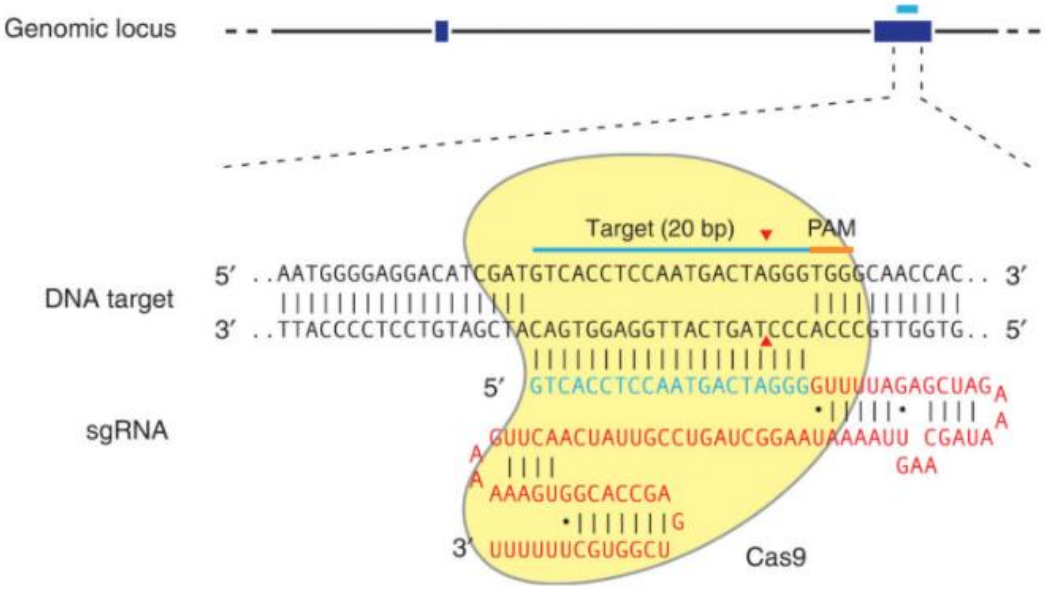

Figure 3.1 - Schematic representation of the RNA-guided Cas9 nuclease.
S. pyogenes Cas9 (yellow) is directed to the genomic DNA by a sgRNA (blue and red). sgRNA binds to the target DNA that is upstream of the 5'-NGG PAM (orange). Adapted from Ran et al., 2013.

In order to perform the knockout of *ADM* and *TFRC* genes, we first constructed the respective CRISPR/Cas9 plasmids using the pSpCas9(BB)-2A-Puro (PX459) backbone vector V2.0. 2 gRNAs were designed for each gene and the gRNA primers are listed in Table 3.1. They were designed and confirmed for the inexistence of off-target activity using the tools mentioned in section 2.1.. The underlined sequences in Table 3.1 correspond to the overhangs created to bind the sites in the plasmid linearized with BbsI restriction enzyme (Figure 3.2).

Table 3.1 – Sequences of the primers used to clone TFRC and ADM gRNAs.

gRNA	Forward primer	Reverse primer
TFRC gRNA1	5´-CACC-GTCATATACCCGGTTCAGCC- 3´	5´-AAAC-GGCTGAACCGGGTATATGAC- 3´
TFRC gRNA2	5´-CACC-GCATTCTCTAACTTGTTTGG- 3´	5´-AAAC-CCAAACAAGTTAGAGAATGC- 3´
ADM gRNA1	5´-CACC-GCGAGCGAACCCAGGTACATC- 3´	5´-AAAC-GATGTACCTGGGTTCGCTCGC- 3´
ADM gRNA2	5´-CACC-GCGACGCGACATCCAACCGAG- 3´	5´-AAAC-CTCGGTTGGATGTCGCGTCGC- 3´

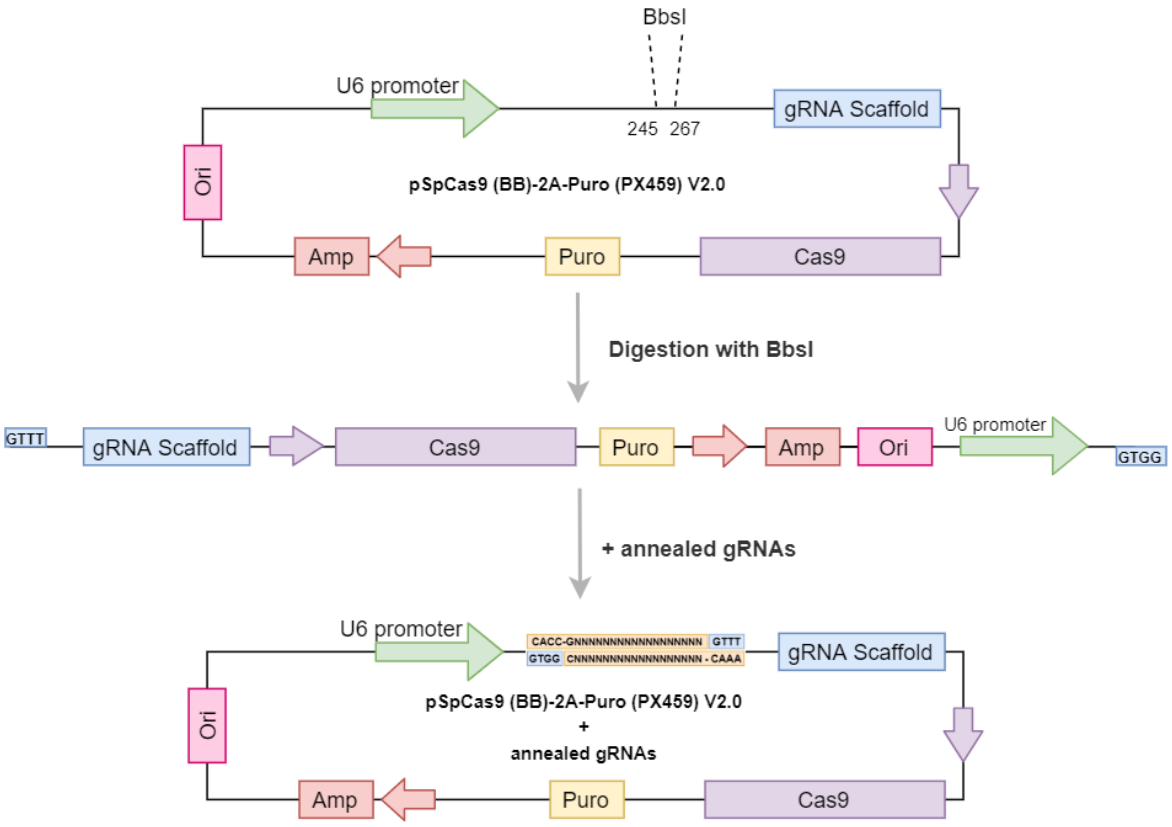

Figure 3.2 – Schematic representation of the linearized plasmid and pX459 plasmid with cloned gRNA.

To clone the gRNAs in the plasmid, first the plasmid needs to be linearized. To this end, the plasmid was digested with the restriction enzyme BbsI. The plasmid

linearization was confirmed through an electrophoresis in a 0.8% agarose gel (Figure 3.3). Only one band was observed confirming the plasmid digestion by BbsI.

Figure 3.3 – Validation of pX459 plasmid linearization.
The digestion product was subjected to an electrophoresis in a 0.8% agarose gel and visualised using Gel Doc™ EZ Imaging System and ChemiDoc™ MP Imaging System (BIO-RAD).

After the plasmid purification, the gRNAs oligonucleotides were annealed and then inserted into the linearized plasmid using the enzyme T4 DNA ligase that performs the ligation reaction. The plasmids were prepared to be introduced in competent bacteria.

The bacterial cells used, STBL4 *E. coli*, were made competent and then transformed. Using 2 control plates with 5 and 50 ng of the circular pX459 plasmid, it was possible to calculate the transformation efficiency using the following equation:

Equation for transformation efficiency (cfu/µg)

$$\frac{cfu\ on\ control\ plate}{ng\ of\ control\ DNA\ plated} \times \frac{10^3\ ng}{\mu g}$$

(cfu – colony forming units)

After the transformation, the following results were obtained:

Control plates:

5 ng of DNA:	**50 ng of DNA:**
Plate 1 – 86 colonies;	Plate 1 – 654 colonies;
Plate 2 – 323 colonies.	Plate 2 – 2760 colonies.

Negative control plates:

Plate 1 – 0 colonies;

Plate 2 – 0 colonies.

The negative control plates had no colonies as expected.

Using Plate 2 plated with 5 ng of DNA: Plate 2 was plated with ~200 µl of bacterial mixture which corresponds to 2.8 ng of DNA.

Using the equation for transformation efficiency:

$$\frac{323}{2.8} \times 10^3 = 1.2 \times 10^5/\mu g$$

The transformation efficiency is $1.2 \times 10^5/\mu g$.

A validation of the positive clones was performed by PCR and observed through an electrophoresis in a 1.5% agarose gel. The results are shown in Figures 3.4 and 3.5.

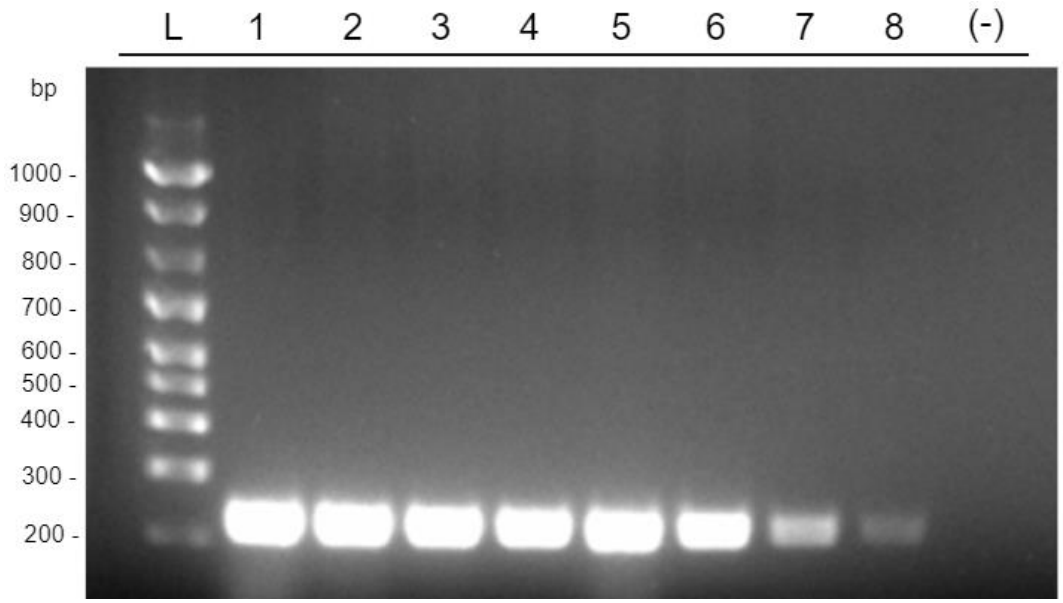

Figure 3.4 – Validation of positive clones by PCR.
L – DNA Ladder - EZ load 1kb Molecular Ruler (BIO-RAD); **1 –** ADM gRNA1; **2 –** TFRC gRNA1; **3 –** TFRC gRNA1; **4 –** TFRC gRNA2; **5 –** TFRC gRNA2; **6 –** TFRC gRNA2; **7 –** ADM gRNA2; **8 –** ADM gRNA2; **(-) –** Negative control. PCR products were subjected to an electrophoresis in a 1.5% agarose gel and visualised using Gel Doc™ EZ Imaging System and ChemiDoc™ MP Imaging System (BIO-RAD).

The results from Figure 3.4 indicate that all the clones (1-8) present a band of approximately 220bp which suggests that the clones are positive. However, the bacterial cultures corresponding to samples 7 and 8 (ADM gRNA2) did not present any overnight growth. After incubating again at the same conditions, samples 7 and 8 still did not present any overnight growth and were discarded. The procedures were repeated in order to clone ADM gRNA2 later and the clones (1-6) were shown positive (Figure 3.5). The negative controls do not show any amplified product which validates the primers' specificity.

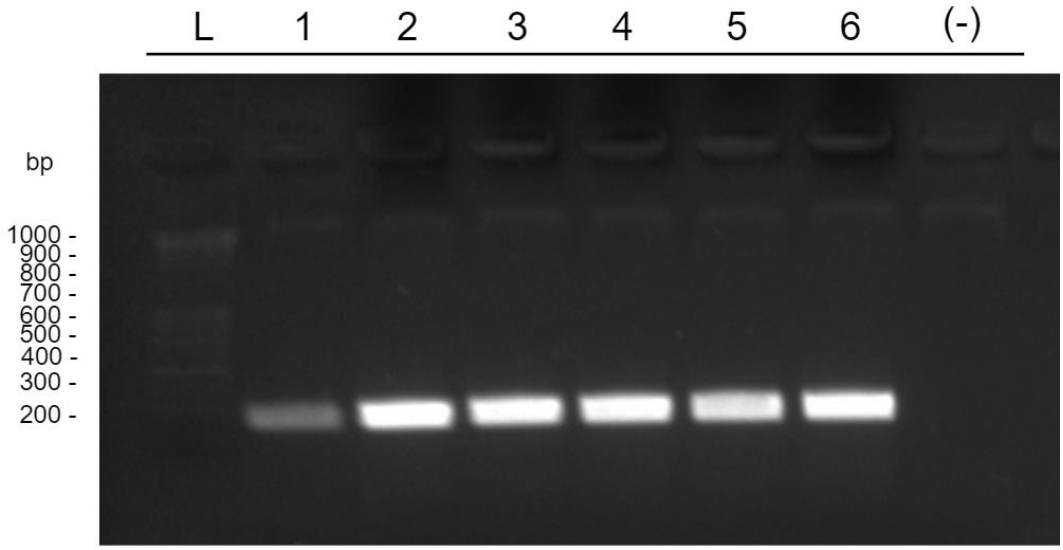

Figure 3.5 – Validation of positive clones by PCR.
L – DNA Ladder - EZ load 1kb Molecular Ruler (BIO-RAD); **1 – 6** ADM gRNA2; **(-) –** Negative control. PCR products were subjected to an electrophoresis in a 1.5% agarose gel and visualised using Gel Doc™ EZ Imaging System and ChemiDoc™ MP Imaging System (BIO-RAD).

The DNA purified was quantified and presented good quality. The cloning of the gRNAs into pX459 V2.0 plasmid was confirmed by sequencing.

3.2. Hypoxia treatment

Wild-type cells were exposed to hypoxia as described in section 2.2.2.4.. UP-029 cells were exposed to hypoxia for 24h and 48h and SEBTA-023 cells for 6h and 24h. Cells' exposure to hypoxia was performed to optimise the Western Blotting conditions while KO cells were being selected. After hypoxia treatment, cells were lysed, and the proteins present in the mixture were extracted, quantified and analysed by Western Blotting (Figures 3.6 and 3.7).

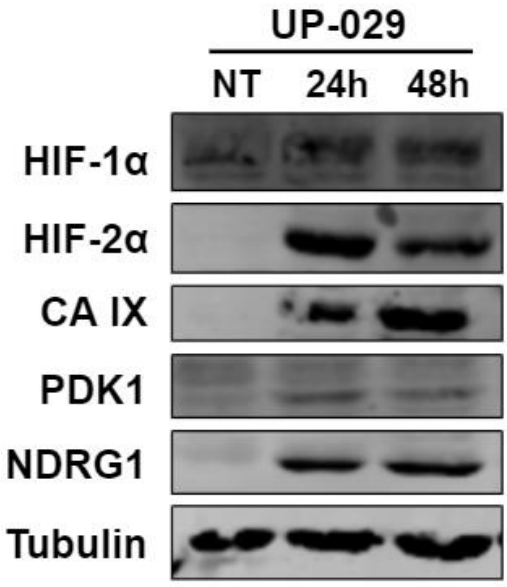

Figure 3.6 – Analysis of hypoxia related proteins in UP-029 cells after hypoxia exposure.
UP-029 cells were incubated under normoxic (NT – Non-treated/normoxia), 24h or 48h of hypoxia (1% O_2). Cells were lysed and 20 µg of each protein extract was subjected to SDS-PAGE and analysed by Western blotting with the antibodies indicated (HIF-1α, HIF-2α, CA IX, PDK1, NDRG1 and α-tubulin). Tubulin was used as a loading control.

Western blot analysis of UP-029 cells showed hypoxia-dependent upregulation of HIF-1α, HIF-2α, CA IX, PDK1 and N-myc Downstream Regulated 1 (NDRG1) after both 24h and 48h of exposure (Figure 3.6). HIF-1α and HIF-2α are induced by hypoxia. CA IX, PDK1 and NDRG1 are HIF-1 targets being their expression regulated by it (Chédeville et al., 2020; J. W. Kim et al., 2006; Proescholdt et al., 2012; Said et al., 2008). Thus, these results validate the presence of a hypoxic environment.

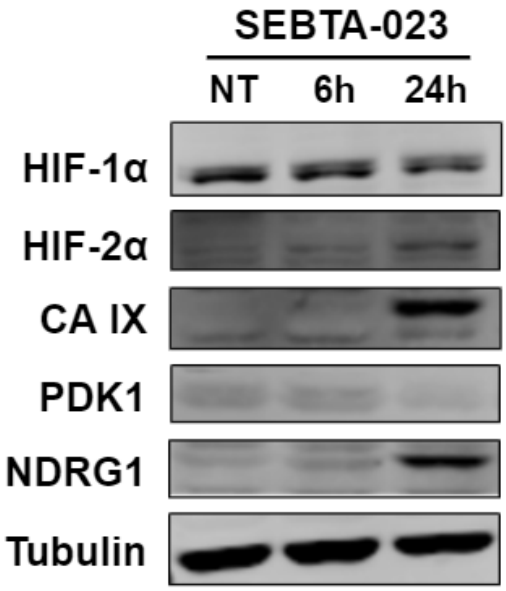

Figure 3.7 – Analysis of hypoxia related proteins in SEBTA-023 cells after hypoxia exposure.
UP-029 cells were incubated under normoxic (NT – Non-treated/normoxia), 6h or 24h of hypoxia (1% O_2). Cells were lysed and 20 µg of each protein extract was subjected to SDS-PAGE and analysed by Western blotting with the antibodies indicated (HIF-1α, HIF-2α, CA IX, PDK1, NDRG1 and α-tubulin). Tubulin was used as a loading control.

Western blot analysis of SEBTA-023 cells showed upregulation of HIF-2α at both 6h and 24h, and CA IX and NDRG1 at 24h of hypoxia exposure. PDK1 presence could not be detected. HIF-1α levels were already high at normoxic conditions and did not change during hypoxia exposure (Figure 3.7). The up-regulation of HIF-2α and the upregulation of HIF-1 targets, CA IX and NDRG1, validate the presence of hypoxic conditions.

Previous western blot analysis from our laboratory demonstrated that PI3K/AKT pathway is highly activated in SEBTA-023 cell line (Chédeville et al., 2020). The increased activation of this pathway, which is usually observed in GBM, might explain the HIF-1α expression detected under normoxic conditions.

3.3. *ADM* and *TFRC* knockout

UP-029 and SEBTA-023 cells were transfected with the plasmids previously prepared in order to knockout *ADM* and *TFRC* genes (Figure 3.8). pX459 plasmid has a gene that confers resistance to puromycin. Puromycin was used as a selective

marker and added to the cells so that the ones without the plasmid die. After puromycin selection, the cells were serially diluted in 96 wells in order to isolate single cell KO clones. To evaluate if the knockout was successful, the cells were analysed by western blotting (Figure 3.8).

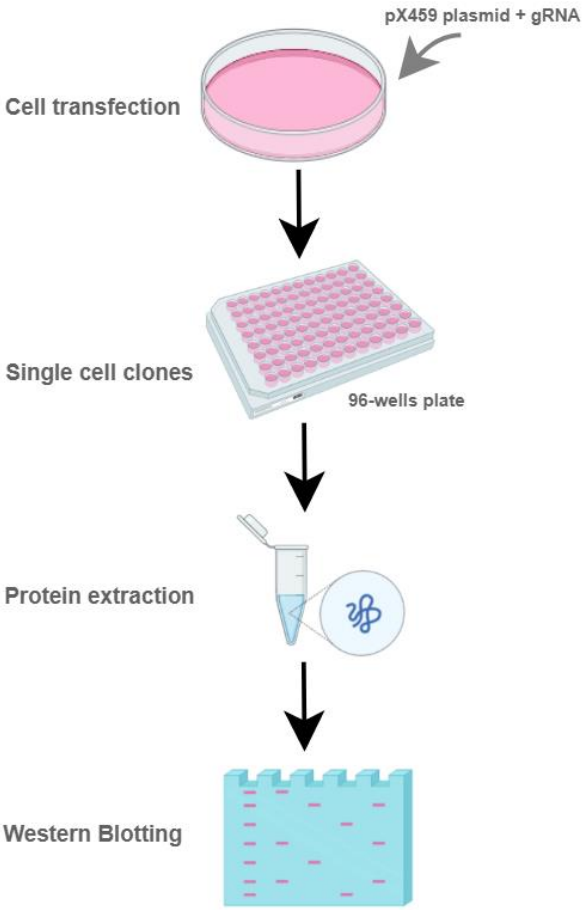

Figure 3.8 - Flow diagram of CRISPR/Cas9 protocol.

ADM is processed in a 6 kDa protein. It could not be detected through western blotting probably due to its size or because it is secreted. Thus, other approaches were used with the aim to overcome this technical difficulty. Besides western blotting, the cell culture medium was analysed to try to confirm the presence of secreted ADM. WT and possible KO cells' medium was analysed through dot blot, ELISA (Bleicher et al., 2018) and PCR (Bhattacharya & van Meir, 2019). However, the techniques could not be optimised due to the COVID-19 pandemic.

UP-029 and SEBTA-023 WT and TFRC gRNA transfected cells were analysed by western blotting. Briefly, cells were lysed, and the proteins present in the mixture were extracted and quantified through a BCA assay. Several western blots were performed (Figures 3.9 – 3.13).

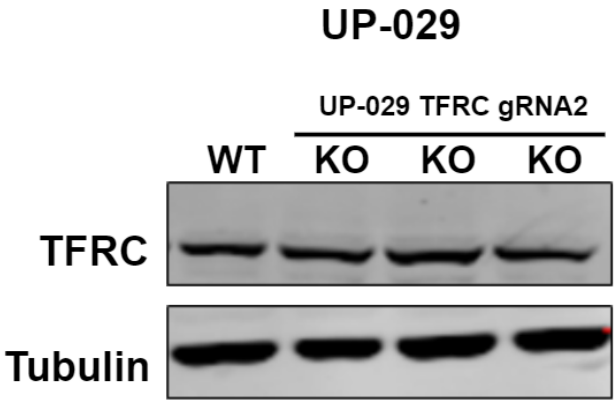

Figure 3.9 – Analysis of UP-029 TFRC gRNA cells.
WT – UP-029 Wild-type; KO – Knockout. Cells were lysed and 20 µg of each protein extract was subjected to SDS-PAGE and analysed by Western blotting with the antibodies indicated (TFRC and α-tubulin). Tubulin was used as a loading control.

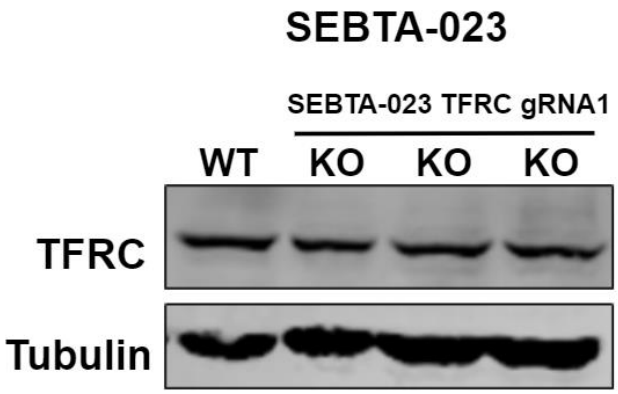

Figure 3.10 – Analysis of SEBTA-023 TFRC gRNA cells.
WT – SEBTA-023 Wild-type; KO – Knockout. Cells were lysed and 20 µg of each protein extract was subjected to SDS-PAGE and analysed by Western blotting with the antibodies indicated (TFRC and α-tubulin). Tubulin was used as a loading control.

Figure 3.11 – Analysis of UP-029 and SEBTA-023 TFRC gRNA cells.
WT 1 – UP-029 Wild-type; WT 2 – SEBTA-023 Wild-type; KO – Knockout. Cells were lysed and the protein extracts were subjected to SDS-PAGE and analysed by Western blotting with the antibodies indicated (TFRC and α-tubulin). Tubulin was used as a loading control.

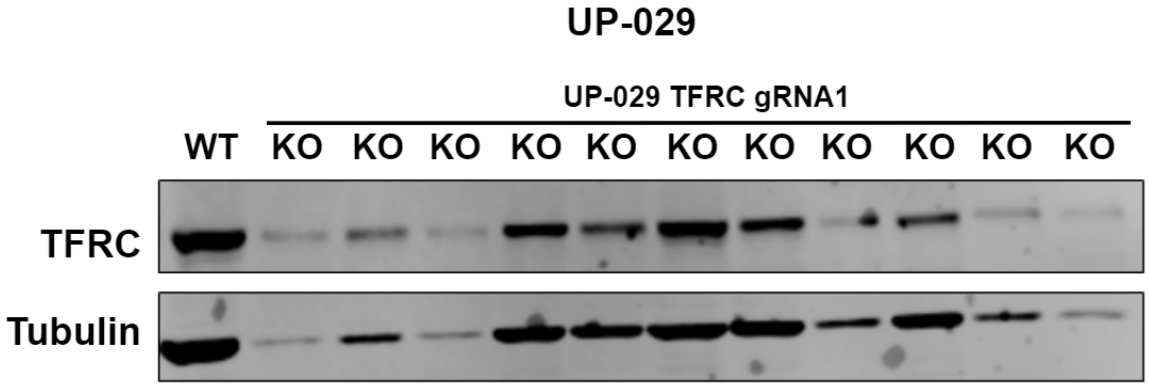

Figure 3.12 – Analysis of UP-029 TFRC gRNA cells.
WT – UP-029 Wild-type; KO – Knockout. Cells were lysed and the protein extracts were subjected to SDS-PAGE and analysed by Western blotting with the antibodies indicated (TFRC and α-tubulin). Tubulin was used as a loading control.

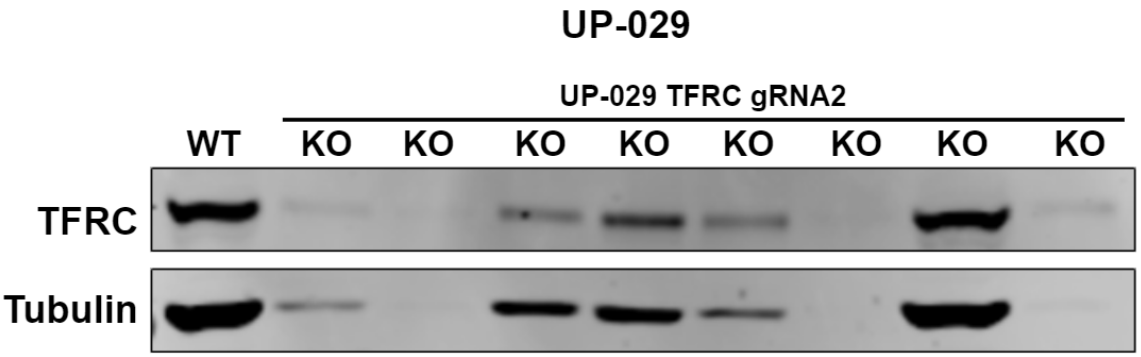

Figure 3.13 – Analysis of UP-029 TFRC gRNA cells.
WT – UP-029 Wild-type; KO – Knockout. Cells were lysed and the protein extracts were subjected to SDS-PAGE and analysed by Western blotting with the antibodies indicated (TFRC and α-tubulin). Tubulin was used as a loading control.

Western blot analysis showed the presence of TFRC in all the TFRC gRNA samples from both UP-029 and SEBTA-023 cell lines. Thus, TFRC knockout was not successful. Some KO samples do not show TFRC or tubulin presence (Figures 3.11-3.13). Figures 3.11-3.13 refer to an initial screening and the protein extracts were not quantified, justifying the difference of tubulin concentrations.

The analysis of TFRC gRNA clones needed to be continued. However, due to the COVID-19 pandemic and the closure of the research facilities, the experiments could not be carried on, and this part of the work could not be finished.

4. Discussion and Conclusions

GBM is one of deadliest types of cancer and is characterised by its aggressiveness and poor patient prognosis. Hypoxia is one of its hallmarks and contributes to its high invasiveness and chemo-resistance (Monteiro et al., 2017). ADM is a hormone that has a strong vasodilatory effect and plays an important role in angiogenesis (Patel et al., 2017). TFRC is a transmembrane protein that interacts with iron-loaded transferrin mediating iron import into the cell (Daniels-Wells & Penichet, 2016). Both are associated with several types of cancer and are regulated by hypoxia (Deville et al., 2010; Shen et al., 2018).

As previously mentioned, our laboratory identified ADM and TFRC as two proteins that are over- and under-expressed, respectively, in hypoxic GBM cells (Chédeville et al., 2020). This study aimed to investigate their role, under normoxia and hypoxia, by performing their knockout in two GBM patient's biopsy-derived cell lines using the CRISPR-Cas9 system.

CRISPR-Cas9 is a genome editing technology that emerged in the last few years. This system relies on the nuclease Cas9 that generates a DSB in the genomic locus of the gene(s) of interest. It consists in inserting a CRISPR-Cas9 plasmid that has a gRNA sequence, that pairs with the complementary DNA target sequence, and guide the Cas9 to the specific site, performing the knockout (Ran et al., 2013).

The gRNAs cloning, using the CRISPR plasmid pSpCas9(BB)-2A-Puro (PX459) vector V2.0, was successful and four plasmids were cloned: TFRC gRNA1, TFRC gRNA2, ADM gRNA1 and ADM gRNA2 (Figures 3.4 and 3.5).

The hypoxia conditions were accessed by analysing the protein expression of HIF alpha subunits and some of HIF-1 targets, in GBM cells, after hypoxia treatment. *CA IX*, *NDRG* and *PDK1* are known to be upregulated by HIF-1 and used as hypoxia markers (Chédeville et al., 2020; J. W. Kim et al., 2006; Proescholdt et al., 2012; Said et al., 2008). HIF-1α, HIF-2α, CA IX, NDRG1 and PDK1 presence was confirmed in UP-029 cells after 24h and 48h of hypoxia exposure (Figure 3.6). HIF-1α, HIF-2α, CAIX and NDRG1 presence was confirmed after 24h of hypoxia exposure in SEBTA-023 cells (Figure 3.7). However, HIF-1α was also present in normoxia conditions which might be explained by the increased activation of PI3K/AKT in SEBTA-023 cell line (Chédeville et al., 2020). These results confirm the presence of hypoxia conditions.

UP-029 and SEBTA-023 were transfected with the ADM and TFRC gRNAs plasmids in order to perform the knockout of *ADM* and *TFRC* genes. Transfected cells were analysed by western blotting.

ADM protein could not be detected by western blotting probably due to its small size (6 kDa) or due to being secreted. Other strategies (dotblot, ELISA (Bleicher et al., 2018), PCR (Bhattacharya & van Meir, 2019)) were used to verify its presence. Unfortunately, the techniques used could not be optimised and were unable to be carried out due to the COVID-19 global pandemic.

Cells transfected with TFRC gRNAs were analysed by western blotting (Figures 3.9-3.13). These results showed that the knockout was not successful. Some KO samples do not show TFRC or tubulin presence (Figures 3.11-3.13). These figures refer to an initial screening in which the protein extracts were not quantified explaining the differences of tubulin concentration. As we cannot infer that there was or not TFRC knockout, these samples would have to be analysed again in order to investigate TFRC absence or presence. Unfortunately, I was unable to analyse more TFRC gRNAs clones due to the COVID-19 global pandemic that caused the closure of the research facilities.

The role of ADM and TFRC in hypoxic GBM could not be investigated. It is paramount to continue this research in order to have a better insight of their function in GBM progression.

5. Future Perspectives

Due to the closure of the research facilities as a consequence of the COVID-19 global pandemic, I was unable to conduct all the experiments planned.

In the future, in order to evaluate ADM and TFRC proteins' role in hypoxic GBM, it is needed to continue to analyse *TFRC* gRNAs clones. UP-029 and SEBTA-023 should be transfected with the CRISPR-Cas9 plasmids constructed. ADM detection experiments should be optimized in order to analyse and isolate *ADM* KO clones.

After obtaining *ADM* and *TFRC* KO clones, these need to be analysed under normoxic and hypoxic conditions and functional assays should be performed to better understand their role in hypoxic GBM.

Tubulogenesis assays should be performed to understand the angiogenic capability of *ADM* KO and WT cells. MTS viability assays should also be performed as well as analyse the cells' sensitivity to oxidative stress (H_2O_2 treatment) for both *TFRC* and *ADM* KO and WT cells.

6. References

Abdullah, K. G., Adamson, C., & Brem, S. (2016). The Molecular Pathogenesis of Glioblastoma. In *Glioblastoma* (pp. 21–31). Elsevier Inc. https://doi.org/10.1016/B978-0-323-47660-7.00003-3

Agnihotri, S., & Zadeh, G. (2016). Metabolic reprogramming in glioblastoma: The influence of cancer metabolism on epigenetics and unanswered questions. *Neuro-Oncology*, *18*(2), 160–172. https://doi.org/10.1093/neuonc/nov125

Aisina, R. B., & Mukhametova, L. I. (2014). Structure and function of plasminogen/plasmin system. *Russian Journal of Bioorganic Chemistry*, *40*(6), 590–605. https://doi.org/10.1134/S1068162014060028

Alberts, B., Johnson, A., Lewis, J., Morgan, D., Raff, M., Roberts, K., & Walter, Peter. (2015). Molecular Biology of the Cell. In *Garland Science* (6th ed.). Garland Science. https://doi.org/10.1292/jvms.17-0659

Alexandrov, L. B., Nik-Zainal, S., Wedge, D. C., Aparicio, S. A. J. R., Behjati, S., Biankin, A. v., Bignell, G. R., Bolli, N., Borg, A., Børresen-Dale, A. L., Boyault, S., Burkhardt, B., Butler, A. P., Caldas, C., Davies, H. R., Desmedt, C., Eils, R., Eyfjörd, J. E., Foekens, J. A., … Stratton, M. R. (2013). Signatures of mutational processes in human cancer. *Nature*, *500*(7463), 415–421. https://doi.org/10.1038/nature12477

Amiri, A., Le, P. U., Moquin, A., Machkalyan, G., Petrecca, K., Gillard, J. W., Yoganathan, N., & Maysinger, D. (2016). Inhibition of carbonic anhydrase IX in glioblastoma multiforme. *European Journal of Pharmaceutics and Biopharmaceutics*, *109*, 81–92. https://doi.org/10.1016/j.ejpb.2016.09.018

Anand, P., Kunnumakara, A. B., Sundaram, C., Harikumar, K. B., Tharakan, S. T., Lai, O. S., Sung, B., & Aggarwal, B. B. (2008). Cancer is a preventable disease that requires major lifestyle changes. *Pharmaceutical Research*, *25*(9), 2097–2116. https://doi.org/10.1007/s11095-008-9661-9

Anjum, K., Shagufta, B. I., Abbas, S. Q., Patel, S., Khan, I., Shah, S. A. A., Akhter, N., & Hassan, S. S. ul. (2017). Current status and future therapeutic perspectives of glioblastoma multiforme (GBM) therapy: A review. *Biomedicine & Pharmacotherapy*, *92*, 681–689. https://doi.org/10.1016/j.biopha.2017.05.125

Aparisi, F., Amado-Labrador, H., Calabuig-Fariñas, S., Torres, S., Herreros-Pomares, A., Jantus-Lewintre, E., Blasco, A., Iranzo, V., & Camps, C. (2019). Passenger mutations in cancer evolution. *Cancer Reports and Reviews*, *3*(3). https://doi.org/10.15761/CRR.1000188

Arvelo, F., Sojo, F., & Cotte, C. (2016). Tumour progression and metastasis. *Ecancer Medical Science*, *10*, 617. https://doi.org/10.3332/ecancer.2016.617

Aurelian, L. (2016). Oncolytic viruses as immunotherapy: Progress and remaining challenges. *OncoTargets and Therapy*, *9*, 2627–2637. https://doi.org/10.2147/OTT.S63049

Bagley, S. J., Desai, A. S., Linette, G. P., June, C. H., & O'Rourke, D. M. (2018). CAR T-cell therapy for glioblastoma: Recent clinical advances and future challenges. *Neuro-Oncology*, *20*(11), 1429–1438. https://doi.org/10.1093/neuonc/noy032

Bao, S., Wu, Q., Sathornsumetee, S., Hao, Y., Li, Z., Hjelmeland, A. B., Shi, Q., Mclendon, R. E., Bigner, D. D., & Rich, J. N. (2006). Stem Cell-like Glioma Cells Promote Tumor Angiogenesis through Vascular Endothelial Growth Factor. *Cancer R*, *66*(16), 7843–7848. https://doi.org/10.1158/0008-5472.CAN-06-1010

Batchelor, T. T., Gerstner, E. R., Ye, X., Desideri, S., Duda, D. G., Peereboom, D., Lesser, G. J., Chowdhary, S., Wen, P. Y., Grossman, S., Supko, J. G., Author, C., Gerstner, E., & Pappas, C. (2017). Feasibility, phase I, and phase II studies of tandutinib, an oral platelet-derived growth factor receptor-β tyrosine kinase inhibitor, in patients with recurrent glioblastoma. *Neuro-Oncology*, *19*(4), 567–575. https://doi.org/10.1093/neuonc/now185

Berghoff, A. S., Kiesel, B., Widhalm, G., Rajky, O., Ricken, G., Wöhrer, A., Dieckmann, K., Filipits, M., Brandstetter, A., Weller, M., Kurscheid, S., Hegi, M. E., Zielinski, C. C., Marosi, C., Hainfellner, J. A., Preusser, M., & Wick, W. (2015). Programmed death ligand 1 expression and tumor-infiltrating lymphocytes in glioblastoma. *Neuro-Oncology*, *17*(8), 1064–1075. https://doi.org/10.1093/neuonc/nou307

Bertout, J. A., Patel, S. A., & Simon, M. C. (2008). The impact of O2 availability on human cancer. *Nature Reviews Cancer*, *8*(12), 967–975. https://doi.org/10.1038/nrc2540

Bhattacharya, D., & van Meir, E. G. (2019). A simple genotyping method to detect small CRISPR-Cas9 induced indels by agarose gel electrophoresis. *Scientific Reports*, *9*(1), 1–7. https://doi.org/10.1038/s41598-019-39950-4

Blasi, F., & Carmeliet, P. (2002). uPAR: A versatile signalling orchestrator. *Nature Reviews Molecular Cell Biology*, *3*(12), 932–943. https://doi.org/10.1038/nrm977

Bleicher, A. v., Unger, H. W., Rogerson, S. J., & Aitken, E. H. (2018). A sandwich enzyme-linked immunosorbent assay for the quantitation of human plasma ferritin. *MethodsX*, *5*(March), 648–651. https://doi.org/10.1016/j.mex.2018.06.010

Brat, D. J., & van Meir, E. G. (2001). Glomeruloid microvascular proliferation orchestrated by VPF/VEGF: A new world of angiogenesis research. *American Journal of Pathology*, *158*(3), 789–796. https://doi.org/10.1016/S0002-9440(10)64025-4

Brat, Daniel J., Castellano-Sanchez, A. A., Hunter, S. B., Pecot, M., Cohen, C., Hammond, E. H., Devi, S. N., Kaur, B., & van Meir, E. G. (2004a). Pseudopalisades in Glioblastoma Are Hypoxic, Express Extracellular Matrix Proteases, and Are Formed by an Actively Migrating Cell Population. *Cancer Research*, *64*(3), 920–927. https://doi.org/10.1158/0008-5472.CAN-03-2073

Brat, Daniel J., Castellano-Sanchez, A. A., Hunter, S. B., Pecot, M., Cohen, C., Hammond, E. H., Devi, S. N., Kaur, B., & van Meir, E. G. (2004b). Pseudopalisades in Glioblastoma Are Hypoxic, Express Extracellular Matrix Proteases, and Are Formed by an Actively Migrating Cell Population. *Cancer Research*, *64*(3), 920–927. https://doi.org/10.1158/0008-5472.CAN-03-2073

Brat, Daniel J., Castellano-Sanchez, A., Kaur, B., & van Meir, E. G. (2002). Genetic and biologic progression in astrocytomas and their relation to angiogenic dysregulation. *Advances in Anatomic Pathology*, *9*(1), 24–36. https://doi.org/10.1097/00125480-200201000-00004

Buddhini, S. (2013). *Hallmarks of Cancer 5: Sustained Angiogenesis*. Scientific American. https://blogs.scientificamerican.com/guest-blog/the-hallmarks-of-cancer-5-sustained-angiogenesis/

Castro-Giner, F., Ratcliffe, P., & Tomlinson, I. (2015). The mini-driver model of polygenic cancer evolution. *Nature Reviews Cancer*, *15*(11), 680–685. https://doi.org/10.1038/nrc3999

Chao, C. C. K. (2014). Mechanisms of p53 degradation. In *Clinica Chimica Acta* (Vol. 438, pp. 139–147). Elsevier B.V. https://doi.org/10.1016/j.cca.2014.08.015

Chavarri-Guerra, Y., Slavin, T. P., Longoria-Lozano, O., & Weitzel, J. N. (2020). Genetic cancer predisposition syndromes among older adults. *Journal of Geriatric Oncology*. https://doi.org/10.1016/j.jgo.2020.01.001

Chédeville, A. L., Lourdusamy, A., Monteiro, A. R., Hill, R., & Madureira, P. A. (2020). Investigating Glioblastoma Response to Hypoxia. *Biomedicines*, *8*(310), 1–30. https://doi.org/10.3390/biomedicines8090310

Cheng, L., Huang, Z., Zhou, W., Wu, Q., Donnola, S., Liu, J. K., Fang, X., Sloan, A. E., Mao, Y., Lathia, J. D., Min, W., McLendon, R. E., Rich, J. N., & Bao, S. (2013). Glioblastoma stem cells generate vascular pericytes to support vessel function and tumor growth. *Cell*, *153*(1), 139–152. https://doi.org/10.1016/j.cell.2013.02.021

Chinnaiyan, P., Won, M., Wen, P. Y., Rojiani, A. M., Werner-Wasik, M., Shih, H. A., Ashby, L. S., Yu, H.-H. M., Stieber, V. W., Malone, S. C., Fiveash, J. B., Mohile, N. A., Ahluwalia, M. S., Wendland, M. M., Stella, P. J., Kee, A. Y., & Mehta, M. P. (2018). A randomized phase II study of everolimus in combination with chemoradiation in newly diagnosed glioblastoma: results of NRG Oncology RTOG 0913. *Radiation Oncology Research*, *20*(5), 3811. https://doi.org/10.1093/neuonc/nox209

Chowdhary, S. A., Ryken, T., & Newton, H. B. (2015). Survival outcomes and safety of carmustine wafers in the treatment of high-grade gliomas: a meta-analysis. *Journal of Neuro-Oncology*, *122*(2), 367–382. https://doi.org/10.1007/s11060-015-1724-2

Chung, I., Osterwald, S., Deeg, K., & Rippe, K. (2012). PML body meets telomere The beginning of an ALTernate ending? *Nucleus*, *3*(3), 263–275. https://doi.org/10.4161/nucl.20326

Clarke, K., Smith, K., Gullick, W. J., & Harris, A. L. (2001). Mutant epidermal growth factor receptor enhances induction of vascular endothelial growth factor by hypoxia and insulin-like growth factor-1 via a PI3 kinase dependent pathway. *British Journal of Cancer*, *84*(10), 1322–1329. https://doi.org/10.1054/bjoc.2001.1805

Cloughesy, T. F., Landolfi, J., Vogelbaum, M. A., Ostertag, D., Elder, J. B., Bloomfield, S., Carter, B., Chen, C. C., Kalkanis, S. N., Kesari, S., Lai, A., Lee, I. Y., Liau, L.

M., Mikkelsen, T., Nghiemphu, P., Piccioni, D., Accomando, W., Diago, O. R., Hogan, D. J., … Walbert, T. (2018). Durable complete responses in some recurrent high-grade glioma patients treated with Toca 511 + Toca FC. *Neuro-Oncology*, *20*(10), 1383–1392. https://doi.org/10.1093/neuonc/noy075

Cloughesy, T., Finocchiaro, G., Belda-Iniesta, C., Recht, L., Brandes, A. A., Pineda, E., Mikkelsen, T., Chinot, O. L., Balana, C., Macdonald, D. R., Westphal, M., Hopkins, K., Weller, M., Bais, C., Sandmann, T., Bruey, J. M., Koeppen, H., Liu, B., Verret, W., … Shames, D. S. (2017). Randomized, double-blind, placebo-controlled, multicenter phase II study of onartuzumab plus bevacizumab versus placebo plus bevacizumab in patients with recurrent glioblastoma: Efficacy, safety, and hepatocyte growth factor and O6-methylguanine-DNA methy. *Journal of Clinical Oncology*, *35*(3), 343–351. https://doi.org/10.1200/JCO.2015.64.7685

Cohen, M. H., Shen, Y. L., Keegan, P., & Pazdur, R. (2009). FDA Drug Approval Summary: Bevacizumab (Avastin®) as Treatment of Recurrent Glioblastoma Multiforme. *The Oncologist*, *14*(11), 1131–1138. https://doi.org/10.1634/theoncologist.2009-0121

Daniels, T. R., Delgado, T., Rodriguez, J. A., Helguera, G., & Penichet, M. L. (2006). The transferrin receptor part I: Biology and targeting with cytotoxic antibodies for the treatment of cancer. In *Clinical Immunology* (Vol. 121, Issue 2, pp. 144–158). Academic Press. https://doi.org/10.1016/j.clim.2006.06.010

Daniels-Wells, T. R., & Penichet, M. L. (2016). Transferrin receptor 1: A target for antibody-mediated cancer therapy. *Immunotherapy*, *8*(9), 991–994. https://doi.org/10.2217/imt-2016-0050

Davis, M. E. (2016). Glioblastoma: Overview of Disease and Treatment. *Clinical Journal of Oncology Nursing*, *20*(5), 2–8. https://doi.org/10.1188/16.CJON.S1.2-8

de Vleeschouwer, S. (2017). *Glioblastoma* (S. de Vleeschouwer, Ed.). https://doi.org/10.15586/codon.glioblastoma.2017

Denton, A. E., Roberts, E. W., & Fearon, D. T. (2018). Stromal Cells in the Tumor Microenvironment. In *Advances in Experimental Medicine and Biology* (Vol. 1060, pp. 99–114). Springer New York LLC. https://doi.org/10.1007/978-3-319-78127-3_6

Derynck, R., & Weinberg, R. A. (2019). EMT and Cancer: More Than Meets the Eye. *Developmental Cell*, *49*(3), 313–316. https://doi.org/10.1016/j.devcel.2019.04.026

Desjardins, A., Gromeier, M., Herndon, J. E., Beaubier, N., Bolognesi, D. P., Friedman, A. H., Friedman, H. S., McSherry, F., Muscat, A. M., Nair, S., Peters, K. B., Randazzo, D., Sampson, J. H., Vlahovic, G., Harrison, W. T., McLendon, R. E., Ashley, D., & Bigner, D. D. (2018). Recurrent Glioblastoma Treated with Recombinant Poliovirus. *New England Journal of Medicine*, *379*(2), 150–161. https://doi.org/10.1056/NEJMoa1716435

Desjardins, A., Vlahovic, G., & Friedman, H. S. (2016). Vaccine Therapy, Oncolytic Viruses, and Gliomas. *Oncology (Williston Park, N.Y.)*, *30*(3), 211–218. https://pubmed.ncbi.nlm.nih.gov/26984213/

Deville, J.-L., Salas, S., Figarella-Branger, D., Ouafik, L. H., & Daniel, L. (2010). Adrenomedullin as a therapeutic target in angiogenesis. *Expert Opinion on Therapeutic Targets*, *14*(10), 1059–1072.

Ding, W.-X., Manley, S., & Ni, H.-M. (2011). The emerging role of autophagy in alcoholic liver disease. *Experimental Biology and Medicine*, *236*(5), 546–556. https://doi.org/10.1258/ebm.2011.010360

Dvorak, H. F. (2002). Vascular permeability factor/vascular endothelial growth factor: A critical cytokine in tumor angiogenesis and a potential target for diagnosis and therapy. *Journal of Clinical Oncology*, *20*(21), 4368–4380. https://doi.org/10.1200/JCO.2002.10.088

Eklund, L., & Saharinen, P. (2013). Angiopoietin signaling in the vasculature. *Experimental Cell Research*, *319*(9), 1271–1280. https://doi.org/10.1016/j.yexcr.2013.03.011

Emara, M., & Allalunis-Turner, J. (2014). Effect of hypoxia on angiogenesis related factors in glioblastoma cells. *Oncology Reports*, *31*(4), 1947–1953. https://doi.org/10.3892/or.2014.3037

Fan, L., Li, J., Yu, Z., Dang, X., & Wang, K. (2014). The Hypoxia-Inducible Factor Pathway, Prolyl Hydroxylase Domain Protein Inhibitors, and Their Roles in Bone Repair and Regeneration. *BioMed Research International*. https://doi.org/10.1155/2014/239356

Favaro, E., Lord, S., Harris, A. L., & Buffa, F. M. (2011). Gene expression and hypoxia in breast cancer. *Genome Medicine*, *3*(8), 55. https://doi.org/10.1186/gm271

Folkins, C., Shaked, Y., Man, S., Tang, T., Lee, C. R., Zhu, Z., Hoffman, R. M., & Kerbel, R. S. (2009). Glioma tumor stem-like cells promote tumor angiogenesis and vasculogenesis via vascular endothelial growth factor and stromal-derived factor 1. *Cancer Research*, *69*(18), 7243–7251. https://doi.org/10.1158/0008-5472.CAN-09-0167

Frantz, C., Stewart, K. M., & Weaver, V. M. (2010). The extracellular matrix at a glance. In *Journal of Cell Science* (Vol. 123, Issue 24, pp. 4195–4200). The Company of Biologists Ltd. https://doi.org/10.1242/jcs.023820

Gilbert, M. R., Dignam, J. J., Armstrong, T. S., Wefel, J. S., Blumenthal, D. T., Vogelbaum, M. A., Colman, H., Chakravarti, A., Pugh, S., Won, M., Jeraj, R., Brown, P. D., Jaeckle, K. A., Schiff, D., Stieber, V. W., Brachman, D. G., Werner-Wasik, M., Tremont-Lukats, I. W., Sulman, E. P., … Mehta, M. P. (2014). A Randomized Trial of Bevacizumab for Newly Diagnosed Glioblastoma. *New England Journal of Medicine*, *370*(8), 699–708. https://doi.org/10.1056/NEJMoa1308573

Glaser, T., Han, I., Wu, L., & Zeng, X. (2017). Targeted nanotechnology in glioblastoma multiforme. *Frontiers in Pharmacology*, *8*(166). https://doi.org/10.3389/fphar.2017.00166

Gray, L. H., Conger, A. D., Ebert, M., Hornsey, S., & Scott, O. C. (1953). The concentration of oxygen dissolved in tissues at the time of irradiation as a factor in radiotherapy. *The British Journal of Radiology*, *26*(312), 638–648. https://doi.org/10.1259/0007-1285-26-312-638

Gupta, R., Chetty, C., Bhoopathi, P., Lakka, S., Mohanam, S., Rao, J. S., & Dinh, D. H. (2011). Downregulation of uPA/uPAR inhibits intermittent hypoxia-induced epithelial-mesenchymal transition (EMT) in DAOY and D283 medulloblastoma cells. *International Journal of Oncology*, *38*(3), 733–744. https://doi.org/10.3892/ijo.2010.883

Haase, S., Garcia-Fabiani, M. B., Carney, S., Altshuler, D., Núñez, F. J., Méndez, F. M., Núñez, F., Lowenstein, P. R., & Castro, M. G. (2018). Mutant ATRX: uncovering a new therapeutic target for glioma. *Expert Opinion on Therapeutic Targets*, *22*(7), 599–613. https://doi.org/10.1080/14728222.2018.1487953

Hanahan, D., & Weinberg, R. A. (2011). Hallmarks of Cancer: The Next Generation. *Cell*, *144*, 646–674. https://doi.org/10.1016/j.cell.2011.02.013

Hanif, F., Muzaffar, K., Perveen, K., Malhi, S. M., & Simjee, S. U. (2017). Glioblastoma multiforme: A review of its epidemiology and pathogenesis through clinical presentation and treatment. *Asian Pacific Journal of Cancer Prevention*, *18*(1), 3–9. https://doi.org/10.22034/APJCP.2017.18.1.3

Hegi, M. E., Diserens, A.-C., Gorlia, T., Hamou, M.-F., de Tribolet, N., Weller, M., Kros, J. M., Hainfellner, J. A., Mason, W., Mariani, L., Bromberg, J. E. C., Hau, P., Mirimanoff, R. O., Cairncross, J. G., Janzer, R. C., & Stupp, R. (2005). MGMT Gene Silencing and Benefit from Temozolomide in Glioblastoma. *New England Journal of Medicine*, *352*(10), 997–1003. https://doi.org/10.1056/NEJMoa043331

Heiden, M. G. V., Cantley, L. C., & Thompson, C. B. (2009). Understanding the warburg effect: The metabolic requirements of cell proliferation. *Science*, *324*(5930), 1029–1033. https://doi.org/10.1126/science.1160809

Helleday, T., Eshtad, S., & Nik-zainal, S. (2014). Mechanisms underlying mutational sigantures in human cancers. *Nature Publishing Group*, *15*(9), 585–598. https://doi.org/10.1038/nrg3729

Hill, R. P., Bristow, R. G., Fyles, A., Koritzinsky, M., Milosevic, M., & Wouters, B. G. (2015). Hypoxia and Predicting Radiation Response. *Seminars in Radiation Oncology*, *25*(4), 260–272. https://doi.org/10.1016/j.semradonc.2015.05.004

Hillen, F., & Griffioen, A. W. (2007). Tumour vascularization: Sprouting angiogenesis and beyond. *Cancer and Metastasis Reviews*, *26*(3–4), 489–502. https://doi.org/10.1007/s10555-007-9094-7

Hottinger, A. F., Pacheco, P., & Stupp, R. (2016). Tumor treating fields: A novel treatment modality and its use in brain tumors. *Neuro-Oncology*, *18*(10), 1338–1349. https://doi.org/10.1093/neuonc/now182

Huang, D., Li, C., & Zhang, H. (2014). Hypoxia and cancer cell metabolism. *Acta Biochimica et Biophysica Sinica*, *46*(3), 214–219. https://doi.org/10.1093/abbs/gmt148

Huang, Jing, Liu, F., Liu, Z., Tang, H., Wu, H., Gong, Q., & Chen, J. (2017). Immune checkpoint in glioblastoma: Promising and challenging. In *Frontiers in Pharmacology* (Vol. 8, Issue MAY, p. 242). Frontiers Media S.A. https://doi.org/10.3389/fphar.2017.00242

Huang, Juan, Yu, J., Tu, L., Huang, N., Li, H., & Luo, Y. (2019). Isocitrate dehydrogenase mutations in glioma: From basic discovery to therapeutics development. *Frontiers in Oncology*, *9*(JUN), 506. https://doi.org/10.3389/fonc.2019.00506

Huang, Z., & Bao, S. D. (2004). Roles of main pro- and anti-angiogenic factors in tumor angiogenesis. *World Journal of Gastroenterology*, *10*(4), 463–470. https://doi.org/10.3748/wjg.v10.i4.463

Jain, R. K., di Tomaso, E., Duda, D. G., Loeffler, J. S., Sorensen, A. G., & Batchelor, T. T. (2007). Angiogenesis in brain tumours. *Nature Reviews Neuroscience*, *8*(8), 610–622. https://doi.org/10.1038/nrn2175

Janke, K., Brockmeier, U., Kuhlmann, K., Eisenacher, M., Nolde, J., Meyer, H. E., Mairbaurl, H., & Metzen, E. (2013). Factor inhibiting HIF-1 (FIH-1) modulates protein interactions of apoptosis-stimulating p53 binding protein 2 (ASPP2). *Journal of Cell Science*, *126*(12), 2629–2640. https://doi.org/10.1242/jcs.117564

Johnsen, K. B., Burkhart, A., Thomsen, L. B., Andresen, T. L., & Moos, T. (2019). Targeting the transferrin receptor for brain drug delivery. *Progress in Neurobiology*, *181*. https://doi.org/10.1016/j.pneurobio.2019.101665

Jones, D. T., Trowbridge, I. S., & Harris, A. L. (2006). Effects of transferrin receptor blockade on cancer cell proliferation and hypoxia-inducible factor function and their differential regulation by ascorbate. *Cancer Research*, *66*(5), 2749–2756. https://doi.org/10.1158/0008-5472.CAN-05-3857

Kalluri, R., & Weinberg, R. A. (2009). The basics of epithelial-mesenchymal transition. *Journal of Clinical Investigation*, *119*(6), 1420–1428. https://doi.org/10.1172/JCI39104

Kamath, A. A., Friedman, D. D., Hassan Akbari, S. A., Kim, A. H., Tao, Y., Luo, J., & Leuthardt, E. C. (2018). Glioblastoma Treated With Magnetic Resonance Imaging-Guided Laser Interstitial Thermal Therapy: Safety, Efficacy, and Outcomes. *Neurosurgery*, *84*(4), 836–843. https://doi.org/10.1093/neuros/nyy375

Kaur, B., Khwaja, F. W., Severson, E. A., Matheny, S. L., Brat, D. J., & van Meir, E. G. (2005). Hypoxia and the hypoxia-inducible-factor pathway in glioma growth and angiogenesis. *Neuro-Oncology*, *7*(2), 134–153. https://doi.org/10.1215/S1152851704001115

Kaur, B., Tan, C., Brat, D. J., & van Meir, E. G. (2004). Genetic and hypoxic regulation of angiogenesis in gliomas. *Journal of Neuro-Oncology*, *70*(2), 229–243. https://doi.org/10.1007/s11060-004-2752-5

Kim, J. W., Tchernyshyov, I., Semenza, G. L., & Dang, C. v. (2006). HIF-1-mediated expression of pyruvate dehydrogenase kinase: A metabolic switch required for cellular adaptation to hypoxia. *Cell Metabolism*, *3*(3), 177–185. https://doi.org/10.1016/j.cmet.2006.02.002

Kim, W., Moon, S.-O., Sung, M. J., Kim, S. H., Lee, S., So, J.-N., & Park, S. K. (2003). Angiogenic role of adrenomedullin through activation of Akt, mitogen-activated protein kinase, and focal adhesion kinase in endothelial cells. *The FASEB Journal*, *17*(13), 1–19. https://doi.org/10.1096/fj.02-1209fje

Klein, G., Vellenga, E., Fraaije, M. W., Kamps, W. A., & de Bont, E. S. J. M. (2004). The possible role of matrix metalloproteinase (MMP)-2 and MMP-9 in cancer, e.g. acute leukemia. *Critical Reviews in Oncology/Hematology*, *50*(2), 87–100. https://doi.org/10.1016/j.critrevonc.2003.09.001

Lang, F. F., Conrad, C., Gomez-Manzano, C., Alfred Yung, W. K., Sawaya, R., Weinberg, J. S., Prabhu, S. S., Rao, G., Fuller, G. N., Aldape, K. D., Gumin, J., Vence, L. M., Wistuba, I., Rodriguez-Canales, J., Villalobos, P. A., Dirven, C. M. F., Tejada, S., Valle, R. D., Alonso, M. M., … Fueyo, J. (2018). Phase I study of DNX-2401 (delta-24-RGD) oncolytic adenovirus: replication and immunotherapeutic effects in recurrent malignant glioma. *Journal of Clinical Oncology*, *36*(14), 1419–1427. https://doi.org/10.1200/JCO.2017.75.8219

Lapointe, S., Mason, W., MacNeil, M., Harlos, C., Tsang, R., Sederias, J., Luchman, H. A., Weiss, S., Rossiter, J. P., Tu, D., Seymour, L., & Smoragiewicz, M. (2019). A phase I study of vistusertib (dual mTORC1/2 inhibitor) in patients with previously treated glioblastoma multiforme: a CCTG study. *Investigational New Drugs*, 1–8. https://doi.org/10.1007/s10637-019-00875-4

Lathia, J. D., Mack, S. C., Mulkearns-Hubert, E. E., Valentim, C. L. L., & Rich, J. N. (2015). Cancer stem cells in glioblastoma. *Genes and Development*, *29*(12), 1203–1217. https://doi.org/10.1101/gad.261982.115

Lawen, A., & Lane, D. J. R. (2013). Mammalian iron homeostasis in health and disease: Uptake, storage, transport, and molecular mechanisms of action. *Antioxidants and Redox Signaling*, *18*(18), 2473–2507. https://doi.org/10.1089/ars.2011.4271

le Rhun, E., Preusser, M., Roth, P., Reardon, D. A., van den Bent, M., Wen, P., Reifenberger, G., & Weller, M. (2019). Molecular targeted therapy of glioblastoma. *Cancer Treatment Reviews*, *80*. https://doi.org/10.1016/j.ctrv.2019.101896

Lee Ventola, C. (2017). Cancer immunotherapy, part 1: Current strategies and agents. *P and T*, *42*(6), 375–383. /pmc/articles/PMC5440098/?report=abstract

Lewandowska, A. M., Rudzki, M., Rudzki, S., Lewandowski, T., & Laskowska, B. (2019). Environmental risk factors for cancer. *Annals of Agricultural and Environmental Medicine*, *26*(1), 1–7. https://doi.org/10.26444/aaem/94299

Liau, L. M., Ashkan, K., Tran, D. D., Campian, J. L., Trusheim, J. E., Cobbs, C. S., Heth, J. A., Salacz, M., Taylor, S., D'Andre, S. D., Iwamoto, F. M., Dropcho, E. J., Moshel, Y. A., Walter, K. A., Pillainayagam, C. P., Aiken, R., Chaudhary, R., Goldlust, S. A., Bota, D. A., … Bosch, M. L. (2018). First results on survival from a large Phase 3 clinical trial of an autologous dendritic cell vaccine in newly diagnosed glioblastoma. *Journal of Translational Medicine*, *16*(1), 1. https://doi.org/10.1186/s12967-018-1507-6

Lim, M., Xia, Y., Bettegowda, C., & Weller, M. (2018). Current state of immunotherapy for glioblastoma. *Nature Reviews Clinical Oncology*, *15*(7), 422–442. https://doi.org/10.1038/s41571-018-0003-5

Loeb, K. R., & Loeb, L. A. (2017). Significance of multiple mutations in cancer. *Carcinogenesis*, *30*(8), 1330–1335. https://doi.org/10.1093/CARCIN

Louis, D. N., Perry, A., Reifenberger, G., von Deimling, A., Figarella-Branger, D., Cavenee, W. K., Ohgaki, H., Wiestler, O. D., Kleihues, P., & Ellison, D. W. (2016). The 2016 World Health Organization Classification of Tumors of the Central Nervous System: a summary. In *Acta Neuropathologica* (Vol. 131, Issue 6, pp. 803–820). Springer Verlag. https://doi.org/10.1007/s00401-016-1545-1

Luo, W., & Wang, Y. (2019). Hypoxia mediates tumor malignancy and therapy resistance. In *Advances in Experimental Medicine and Biology* (Vol. 1136, pp. 1–18). Springer New York LLC. https://doi.org/10.1007/978-3-030-12734-3_1

Mahase, S., Rattenni, R. N., Wesseling, P., Leenders, W., Baldotto, C., Jain, R., & Zagzag, D. (2017). Hypoxia-Mediated Mechanisms Associated with Antiangiogenic Treatment Resistance in Glioblastomas. *The American Journal of Pathology*, *187*(5), 940–953. https://doi.org/10.1016/j.ajpath.2017.01.010

Mahon, P. C., Hirota, K., & Semenza, G. L. (2001). FIH-1: A novel protein that interacts with HIF-1α and VHL to mediate repression of HIF-1 transcriptional activity. *Genes and Development*, *15*(20), 2675–2686. https://doi.org/10.1101/gad.924501

Maier-Hauff, K., Ulrich, F., Nestler, D., Niehoff, H., Wust, P., Thiesen, B., Orawa, H., Budach, V., & Jordan, A. (2011). Efficacy and safety of intratumoral thermotherapy using magnetic iron-oxide nanoparticles combined with external beam radiotherapy on patients with recurrent glioblastoma multiforme. *Journal of Neuro-Oncology*, *103*(2), 317–324. https://doi.org/10.1007/s11060-010-0389-0

Majmundar, A. J., Wong, W. J., & Simon, M. C. (2010). Hypoxia-Inducible Factors and the Response to Hypoxic Stress. *Molecular Cell*, *40*(2), 294–309. https://doi.org/10.1016/j.molcel.2010.09.022

Maki, T., Ihara, M., Fujita, Y., Nambu, T., Harada, H., Ito, H., Nakao, K., Tomimoto, H., & Takahashi, R. (2011). Angiogenic roles of adrenomedullin through vascular endothelial growth factor induction. *NeuroReport*, *22*(9), 442–447. https://doi.org/10.1097/WNR.0b013e32834757e4

Malta, T. M., de Souza, C. F., Sabedot, T. S., Silva, T. C., Mosella, M. S., Kalkanis, S. N., Snyder, J., Castro, A. V. B., & Noushmehr, H. (2017). Glioma CpG island methylator phenotype (G-CIMP): Biological and clinical implications. *Neuro-Oncology*, *20*(5), 608–620. https://doi.org/10.1093/neuonc/nox183

Martikainen, M., & Essand, M. (2019). Virus-Based Immunotherapy of Glioblastoma. *Cancers*, *11*(2), 186. https://doi.org/10.3390/cancers11020186

Martinez, A., Vos, Michele., Guédez, L., Kaur, G., Chen, Z., Garayoa, M., Pío, R., Stetler-Stevenson, W. G., Kleinman, H. K., & Cuttitta, F. (2002). The Effects of Adrenomedullin Overexpression in Breast Tumor Cells. *Journal of National Cancer Institute*, *94*(16), 1226–1237. https://doi.org/10.1093/jnci/94.16.1226

Masson, N., & Ratcliffe, P. J. (2003). HIF prolyl and asparaginyl hydroxylases in the biological response to intracellular O2 levels. *Journal of Cell Science*, *116*(15), 3041–3049. https://doi.org/10.1242/jcs.00655

McGranahan, T., Therkelsen, K. E., Ahmad, S., & Nagpal, S. (2019). Current State of Immunotherapy for Treatment of Glioblastoma. *Current Treatment Options in Oncology*, *20*(3), 24. https://doi.org/10.1007/s11864-019-0619-4

Metellus, P., Voutsinos-Porche, B., Nanni-Metellus, I., Colin, C., Fina, F., Berenguer, C., Dussault, N., Boudouresque, F., Loundou, A., Intagliata, D., Chinot, O., Martin, P., Figarella-Branger, D., & Ouafik, L. (2011). Adrenomedullin expression and regulation in human glioblastoma, cultured human glioblastoma cell lines and pilocytic astrocytoma. *European Journal of Cancer*, *47*(11), 1727–1735. https://doi.org/10.1016/j.ejca.2011.02.021

Miller, M. E. (2018). *Cancer* (A. M. Campbell, Ed.; 1st ed.). Momentum Press.

Moghadam, A. R., Patrad, E., Tafsiri, E., Peng, W., Fangman, B., Pluard, T. J., Accurso, A., Salacz, M., Shah, K., Ricke, B., Bi, D., Kimura, K., Graves, L., Najad, M. K., Dolatkhah, R., Sanaat, Z., Yazdi, M., Tavakolinia, N., Mazani, M., … Farassati, F. (2017). Ral signaling pathway in health and cancer. In *Cancer Medicine* (Vol. 6, Issue 12, pp. 2998–3013). Blackwell Publishing Ltd. https://doi.org/10.1002/cam4.1105

Mohammadi, A. M., Hawasli, A. H., Rodriguez, A., Schroeder, J. L., Laxton, A. W., Elson, P., Tatter, S. B., Barnett, G. H., & Leuthardt, E. C. (2014). The role of laser interstitial thermal therapy in enhancing progression-free survival of difficult-to-access high-grade gliomas: A multicenter study. *Cancer Medicine*, *3*(4), 971–979. https://doi.org/10.1002/cam4.266

Monteiro, A., Hill, R., Pilkington, G., & Madureira, P. (2017). The Role of Hypoxia in Glioblastoma Invasion. *Cells*, *6*(4), 45. https://doi.org/10.3390/cells6040045

Muz, B., de La Puente, P., Azab, F., & Azab, A. K. (2015). The role of hypoxia in cancer progression, angiogenesis, metastasis, and resistance to therapy. *Hypoxia*, *3*, 83–92. https://doi.org/10.2147/HP.S93413

Nag, S., Qin, J., Srivenugopal, K. S., Wang, M., & Zhang, R. (2013). The MDM2-p53 pathway revisited. *Journal of Biomedical Research*, *27*(4), 254–271. https://doi.org/10.7555/JBR.27.20130030

Nandakumar, P., Mansouri, A., & Das, S. (2017). The role of ATRX in glioma biology. *Frontiers in Oncology*, *7*(236). https://doi.org/10.3389/fonc.2017.00236

Neel, N. F., Martin, T. D., Stratford, J. K., Zand, T. P., Reiner, D. J., & Der, C. J. (2011). The RalGEF-ral effector signaling network: The road less traveled for anti-ras drug discovery. *Genes and Cancer*, *2*(3), 275–287. https://doi.org/10.1177/1947601911407329

Nelson, D. L., & Cox, M. M. (2013). *Lehninger Principles of Biochemistry* (6th ed.). W.H. Freeman.

Nikitenko, L. L., Fox, S. B., Kehoe, S., Rees, M. C. P., & Bicknell, R. (2006). Adrenomedullin and tumour angiogenesis. *Briti*, *94*, 1–7. https://doi.org/10.1038/sj.bjc.6602832

Nomura, M., Yamagishi, S., Harada, S., Yamashima, T., Yamashita, J., & Yamamoto, H. (1998). Placenta growth factor (PlGF) mRNA expression in brain tumors. *Journal of Neuro-Oncology*, *40*(2), 123–130. https://doi.org/10.1023/A:1006198422718

Nørøxe, D. S., Poulsen, H. S., & Lassen, U. (2016). Hallmarks of glioblastoma: A systematic review. In *ESMO Open* (Vol. 1, Issue 6). BMJ Publishing Group. https://doi.org/10.1136/esmoopen-2016-000144

Nussinov, R., & Tsai, C. J. (2015). “Latent drivers” expand the cancer mutational landscape. *Current Opinion in Structural Biology*, *32*, 25–32. https://doi.org/10.1016/j.sbi.2015.01.004

Oehler, M. K., Norbury, C., Hague, S., Rees, M. C. P., & Bicknell, R. (2001). Adrenomedullin inhibits hypoxic cell death by upregulation of Bcl-2 in endometrial cancer cells: A possible promotion mechanism for tumour growth. *Oncogene*, *20*(23), 2937–2945. https://doi.org/10.1038/sj.onc.1204422

Ohgaki, H., Dessen, P., Jourde, B., Horstmann, S., Nishikawa, T., di Patre, P. L., Burkhard, C., Schüler, D., Probst-Hensch, N. M., Maiorka, P. C., Baeza, N., Pisani, P., Yonekawa, Y., Yasargil, M. G., Lütolf, U. M., & Kleihues, P. (2004). Genetic pathways to glioblastoma: A population-based study. *Cancer Research*, *64*(19), 6892–6899. https://doi.org/10.1158/0008-5472.CAN-04-1337

Osuka, S., & van Meir, E. G. (2017). Overcoming therapeutic resistance in glioblastoma: the way forward. *Journal of Clinical Investigation*, *127*(2), 415–426. https://doi.org/10.1172/JCI89587

Paolillo, M., Boselli, C., & Schinelli, S. (2018). Glioblastoma under siege: An overview of current therapeutic strategies. *Brain Sciences*, *8*(15). https://doi.org/10.3390/brainsci8010015

Pastorekova, S., & Gillies, R. J. (2019). The role of carbonic anhydrase IX in cancer development: links to hypoxia, acidosis, and beyond. In *Cancer and Metastasis Reviews* (Vol. 38, Issues 1–2, pp. 65–77). Springer New York LLC. https://doi.org/10.1007/s10555-019-09799-0

Patel, P., Mishra, A., Sheikh, A. A., & Kumar, K. (2017). Adrenomedullin : A novel peptide hormone : A review. *Journal of Pharmacognosy and Phytochemistry*, *6*(6), 2068–2073.

Paw, I., Carpenter, R. C., Watabe, K., Debinski, W., & Lo, H.-W. (2015). Mechanisms Regulating Glioma Invasion. *Cancer Lett*, *362*(1), 1–7. https://doi.org/10.1016/j.canlet.2015.03.015

Pawlik, T. M., & Keyomarsi, K. (2004). Role of cell cycle in mediating sensitivity to radiotherapy. *International Journal of Radiation Oncology Biology Physics*, *59*(4), 928–942. https://doi.org/10.1016/j.ijrobp.2004.03.005

Pecorino, L. (2012). *Molecular Biology of Cancer: Mechanisms, Targets, and Therapeutics*. http://books.google.com/books?id=tI_vcU85QU4C&pgis=1

Peyssonnaux, C., Nizet, V., & Johnson, R. S. (2008). Role of the hypoxia inducible factors HIF in iron metabolism. *Cell Cycle*, *7*(1), 28–32. https://doi.org/10.4161/cc.7.1.5145

Preusser, M., & Weller, M. (2017). *Neuro-oncology Essentials for clinicians ESMO*. ESMO Press.

Prior, R., Reifenberger, G., & Wechsler, W. (1989). Nerve growth factor receptor in tumours of the human nervous system: Immunohistochemical analysis of receptor

expression and tumour growth fraction. *Pathology Research and Practice*, *185*(3), 332–338. https://doi.org/10.1016/S0344-0338(89)80008-1

Proescholdt, M. A., Mayer, C., Kubitza, M., Schubert, T., Liao, S. Y., Stanbridge, E. J., Ivanov, S., Oldfield, E. H., Brawanski, A., & Merrill, M. J. (2005). Expression of hypoxia-inducible carbonic anhydrases in brain tumors. *Neuro-Oncology*, *7*(4), 465–475. https://doi.org/10.1215/S1152851705000025

Proescholdt, M. A., Merrill, M. J., Stoerr, E. M., Lohmeier, A., Pohl, F., & Brawanski, A. (2012). Function of carbonic anhydrase IX in glioblastoma multiforme. *Neuro-Oncology*, *14*(11), 1357–1366. https://doi.org/10.1093/neuonc/nos216

Raghu, H., Gondi, C. S., Dinh, D. H., Gujrati, M., & Rao, J. S. (2011). Specific knockdown of uPA/uPAR attenuates invasion in glioblastoma cells and xenografts by inhibition of cleavage and trafficking of Notch -1 receptor. *Molecular Cancer*, *10*(1), 130. https://doi.org/10.1186/1476-4598-10-130

Rajaratnam, V., Islam, M. M., Yang, M., Slaby, R., Ramirez, H. M., & Mirza, S. P. (2020). Glioblastoma: Pathogenesis and Current Status of Chemotherapy and Other Novel Treatments. *Cancers*, *12*(4), 937. https://doi.org/10.3390/cancers12040937

Ran, F. A., Hsu, P. D., Wright, J., Agarwala, V., Scott, D. A., & Zhang, F. (2013). Genome engineering using the CRISPR-Cas9 system. *Nature Protocols*, *8*(11), 2281–2308. https://doi.org/10.1038/nprot.2013.143.Genome

Ravi, R., Mookerjee, B., Bhujwalla, Z. M., Sutter, C. H., Artemov, D., Zeng, Q., Dillehay, L. E., Madan, A., Semenza, G. L., & Bedi, A. (2000). Regulation of tumor angiogenesis by p53-induced degradation of hypoxia-inducible factor 1. *Genes and Development*, *14*, 34–44. www.genesdev.org

Riabov, V., Gudima, A., Wang, N., Mickley, A., Orekhov, A., & Kzhyshkowska, J. (2014). Role of tumor associated macrophages in tumor angiogenesis and lymphangiogenesis. *Frontiers in Physiology*, *5*(75), 1–13. https://doi.org/10.3389/fphys.2014.00075

Ribatti, D., Nico, B., Spinazzi, R., Vacca, A., & Nussdorfer, G. G. (2005). The role of adrenomedullin in angiogenesis. *Peptides*, *26*(9), 1670–1675. https://doi.org/10.1016/j.peptides.2005.02.017

Rong, Y., Durden, D. L., van Meir, E. G., & Brat, D. J. (2006). “Pseudopalisading” necrosis in glioblastoma: A familiar morphologic feature that links vascular pathology, hypoxia, and angiogenesis. *Journal of Neuropathology and Experimental Neurology*, *65*(6), 529–539. https://doi.org/10.1097/00005072-200606000-00001

Ryland, G. L., Doyle, M. A., Goode, D., Boyle, S. E., Choong, D. Y. H., Rowley, S. M., Li, J., Bowtell, D. D., Tothill, R. W., Campbell, I. G., & Gorringe, K. L. (2015). Loss of heterozygosity: What is it good for? *BMC Medical Genomics*, *8*(1), 45. https://doi.org/10.1186/s12920-015-0123-z

Said, H. M., Polat, B., Staab, A., Hagemann, C., Stein, S., Flentje, M., Theobald, M., Katzer, A., & Vordermark, D. (2008). Rapid detection of the hypoxia-regulated CA-IX and NDRG1 gene expression in different glioblastoma cells in vitro. *Oncology Reports*, *20*(2), 413–419. https://doi.org/10.3892/or_00000023

Sarkaria, J. N., Hu, L. S., Parney, I. F., Pafundi, D. H., Brinkmann, D. H., Laack, N. N., Giannini, C., Burns, T. C., Kizilbash, S. H., Laramy, J. K., Swanson, K. R., Kaufmann, T. J., Brown, P. D., Agar, N. Y. R., Galanis, E., Buckner, J. C., & Elmquist, W. F. (2018). Is the blood-brain barrier really disrupted in all glioblastomas? A critical assessment of existing clinical data. *Neuro-Oncology*, *20*(2), 184–191. https://doi.org/10.1093/neuonc/nox175

Sayegh, E. T., Oh, T., Fakurnejad, S., Bloch, O., & Parsa, A. T. (2014). Vaccine therapies for patients with glioblastoma. In *Journal of Neuro-Oncology* (Vol. 119, Issue 3, pp. 531–546). Springer New York LLC. https://doi.org/10.1007/s11060-014-1502-6

Schaller, J., & Gerber, S. S. (2011). The plasmin-antiplasmin system: structural and functional aspects. *Cellular and Molecular Life Sciences*, *68*, 785–801. https://doi.org/10.1007/s00018-010-0566-5

Schell, D. A., Vari, R. C., & Samson, W. K. (1996). Adrenomedullin : A Newly Discovered Hormone Controlling. *Trends in Endocrinology and Metabolism*, *7*, 7–13.

Schiff, D., Jaeckle, K. A., Anderson, S. K., Galanis, E., Giannini, C., Buckner, J. C., Stella, P., Flynn, P. J., Erickson, B. J., Schwerkoske, J. F., Kaluza, V., Twohy, E., Dancey, J., Wright, J., & Sarkaria, J. N. (2018). Phase 1/2 trial of temsirolimus and sorafenib in the treatment of patients with recurrent glioblastoma: North Central Cancer Treatment Group Study/Alliance N0572. *Cancer*, *124*(7), 1455–1463. https://doi.org/10.1002/cncr.31219

Schito, L. (2019). Hypoxia-dependent angiogenesis and lymphangiogenesis in cancer. In *Advances in Experimental Medicine and Biology* (Vol. 1136, pp. 71–85). Springer New York LLC. https://doi.org/10.1007/978-3-030-12734-3_5

Schofield, C. J., & Ratcliffe, P. J. (2004). Oxygen sensing by HIF hydroxylases. *Nature Reviews Molecular Cell Biology*, *5*(5), 343–354. https://doi.org/10.1038/nrm1366

Schwarzenbach, H. (2013). Loss of Heterozygosity. In *Brenner's Encyclopedia of Genetics: Second Edition* (pp. 271–273). Elsevier Inc. https://doi.org/10.1016/B978-0-12-374984-0.00882-2

Sepúlveda-Sánchez, J. M., Ángeles Vaz, M., Balañá, C., Gil-Gil, M., Reynés, G., Gallego, Ó., Martínez-García, M., Vicente, E., Quindós, M., Luque, R., Ramos, A., Ruano, Y., Pérez-Segura, P., Benavides, M., Sánchez-Gómez, P., & Hernández-Laín, A. (2017). Phase II trial of dacomitinib, a pan-human EGFR tyrosine kinase inhibitor, in recurrent glioblastoma patients with EGFR amplification. *Neuro-Oncology*, *19*(11), 1522–1531. https://doi.org/10.1093/neuonc/nox105

Shackelford, D. B., & Shaw, R. J. (2009). The LKB1-AMPK pathway: Metabolism and growth control in tumour suppression. In *Nature Reviews Cancer* (Vol. 9, Issue 8, pp. 563–575). https://doi.org/10.1038/nrc2676

Shen, Y., Li, X., Dong, D., Zhang, B., Xue, Y., & Shang, P. (2018). Transferrin receptor 1 in cancer: a new sight for cancer therapy. *Am J Cancer Res*, *8*(6), 916–931. www.ajcr.us/

Shergalis, A., Bankhead, A., Luesakul, U., Muangsin, N., & Neamati, N. (2018). Current challenges and opportunities in treating glioblastomas. *Pharmacological Reviews*, *70*(3), 412–445. https://doi.org/10.1124/pr.117.014944

Shibuya, M. (2013). Vascular endothelial growth factor and its receptor system: physiological functions in angiogenesis and pathological roles in various diseases. *Journal of Biochemistry*, *153*(1), 13–19. https://doi.org/10.1093/jb/mvs136

Siebzehnrubl, F. A., Silver, D. J., Tugertimur, B., Deleyrolle, L. P., Siebzehnrubl, D., Sarkisian, M. R., Devers, K. G., Yachnis, A. T., Kupper, M. D., Neal, D., Nabilsi, N. H., Kladde, M. P., Suslov, O., Brabletz, S., Brabletz, T., Reynolds, B. A., & Steindler, D. A. (2013). The ZEB1 pathway links glioblastoma initiation, invasion and chemoresistance. *EMBO Molecular Medicine*, *5*(8), 1196–1212. https://doi.org/10.1002/emmm.201302827

Srinivasan, S., Chitalia, V., Meyer, R. D., Hartsough, E., Mehta, M., Harrold, I., Anderson, N., Feng, H., Smith, L. E. H., Jiang, Y., Costello, C. E., Rahimi, N., & Edu, N. (2015). Hypoxia-induced expression of phosducin-like 3 regulates expression of VEGFR-2 and promotes angiogenesis HHS Public Access. *Angiogenesis*, *18*(4), 449–462. https://doi.org/10.1007/s10456-015-9468-3

Srivastava, C., Irshad, K., Dikshit, B., Chattopadhyay, P., Sarkar, C., Gupta, D. K., Sinha, S., & Chosdol, K. (2018). FAT1 modulates EMT and stemness genes expression in hypoxic glioblastoma. *International Journal of Cancer*, *142*(4), 805–812. https://doi.org/10.1002/ijc.31092

Srivastava, S., Jackson, C., Kim, T., Choi, J., & Lim, M. (2019). A Characterization of Dendritic Cells and Their Role in Immunotherapy in Glioblastoma: From Preclinical Studies to Clinical Trials. *Cancers*, *11*(4), 537. https://doi.org/10.3390/cancers11040537

Strachan, T. O. M., & Read, A. (2011). Human Molecular Genetics. In *Garland Science* (4th ed.). Garland Science.

Stratton, M. R., Campbell, P. J., & Futreal, P. A. (2009). The cancer genome. *Nature Reviews*, *458*, 719–724. https://doi.org/10.1038/nature07943

Stupp, R., Mason, W. P., van den Bent, M. J., Weller, M., Fisher, B., Taphoorn, M. J. B., Belanger, K., Brandes, A. A., Marosi, C., Bogdahn, U., Curschmann, J., Janzer, R. C., Ludwin, S. K., Gorlia, T., Allgeier, A., Lacombe, D., Cairncross, J. G., Eisenhauer, E., & Mirimanoff, R. O. (2005). Radiotherapy plus Concomitant and Adjuvant Temozolomide for Glioblastoma. *The New England Journal of Medicine*, *352*(10), 987–996. https://doi.org/10.1056/NEJMoa043330

Stupp, R., Taillibert, S., Kanner, A. A., Kesari, S., Steinberg, D. M., Toms, S. A., Taylor, L. P., Lieberman, F., Silvani, A., Fink, K. L., Barnett, G. H., Zhu, J. J., Henson, J. W., Engelhard, H. H., Chen, T. C., Tran, D. D., Sroubek, J., Tran, N. D., Hottinger, A. F., … Ram, Z. (2015). Maintenance therapy with tumor-Treating fields plus temozolomide vs temozolomide alone for glioblastoma a randomized clinical trial. *JAMA*, *314*(23), 2535–2543. https://doi.org/10.1001/jama.2015.16669

Stupp, R., Taillibert, S., Kanner, A., Read, W., Steinberg, D. M., Lhermitte, B., Toms, S., Idbaih, A., Ahluwalia, M. S., Fink, K., di Meco, F., Lieberman, F., Zhu, J. J., Stragliotto, G., Tran, D. D., Brem, S., Hottinger, A. F., Kirson, E. D., Lavy-Shahaf,

G., … Ram, Z. (2017). Effect of tumor-treating fields plus maintenance temozolomide vs maintenance temozolomide alone on survival in patients with glioblastoma a randomized clinical trial. *JAMA*, *318*(23), 2306–2316. https://doi.org/10.1001/jama.2017.18718

Stupp, R., Wong, E. T., Kanner, A. A., Steinberg, D., Engelhard, H., Heidecke, V., Kirson, E. D., Taillibert, S., Liebermann, F., Dbalý, V., Ram, Z., Villano, J. L., Rainov, N., Weinberg, U., Schiff, D., Kunschner, L., Raizer, J., Honnorat, J., Sloan, A., … Gutin, P. H. (2012). NovoTTF-100A versus physician's choice chemotherapy in recurrent glioblastoma: A randomised phase III trial of a novel treatment modality. *European Journal of Cancer*, *48*(14), 2192–2202. https://doi.org/10.1016/j.ejca.2012.04.011

Takano, S., Yoshii, Y., Kondo, S., Suzuki, H., Maruno, T., Shirai, S., & Nose, T. (1996). Concentration of Vascular Endothelial Growth Factor in the Serum and Tumor Tissue of Brain Tumor Patients. *Cancer Research*, *56*(9), 2185–2190.

Taphoorn, M. J. B., Dirven, L., Kanner, A. A., Lavy-Shahaf, G., Weinberg, U., Taillibert, S., Toms, S. A., Honnorat, J., Chen, T. C., Sroubek, J., David, C., Idbaih, A., Easaw, J. C., Kim, C. Y., Bruna, J., Hottinger, A. F., Kew, Y., Roth, P., Desai, R., … Stupp, R. (2018). Influence of treatment with tumor-treating fields on health-related quality of life of patients with newly diagnosed glioblastoma a secondary analysis of a randomized clinical trial. *JAMA Oncology*, *4*(4), 495–504. https://doi.org/10.1001/jamaoncol.2017.5082

Taylor, J. W., Parikh, M., Phillips, J. J., James, C. D., Molinaro, A. M., Butowski, N. A., Clarke, J. L., Oberheim-Bush, N. A., Chang, S. M., Berger, M. S., & Prados, M. (2018). Phase-2 trial of palbociclib in adult patients with recurrent RB1-positive glioblastoma. *Journal of Neuro-Oncology*, *140*(2). https://doi.org/10.1007/s11060-018-2977-3

Thomas, J. G., Rao, G., Kew, Y., & Prabhu, S. S. (2016). Laser interstitial thermal therapy for newly diagnosed and recurrent glioblastoma. *Neurosurgical Focus*, *41*(4). https://doi.org/10.3171/2016.7.FOCUS16234

Tivnan, A., Heilinger, T., Lavelle, E. C., & Prehn, J. H. M. (2017). Advances in immunotherapy for the treatment of glioblastoma. *Journal of Neuro-Oncology*, *131*, 1–9. https://doi.org/10.1007/s11060-016-2299-2

Valdez, J. M., Nichols, K. E., & Kesserwan, C. (2017). Li-Fraumeni syndrome: a paradigm for the understanding of hereditary cancer predisposition. *British Journal of Haematology*, *176*(4), 539–552. https://doi.org/10.1111/bjh.14461

van Zijl, F., Krupitza, G., & Mikulits, W. (2011). Initial steps of metastasis: Cell invasion and endothelial transmigration. *Mutation Research - Reviews in Mutation Research*, *728*(1–2), 23–34. https://doi.org/10.1016/j.mrrev.2011.05.002

Verhaak, R. G., Hoadley, K. A., Purdom, E., Wang, V., Qi, Y., Wilkerson, M. D., Ryan Miller, C., Ding, L., Golub, T., Mesirov, J. P., Alexe, G., Lawrence, M., Tamayo, P., Weir, B. A., Gabrie, S., Winckler, W., Gupta, S., Jakkula, L., Feiler, H. S., … David James, C. (2010a). An integrated genomic analysis identifies clinically relevant subtypes of glioblastoma characterized by abnormalities in PDGFRA, IDH1, EGFR and NF1. *Cancer Cell*, *17*(1), 98. https://doi.org/10.1016/j.ccr.2009.12.020

Verhaak, R. G., Hoadley, K. A., Purdom, E., Wang, V., Qi, Y., Wilkerson, M. D., Ryan Miller, C., Ding, L., Golub, T., Mesirov, J. P., Alexe, G., Lawrence, M., Tamayo, P., Weir, B. A., Gabrie, S., Winckler, W., Gupta, S., Jakkula, L., Feiler, H. S., … David James, C. (2010b). An integrated genomic analysis identifies clinically relevant subtypes of glioblastoma characterized by abnormalities in PDGFRA, IDH1, EGFR and NF1. *Cancer Cell*, *17*(1), 98. https://doi.org/10.1016/j.ccr.2009.12.020

Vlahovic, G., Fecci, P. E., Reardon, D., & Sampson, J. H. (2015). Programmed death ligand 1 (PD-L1) as an immunotherapy target in patients with glioblastoma: Table 1. *Neuro-Oncology*, *17*(8), 1043–1045. https://doi.org/10.1093/neuonc/nov071

Vollmann-Zwerenz, A., Leidgens, V., Feliciello, G., Klein, C. A., & Hau, P. (2020). Tumor Cell Invasion in Glioblastoma. *International Journal of Molecular Sciences*, *21*(6), 1932. https://doi.org/10.3390/ijms21061932

Walker, C., Mojares, E., & del Río Hernández, A. (2018). Role of extracellular matrix in development and cancer progression. In *International Journal of Molecular Sciences* (Vol. 19, Issue 10). MDPI AG. https://doi.org/10.3390/ijms19103028

Walsh, J. C., Lebedev, A., Aten, E., Madsen, K., Marciano, L., & Kolb, H. C. (2014). The clinical importance of assessing tumor hypoxia: Relationship of tumor hypoxia to prognosis and therapeutic opportunities. *Antioxidants and Redox Signaling*, *21*(10), 1516–1554. https://doi.org/10.1089/ars.2013.5378

Wang, Y., Liu, T., Yang, N., Xu, S., Li, X., & Wang, D. (2016). Hypoxia and macrophages promote glioblastoma invasion by the CCL4-CCR5 axis. *Oncology Reports*, *36*(6), 3522–3528. https://doi.org/10.3892/or.2016.5171

Warburg, O. (1925). The metabolism of carcinoma cells 1. *The Journal of Cancer Research*, *9*(1), 148–163. https://doi.org/10.1158/jcr.1925.148

Weiderpass, E. (2010). Lifestyle and Cancer Risk. *Journal of Preventive Medicine and Public Health*, *43*(6), 459. https://doi.org/10.3961/jpmph.2010.43.6.459

Weinberg, R. A. (1996). How cancer arises. *Scientific American*, *275*(3), 62–70. https://doi.org/10.1038/scientificamerican0996-62

Weinberg, R. A. (2014). *The Biology of Cancer* (Second). Garland Science.

Wen, P. Y., Touat, M., Alexander, B. M., Mellinghoff, I. K., Ramkissoon, S., McCluskey, C. S., Pelton, K., Haidar, S., Basu, S. S., Gaffey, S. C., Brown, L. E., Martinez-Ledesma, J. E., Wu, S., Kim, J., Wei, W., Park, M. A., Huse, J. T., Kuhn, J. G., Rinne, M. L., … Ligon, K. L. (2019). Buparlisib in patients with recurrent glioblastoma harboring phosphatidylinositol 3-kinase pathway activation: An open-label, multicenter, multi-arm, phase II trial. *Journal of Clinical Oncology*, *37*(9), 741–750. https://doi.org/10.1200/JCO.18.01207

Werner, C., Doenst, T., & Schwarzer, M. (2016). Metabolic Pathways and Cycles. In *The Scientist's Guide to Cardiac Metabolism* (pp. 39–55). Elsevier Inc. https://doi.org/10.1016/B978-0-12-802394-5/00004-2

Wilson, K., & Walker, J. (2010). Principles and Techniques of Biochemistry and Molecular Biology. In *Cambridge University Press* (7th ed.). Cambrigde University Press. https://doi.org/10.1017/CBO9780511813412.007

Xie, Q., Mittal, S., & Berens, M. E. (2014). Targeting adaptive glioblastoma: an overview of proliferation and invasion. *Neuro-Oncology*, *16*(12), 1575–1584. https://doi.org/10.1093/neuonc/nou147

Yang, P.-C., & Mahmood, T. (2012). Western blot: Technique, theory, and trouble shooting. *North American Journal of Medical Sciences*, *4*(9), 429. https://doi.org/10.4103/1947-2714.100998

Young, R. M., Jamshidi, A., Davis, G., & Sherman, J. H. (2015). Current trends in the surgical management and treatment of adult glioblastoma. *Ann Transl Med*, *3*(9), 121. https://doi.org/10.3978/j.issn.2305-5839.2015.05.10

Yu, A., Faiq, N., Green, S., Lai, A., Green, R., Hu, J., Cloughesy, T. F., Mellinghoff, I., & Nghiemphu, P. L. (2017). Report of safety of pulse dosing of lapatinib with temozolomide and radiation therapy for newly-diagnosed glioblastoma in a pilot phase II study. *Journal of Neuro-Oncology*, *134*(2), 357–362. https://doi.org/10.1007/s11060-017-2533-6

Yu, Z., Pestell, T. G., Lisanti, M. P., & Pestell, R. G. (2012). Cancer Stem Cells. *International Journal of Biochemistry & Cell Biology*, *44*(12), 2144–2151. https://doi.org/10.1016/j.biocel.2012.08.022

Yuan, Y., Jiang, Y. C., Sun, C. K., & Chen, Q. M. (2016). Role of the tumor microenvironment in tumor progression and the clinical applications. *Oncology Reports*, *35*(5), 2499–2515. https://doi.org/10.3892/or.2016.4660

Zbytek, B., Carlson, J. A., Granese, J., Ross, J., Mihm, M., & Slominski, A. (2008). Current concepts of metastasis in melanoma. *Expert Review of Dermatology*, *3*(5), 569–585. https://doi.org/10.1586/17469872.3.5.569

Zhang, L., Huang, Y., Lindstrom, A. R., Lin, T. Y., Lam, K. S., & Li, Y. (2019). Peptide-based materials for cancer immunotherapy. *Theranostics*, *9*(25), 7807–7825. https://doi.org/10.7150/thno.37194

Appendices

Appendix A: Plasmid and primers used for cloning.

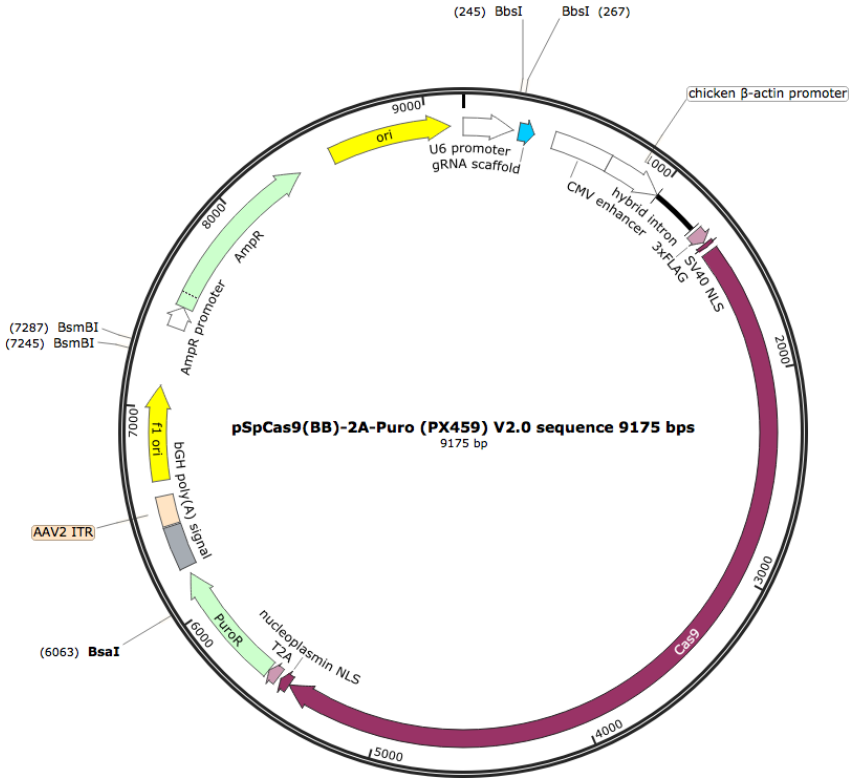

Figure A.1 – Plasmid pSpCas9(BB)-2A-Puro (PX459) V2.0 sequence map (Addgene #62988).
The figure shows the map of the PX459 plasmid used. The plasmid contains Puro (Puromycin) and Amp (Ampicillin) resistance genes (green), replication origin (ori) (yellow), Cas9 gene (dark pink), Cytomegalovirus (CMV) enhancer (white), U6 promoter (white) and gRNA scaffold (blue).

Table A.1 – U6 Forward primer sequence.
(Ran et al., 2013)

Primer	Sequence
U6 Forward primer	5'-GAGGGCCTATTTCCCATGATTCC-3'

Appendix B: Compositions of the solutions and mediums used.

10X DNA Loading buffer

-50% glycerol

-100mM Tris pH 7.5

-10mM EDTA pH 8

-Bromophenol blue and xylene cyanol

SOC medium

-2% tryptone

-0.5% yeast extract

-10 mM NaCl

-2.5 mM KCl

-10 mM $MgCl_2$

-10 mM $MgSO_4$

-20 mM glucose

Lysis Buffer

-1% NP-40

-20nM NaCl

-50mM Tris pH=7.5

-5mM EDTA

-Protease inhibitor cocktail (BIO-RAD)

10X Running Buffer

-250mM Tris base

-2.5M glycine

-1% SDS

Gels were run using 1X Running Buffer

10X Transfer Buffer

-250mM Tris base

-2M glycine

Gels were transferred using 1X Transfer Buffer with 20% of methanol.

4X Protein Loading Buffer

-8% SDS

-120mM Tris-HCl pH 6.8

-20% Glycerol

-0.02% Bromophenol blue

-20% β-mercaptoehanol

The proteins were prepared in 1X Protein Loading Buffer.

20X TBS buffer

-20mM Tris pH 7.5

-120mM NaCl

Working solution: 1X TBS-T (1X TBS + 0.05% Tween-20)

xxx

Appendix C : DNA and protein markers used.

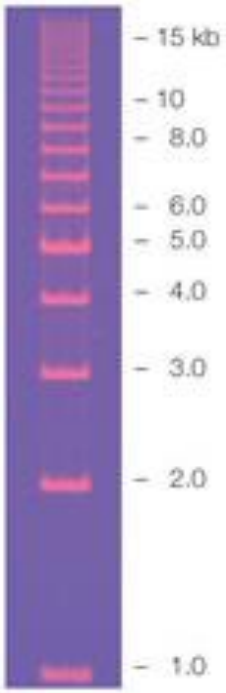

Figure C.1 - EZ load 1kb Molecular Ruler - DNA ladder (BIO-RAD).

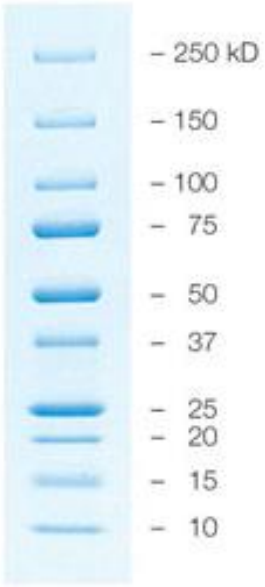

Figure C.2 - Precision Plus Protein All Blue Standards marker (BIO-RAD).